Fermion degrees of freedom in the interacting boson model

Slobodan Brant

Department of Physics, Faculty of Science
University of Zagreb
Zagreb
Croatia

1. Structure of odd-even nuclei in the interacting boson-fermion model
2. High spin states in the interacting boson and interacting boson-fermion model
3. Structure of odd-odd nuclei in the interacting boson-fermion-fermion model
4. β decay in the interacting boson-fermion model

1.

Structure of odd-even nuclei in the interacting boson fermion model

Shell model $\longrightarrow$ matrix elements of the effective interaction between identical nucleons are strongly attractive when the two nucleons are in a $J = 0$ state and remain attractive when the two nucleons are in a $J = 2$ state. They become repulsive for $J \geq 4$.

Nucleons tend to form pairs with angular momentum $J = 0$ or $J = 2$

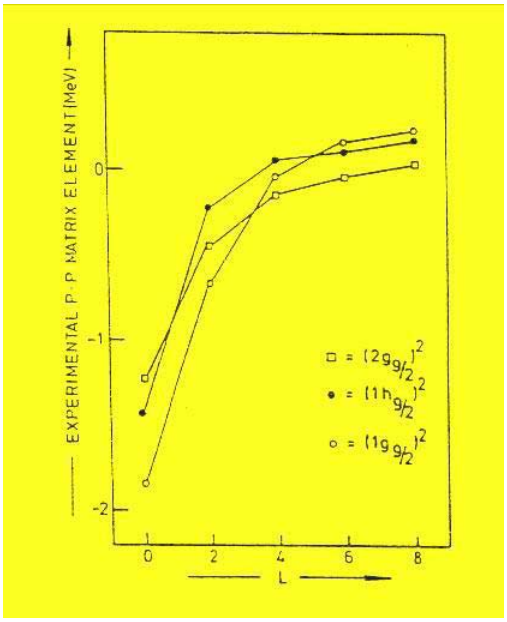

Generalized seniority scheme: generalization of the seniority scheme to several non-degenerate orbits. The number of active nucleons is counted in respect to the nearest closed shell (valence nucleons). Contributions from orbitals outside the valence shell can be neglected since they lie at a too high energy.

A collective $J = 0$ pair is generated by the operator

$$S^\dagger = \sum_j \alpha_j S_j^\dagger$$

$$S_j^\dagger = \frac{1}{2}\sqrt{2j+1}\ (c_j^\dagger \tilde{c}_j)^{(0)}$$

State with generalized seniority $w = 0$ and $n = 2N$ particles

$$|n,\ J = 0,\ w = 0\rangle = (S^\dagger)^N\ |0\rangle$$

An excited 2^+ state is generated by the operator that creates a collective state with $J = 2$ and $w = 2$

$$D^\dagger = \sum_{jj'} \frac{1}{2}\beta_{jj'}\sqrt{1+\delta_{jj'}}\ (c_j^\dagger \tilde{c}_{j'})^{(2)}$$

State with generalized seniority $w = 2$, $J = 2$ and $n = 2N$ particles

$$|n,\ J = 2,\ w = 2\rangle = D^\dagger (S^\dagger)^{N-1}\ |0\rangle$$

The structure coefficients α_j and $\beta_{jj'}$ can be obtained by diagonalizing the shell model interaction in the space of all $w = 0, 2$ states.

Instead of having to use the full shell model space, it is sufficient to consider the much smaller (S, D) subspace.

- Low-lying collective states can be described very well
- Non collective states can not be described
- The matrix elements of the fermion operators in the (S, D) subspace can be cumbersome
- The space built on S and D fermion pairs is mapped onto a corresponding space built on s and d boson degrees of freedom
- For states containing more than one D fermion pair we have to map the component of the state which is orthogonal to all the states containing fewer D fermion pairs

$$
\begin{aligned}
|S^N,\ L=0\rangle &\longrightarrow |s^N,\ L=0\rangle \\
|D\ S^{N-1},\ L=2\rangle &\longrightarrow |d\ s^{N-1},\ L=2\rangle \\
|D^m\ S^{N-m},\ L\rangle_{\ orth} &\longrightarrow |d^m\ s^{N-m},\ L\rangle
\end{aligned}
$$

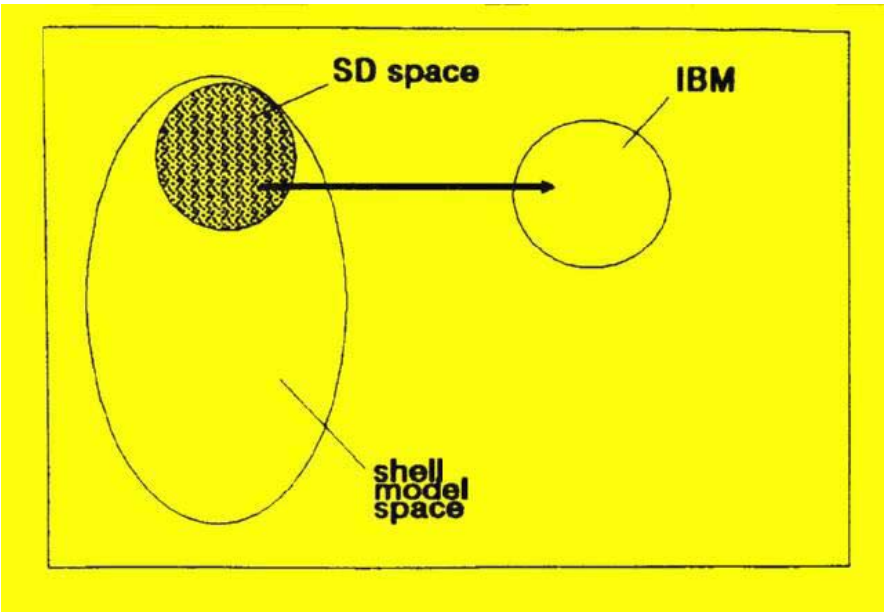

- By equating matrix elements in (S, D) and (s, d) spaces the operators in the (s, d) space are obtained
- Since the S and D fermion pairs are always pairs of like nucleons (two protons or two neutrons), one has proton (s_π, d_π) and neutron (s_ν, d_ν) bosons. The model is called IBM-2.

$$H_B = \epsilon_d \left(\hat{n}_{d_\nu} + \hat{n}_{d_\pi}\right) + \kappa \left(Q^B_\nu \cdot Q^B_\pi\right) + M_{\nu\pi} + V_{\nu\nu} + V_{\pi\pi}$$

$$\begin{aligned} Q^B_\nu &= d^\dagger_\nu s_\nu + s^\dagger_\nu \tilde{d}_\nu + \chi_\nu \left[d^\dagger_\nu \tilde{d}_\nu\right]^{(2)} \\ Q^B_\pi &= d^\dagger_\pi s_\pi + s^\dagger_\pi \tilde{d}_\pi + \chi_\pi \left[d^\dagger_\pi \tilde{d}_\pi\right]^{(2)} \end{aligned}$$

$$\begin{aligned} M_{\nu\pi} = & \frac{1}{2}\xi_2 \left((d^\dagger_\nu s^\dagger_\pi - d^\dagger_\pi s^\dagger_\nu) \cdot (\tilde{d}_\nu s_\pi - \tilde{d}_\pi s_\nu)\right) \\ & - \sum_{K=1,3} \xi_K \left([d^\dagger_\nu d^\dagger_\pi]^{(K)} \cdot [\tilde{d}_\nu \tilde{d}_\pi]^{(K)}\right) \end{aligned}$$

$$V_{\nu\nu} = \frac{1}{2} \sum_{L=0,2,4} c^\nu_L \left([d^\dagger_\nu d^\dagger_\nu]^{(L)} \cdot [\tilde{d}_\nu \tilde{d}_\nu]^{(L)}\right)$$

$$V_{\pi\pi} = \frac{1}{2} \sum_{L=0,2,4} c^\pi_L \left([d^\dagger_\pi d^\dagger_\pi]^{(L)} \cdot [\tilde{d}_\pi \tilde{d}_\pi]^{(L)}\right)$$

- The major part of the interaction between like particles is contained in the boson energies and a smaller in the $V_{\nu\nu}$ and $V_{\pi\pi}$ terms.
- The $Q^B_\nu \cdot Q^B_\pi$ interaction is the boson image of the neutron-proton quadrupole-quadrupole interaction.
- $M_{\nu\pi}$ (Majorana term) shifts up all states that are not totally symmetric in the neutron-proton degree of freedom. It is a consequence of the truncation of the basis to s and d bosons only.

Introducing the concept of F spin, the IBM-1 Hamiltonian can be obtained by projecting out the part that acts only on the maximal F spin subspace (on states that are totally symmetric in the neutron-proton degree of freedom).

$$\begin{aligned} H_B = & \varepsilon\, \hat{N} + \frac{1}{2}\, v_0 \, \left([d^\dagger d^\dagger]_{(0)} [\tilde{s}\tilde{s}]_{(0)} + h.c.\right)_{(0)} \\ & + \frac{1}{\sqrt{2}}\, v_2 \, \left([d^\dagger d^\dagger]_{(2)} [\tilde{d}\tilde{s}]_{(2)} + h.c.\right)_{(0)} \\ & + \sum_{L=0,2,4} \frac{1}{2}\, C_L \, \sqrt{2L+1} \, \left([d^\dagger d^\dagger]_{(L)} [\tilde{d}\tilde{d}]_{(L)}\right)_{(0)} \end{aligned}$$

LIMITS

$$
\begin{array}{lll}
U(6) \supset U(5) \supset O(5) \supset O(3) \supset O(2) & & \textit{vibrational limit} \\
U(6) \supset SU(3) \supset O(3) \supset O(2) & & \textit{rotational limit} \\
U(6) \supset O(6) \supset O(5) \supset O(3) \supset O(2) & & \gamma - \textit{soft limit}
\end{array}
$$

The Lie algebra U(6) admits:

- Schwinger boson realization in terms of 6 bosons s, d_μ
- Holstein-Primakoff boson realization in terms of 5 bosons b_μ

$$
\begin{aligned}
d^\dagger_{2\mu} &\longleftrightarrow b^\dagger_{2\mu} \\
s^\dagger &\longleftrightarrow \sqrt{N - \sum_\mu b^\dagger_{2\mu} b_{2\mu}}
\end{aligned}
$$

- In the IBFM an odd-nucleon operator $a^\dagger_j$ is introduced in addition to the s and d boson operators.
- The states in the IBFM model space can be related to the shell model basis by using the generalized seniority scheme.
- The odd-nucleon operator $a^\dagger_j$ should not be regarded as a nucleon creation operator (in the shell model sense) but as a generalized seniority raising operator.

$$
\begin{aligned}
a^\dagger_j \, |s^N\rangle = |j s^N\rangle &\longleftrightarrow |n = 2N+1, J = j, w = 1\rangle \\
(a^\dagger_j d^\dagger)^{(J)} \, |s^{N-1}\rangle = |(jd)^{(J)} s^{N-1}\rangle &\longleftrightarrow |n = 2N+1, J, w = 3\rangle
\end{aligned}
$$

- The operator $a^\dagger_j$ operating on an N boson state with n_d d -bosons creates a state which corresponds to a shell model state with $n = 2N + 1$ and $w = 2n_d + 1$.
- For the shell model single-nucleon operator $c^\dagger_j$
  $c^\dagger_j \, |w = 2\rangle = \alpha |w = 1\rangle + \beta |w = 3\rangle$
- For the odd-nucleon operator $a^\dagger_j$
  $a^\dagger_j \, |w = 2\rangle = |w = 3\rangle$

A microscopic theory for a system that includes both fermionic and bosonic degrees of freedom is complicated.

The dominant interaction in the coupling of the odd-particle to the bosons is the proton-neutron quadrupole interaction → construction of the IBFM image of the shell model quadrupole operator.

There are several methods for obtaining the IBFM image of the shell model quadrupole operator. One of them is to introduce the pseudo particle operator $\check{c}_j^\dagger$ (Scholten).

Condition:

The matrix elements of $\check{c}_j^\dagger$ in the IBFM space are equal to the matrix elements of $c_j^\dagger$ in the shel model space.

For $w \leq 1$ (α_j are the coefficients which enter in the definition of the S pair operator):

$$\hat{n} = \sum_j \alpha_j^2 \sum_m c_{jm}^\dagger c_{jm} = \sum_j \alpha_j^2 \hat{n}_j$$

$$\langle S^N |\ \hat{n}\ | S^N \rangle = 2N$$

Effective degeneracy

$$\Omega_e = \sum_j \alpha_j^2 \Omega_j$$

Here the spherical shell model OCCUPATION PROBABILITIES v_j^2 are introduced
($u_j^2 + v_j^2 = 1$).

$$v_j^2 = n_j/(2j+1)$$

$$n_j = \langle S^N |\ \hat{n}_j\ | S^N \rangle \approx 2N\alpha_j^2 \frac{\Omega_j}{\Omega_e}$$

$$v_j^2 = \alpha_j^2 N/\Omega_e$$

$$\langle S^N j' \parallel c_j^\dagger \parallel S^N \rangle = -\hat{j} u_j \delta_{jj'} = u_j \langle s^N j' \parallel a_j^\dagger \parallel s^N \rangle$$
$$\langle S^N \parallel c_j^\dagger \parallel S^{N-1} j' \rangle = \hat{j} v_j \delta_{jj'} = v_j \langle s^N \parallel (s^\dagger \tilde{a}_j)^{(j)} \parallel s^{N-1} j' \rangle / \sqrt{N}$$

For $w \leq 3$ similar expressions can be obtained. Finally, the IBFM image of the shell model single-nucleon creation operator is

$$\begin{aligned} \check{c}_j^\dagger &= u_j a_j^\dagger - \sum_{j'} \frac{v_j}{\sqrt{N}} \sqrt{\frac{10}{2j+1}} \beta_{j'j} (K_\beta)^{-1} s^\dagger (\tilde{d}\, a_{j'}^\dagger)^{(j)} \\ &+ \frac{v_j}{\sqrt{N}} (s^\dagger \tilde{a}_j)^{(j)} + \sum_{j'} u_j \sqrt{\frac{10}{2j+1}} \beta_{j'j} (K_\beta)^{-1} (d^\dagger \tilde{a}_{j'})^{(j)} \end{aligned}$$

$$K_\beta^2 = \sum_{jj'} \beta_{j'j}^2$$

The coefficients $\beta_{j'j}$ define the microscopic structure of the d-boson.

The matrix elements of the quadrupole operator $\sum_{jj'} Q_{jj'}\ (c_j^\dagger \tilde{c}_{j'})^{(2)}$ in the fermion space are replaced by the matrix elements of the pseudo particle operator $\check{c}_j^\dagger$ acting in the boson space giving the quadrupole operator expressed in terms of boson and odd-particle operators.

$$\begin{aligned} Q^{(2)} &= Q_B^{(2)} + Q_F^{(2)} \\ Q_B^{(2)} &= [s^\dagger \tilde{d} + d^\dagger \tilde{s}]^{(2)} + \chi [d^\dagger \tilde{d}]^{(2)} \\ Q_F^{(2)} &= \sum_{jj'} Q_{jj'}\ (u_j u_{j'} - v_j v_{j'})\ (a_j^\dagger \tilde{a}_{j'})^{(2)} \\ &- \sqrt{\frac{10}{N}} \sum_{jj'j''} Q_{jj'} (u_j v_{j'} + v_j u_{j'}) \beta_{j''j} [(d^\dagger \tilde{a}_{j''})^{(j)} (\tilde{s} a_{j'}^\dagger)^{(j')}]^{(2)} (\hat{j} K_\beta)^{-1} \end{aligned}$$

The boson-fermion interaction can be generated by the interaction between like particles or by the proton-neutron quadrupole interaction. The structure of the interactions is identical. The product of $Q_B^{(2)}$ and $Q_F^{(2)}$ contributes to the boson-fermion interaction. By maping the basis from IBM-2 onto IBM-1 and taking terms up to the second order in d-boson operators the standard form of the boson-fermion interaction is obtained.

The IBFM-1 Hamiltonian for an odd-even nucleus

$$H = H_B + H_F + V_{BF}$$

H_B is the boson Hamiltonian of IBM-1 describing a system of N interacting bosons (correlated S and D pairs) that approximate the valence nucleon pairs:

$$\begin{aligned} H_B &= \varepsilon\, \hat{N} + \frac{1}{2}\, v_0 \left([d^\dagger \times d^\dagger]_{(0)} \times [\tilde{s} \times \tilde{s}]_{(0)} + h.c. \right)_{(0)} \\ &+ \frac{1}{\sqrt{2}}\, v_2 \left([d^\dagger \times d^\dagger]_{(2)} \times [\tilde{d} \times \tilde{s}]_{(2)} + h.c. \right)_{(0)} \\ &+ \sum_{L=0,2,4} \frac{1}{2}\, C_L \sqrt{2L+1} \left([d^\dagger \times d^\dagger]_{(L)} \times [\tilde{d} \times \tilde{d}]_{(L)} \right)_{(0)} \end{aligned}$$

$$n_s = N - n_d$$

H_F is the fermion Hamiltonian containing quasiparticle energies of odd protons or neutrons. The quasiparticle energies and occupation probabilities contained in the fermion Hamiltonian, and other terms, are obtained in a BCS calculation with some standard set of single fermion energies.

$$H_F = \sum_i \varepsilon_i\, a_i^\dagger \tilde{a}_i$$

V_{BF} is the IBFM-1 boson-fermion interaction containing the dynamical, exchange and monopole term.

- The dynamical interaction V_{DYN} represents the direct component of the quadrupole interaction between the odd particle and the bosons.
- The exchange interaction V_{EXC} is due to the two-particle nature of the bosons, bringing the Pauli exclusion principle into play.
- The monopole interaction V_{MON} can result from a variety of causes, in particular from the blocking of certain degrees of freedom by the odd particle.

$$V_{BF} \;=\; V_{DYN} + V_{EXC} + V_{MON}$$

$$V_{DYN} \;=\; \Gamma_0 \sum_{j_1 j_2} \sqrt{5}\,(u_{j_1}u_{j_2} - v_{j_1}v_{j_2})\,\langle j_1 \parallel Y_2 \parallel j_2\rangle\,\left([a^\dagger_{j_1} \times \tilde{a}_{j_2}]^{(2)} \times Q_B^{(2)}\right)^{(0)}$$

$Q_B^{(2)}$ is the standard boson quadrupole operator

$$Q_B^{(2)} = [s^\dagger \times \tilde{d} + d^\dagger \times \tilde{s}]^{(2)} + \chi[d^\dagger \times \tilde{d}]^{(2)}$$

$$V_{EXC} \;=\; \Lambda_0 \sum_{j_1 j_2 j_3} (-2)\,\sqrt{\frac{5}{2j_3+1}}\,(u_{j_1}v_{j_3} + v_{j_1}u_{j_3})\;\;(u_{j_2}v_{j_3} + v_{j_2}u_{j_3})$$
$$\langle j_3 \parallel Y_2 \parallel j_1\rangle\,\langle j_3 \parallel Y_2 \parallel j_2\rangle\;:\left([a^\dagger_{j_1} \times \tilde{d}\,]_{j_3} \times [\tilde{a}_{j_2} \times d^\dagger\,]_{j_3}\right)^{(0)}:$$

$$V_{MON} \;=\; A_0 \sum_j \sqrt{5}\,(2j+1)\,\left([a^\dagger_j \times \tilde{a}_j]^{(0)} \times [d^\dagger \times \tilde{d}]^{(0)}\right)^{(0)}$$

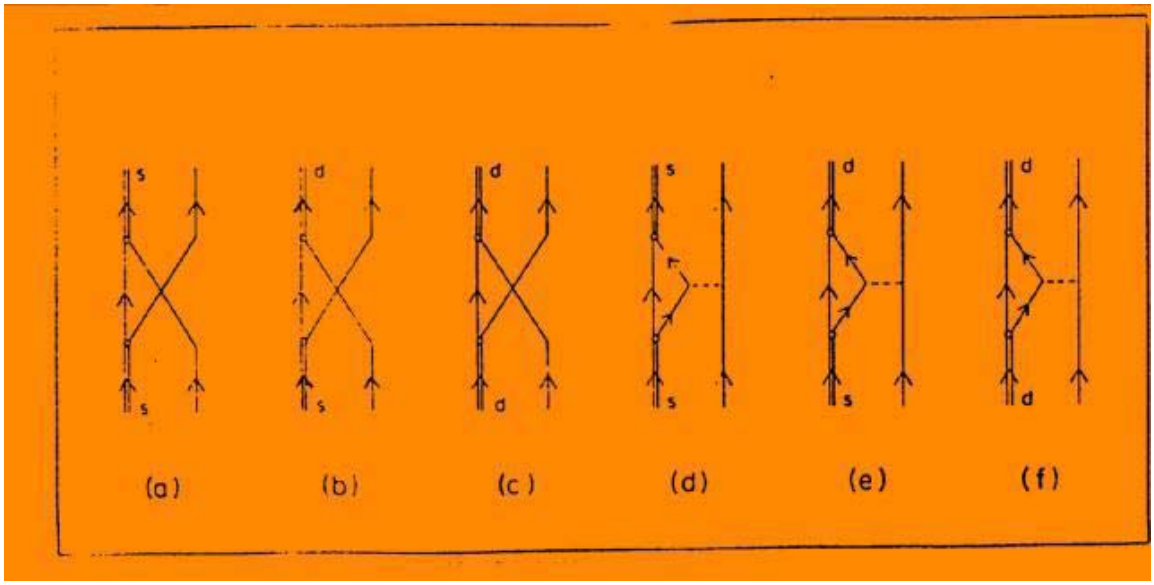

(a), (b), (c) exchange terms
(d), (e), (f) direct terms

The structure coefficients:

- The coefficients v_j are related to the structure coefficients of the fermion S-pair state, which is the microscopic equivalent of the s boson. In practice, they are the occupation probabilities of the single-particle orbits, as follows from a spherical BCS calculation.

- The coefficients $\beta_{j_a j_b} = (u_{j_a} v_{j_b} + v_{j_a} u_{j_b}) \langle j_a \parallel Y_2 \parallel j_b \rangle$ are the structure coefficients of the d boson.

The electromagnetic operators have the form:

$$M(E2) = M_B(E2) + M_F(E2)$$

$$M_B(E2) = \frac{3}{4\pi} R_0^2 \, e^{VIB} \left([s^\dagger \times \tilde{d} + d^\dagger \times \tilde{s}]^{(2)} + \chi [d^\dagger \times \tilde{d}]^{(2)} \right)$$

$$R_0^2 = 0.0144 \; A^{\frac{2}{3}} \qquad barn$$

$$M_F(E2) = \frac{3}{5} R_0^2 \, e_F \, Y_2$$

Common notation:

$$\frac{3}{4\pi} R_0^2 \, e^{VIB} = e_B$$

$$\vec{M}(M1) \;=\; \vec{M}_B(M1) + \vec{M}_F(M1)$$

$$\vec{M}_B(M1) \;=\; \sqrt{\frac{3}{4\pi}}\,\sqrt{10}\,g_R\,[d^\dagger \times \tilde{d}]^{(1)}$$

$$\vec{M}_F(M1) \;=\; \sqrt{\frac{3}{4\pi}}\,[\,g_l\,\vec{l} \;+\; g_s\,\vec{s} \;+\; g_T\,(Y_2 \;\times\; \vec{s}\,)_1\,]$$

Common notations:

$$\sqrt{\frac{3}{4\pi}}\,g_R \;=\; g_B$$

IBFM (and its extensions) provide a consistent description of nuclear structure phenomena in:

- spherical nuclei
- deformed nuclei
- transitional nuclei

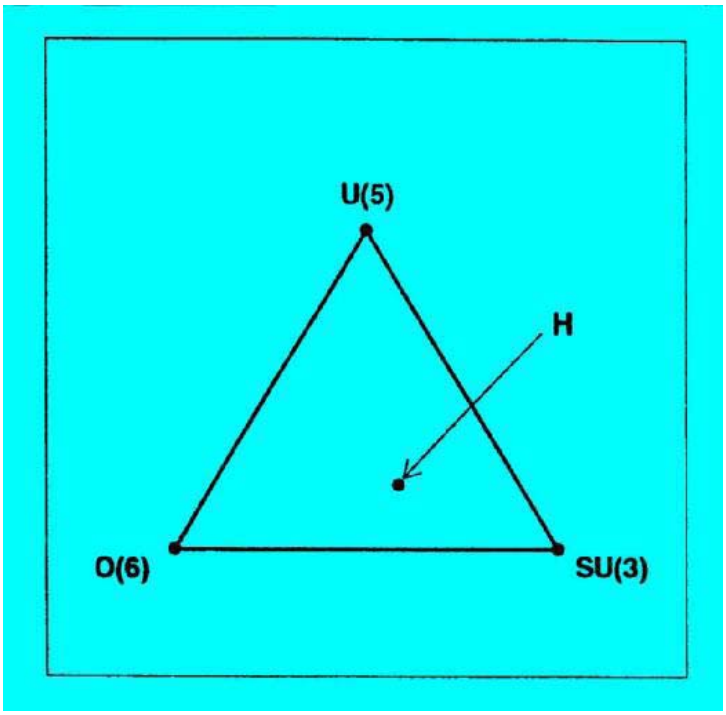

Spherical nuclei

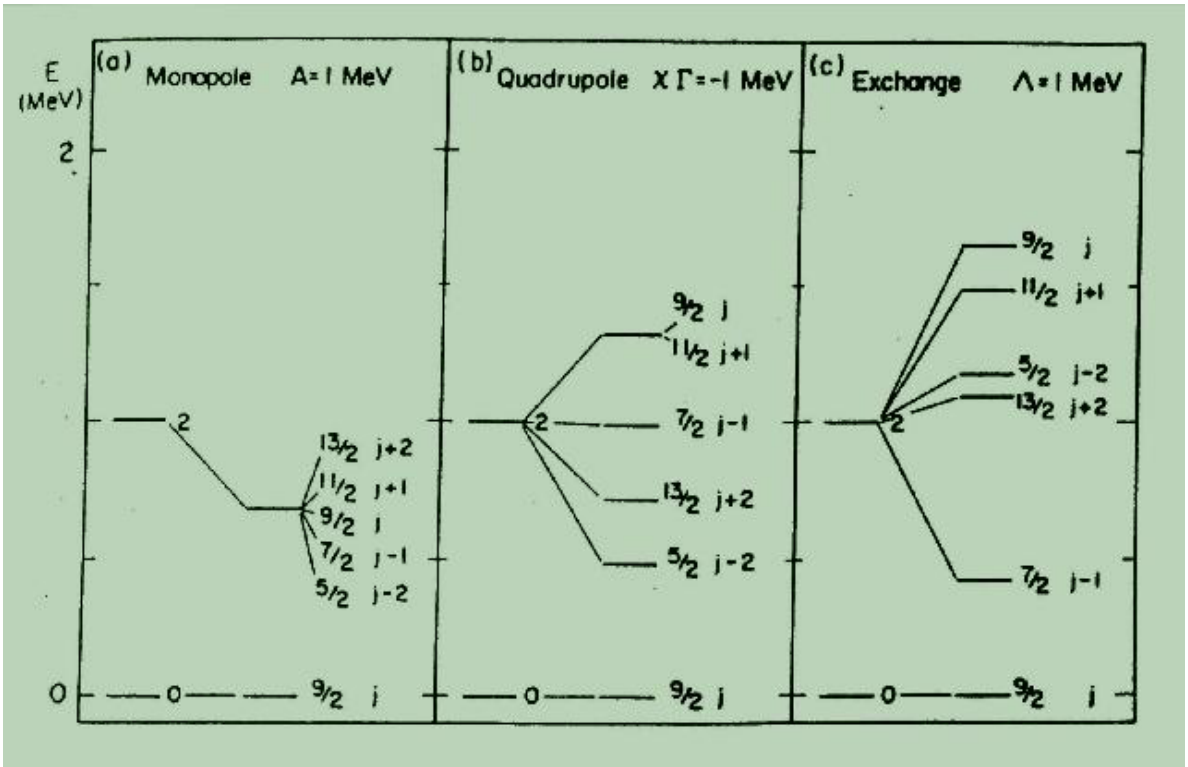

Scholten

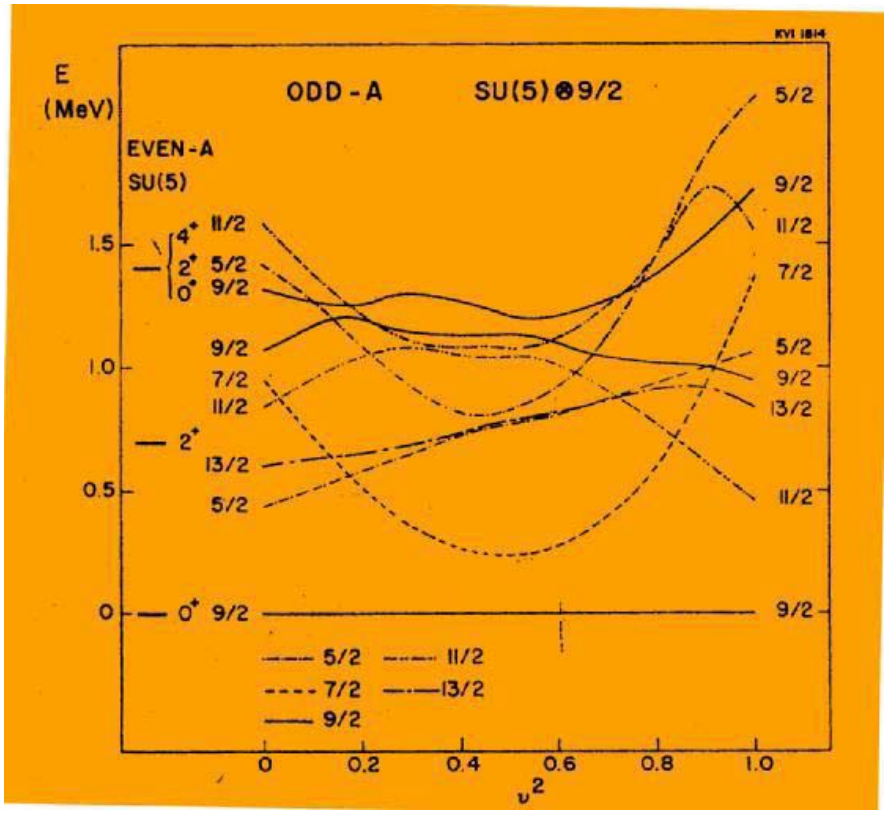

Scholten

Deformed nuclei

j = 9/2 Iachello, PRL 43

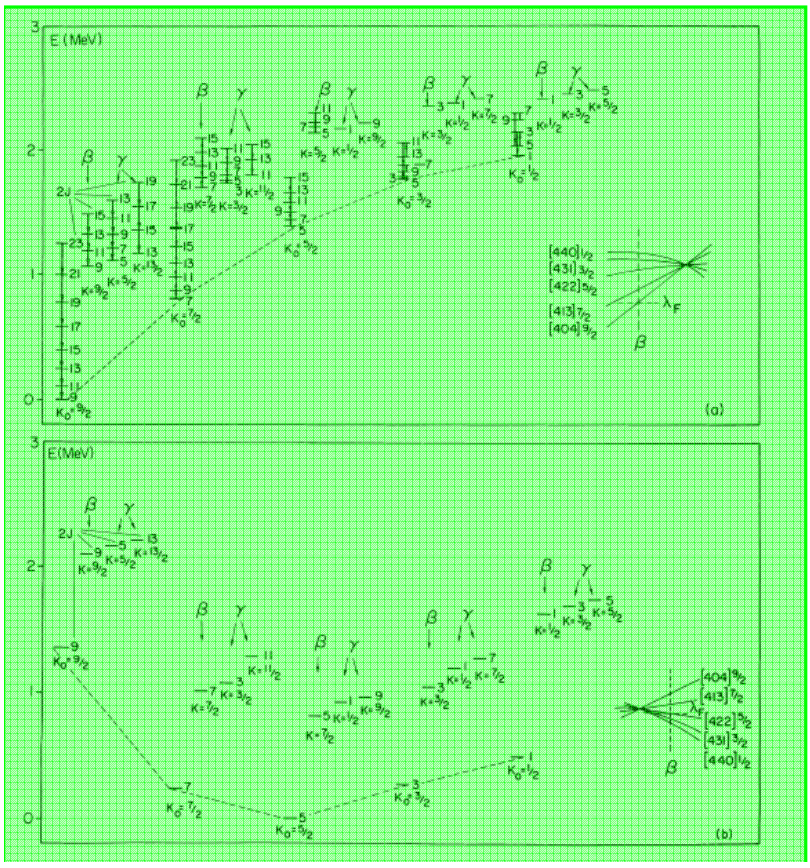

Λ = 0

The levels are arranged into bands denoted by the lowest value of the angular momentum K, contained in the band.

This quantum number is only approximately equivalent to the quantum number K in the Nilsson model.

In the inset, the corresponding situation in the Nilsson model is shown.

Λ ≠ 0

The IBFM generates bands that are analogous to the bands which can be constructed in the Nilsson model. In addition, it generates bands that could be called β and γ bands. While here they arise automatically, in the Nilsson model they must be either placed ad hoc or calculated by use of other methods.

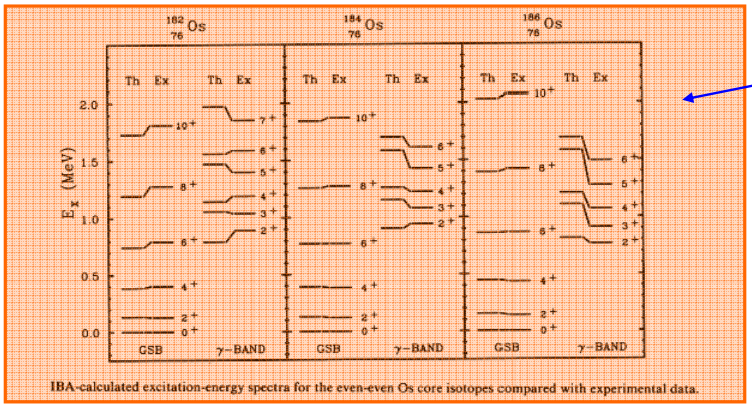

IBA-calculated excitation-energy spectra for the even-even Os core isotopes compared with experimental data.

Prolate

Scholten, PRC 37

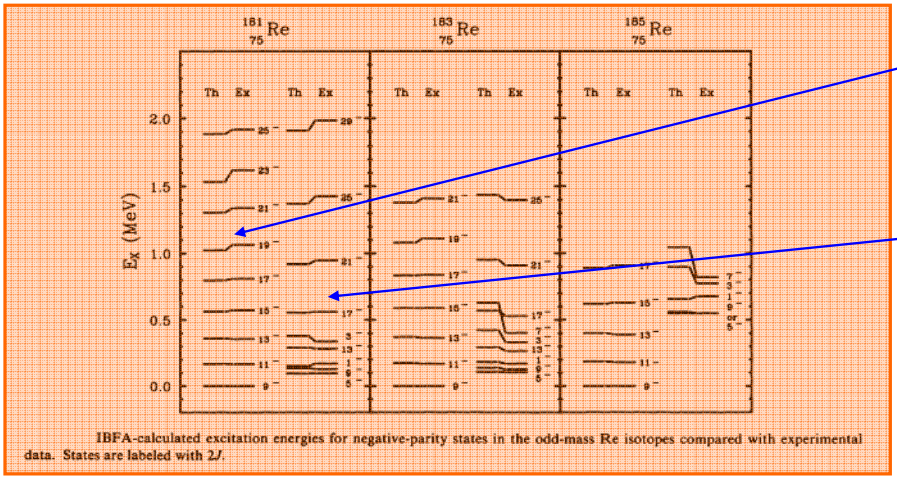

IBFA-calculated excitation energies for negative-parity states in the odd-mass Re isotopes compared with experimental data. States are labeled with $2J$.

$K^\pi = 9/2^-$
$(\pi\, h_{11/2})$

$v^2 = 0.62$

$K^\pi = 1/2^-$
$(\pi\, h_{9/2})$

$V^2 = 0.05$

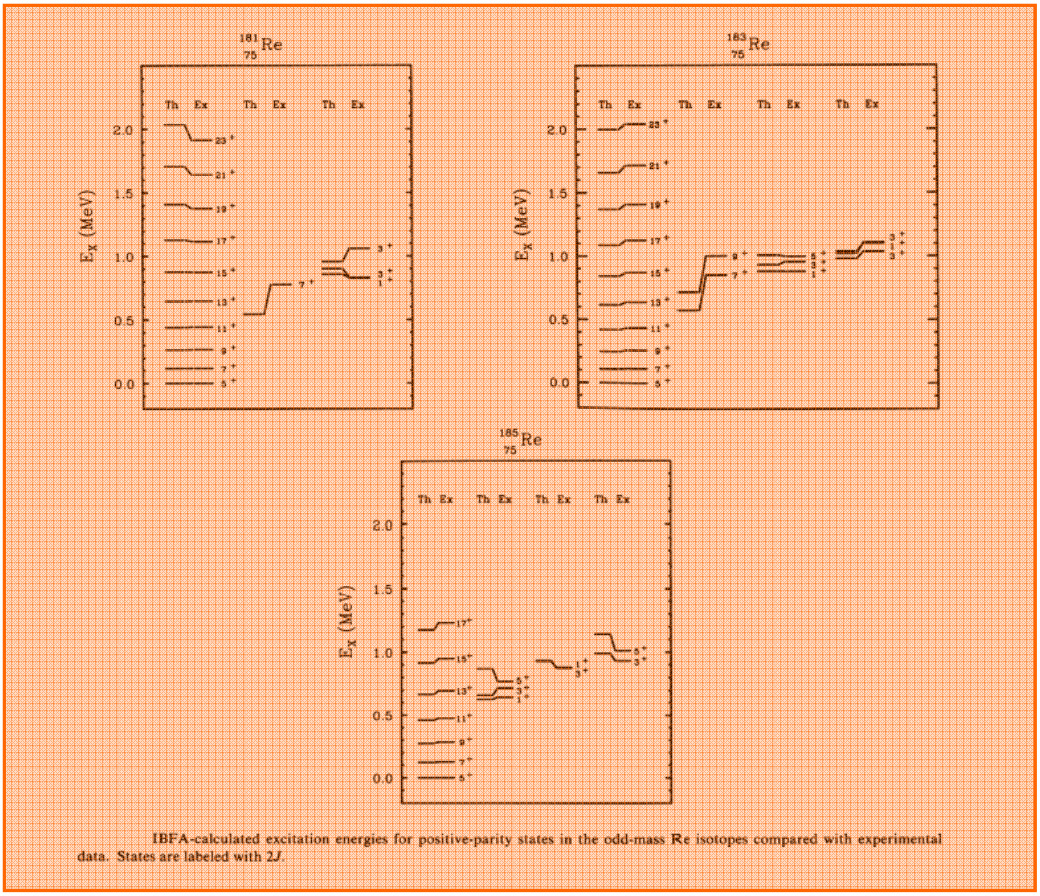

IBFA-calculated excitation energies for positive-parity states in the odd-mass Re isotopes compared with experimental data. States are labeled with $2J$.

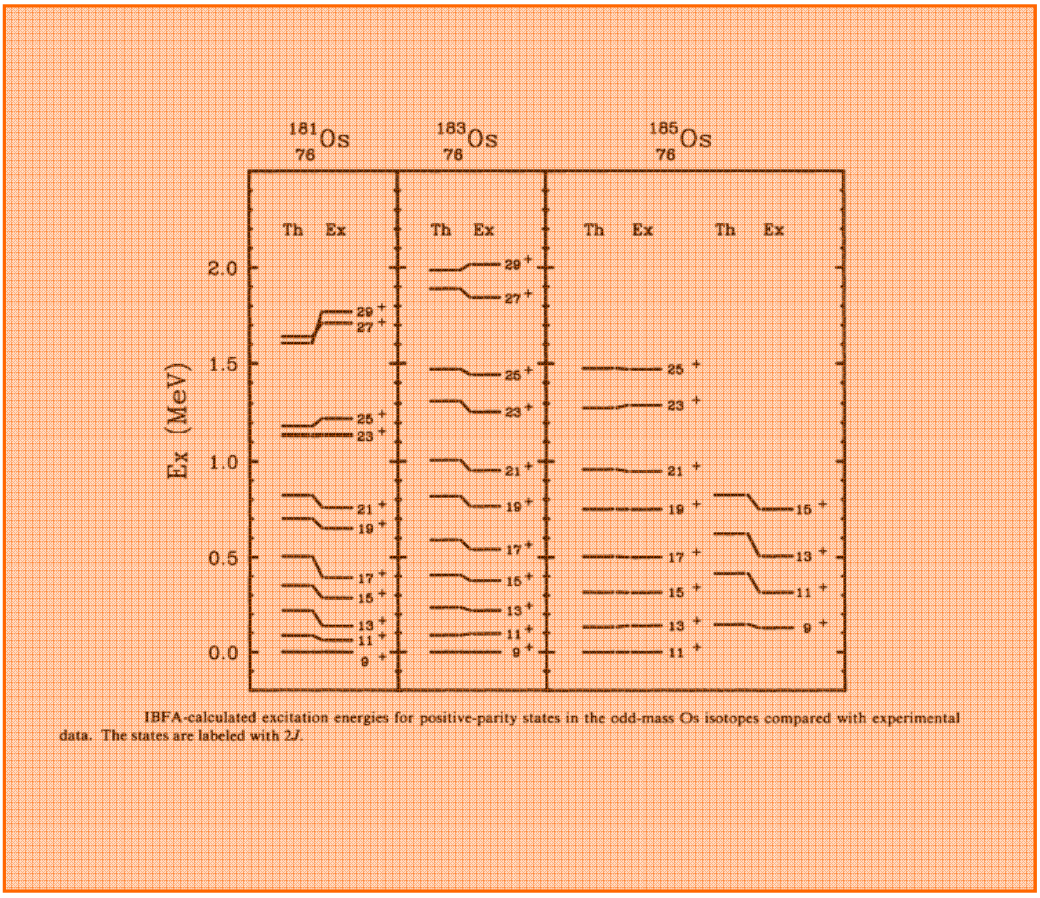

IBFA-calculated excitation energies for positive-parity states in the odd-mass Os isotopes compared with experimental data. The states are labeled with $2J$.

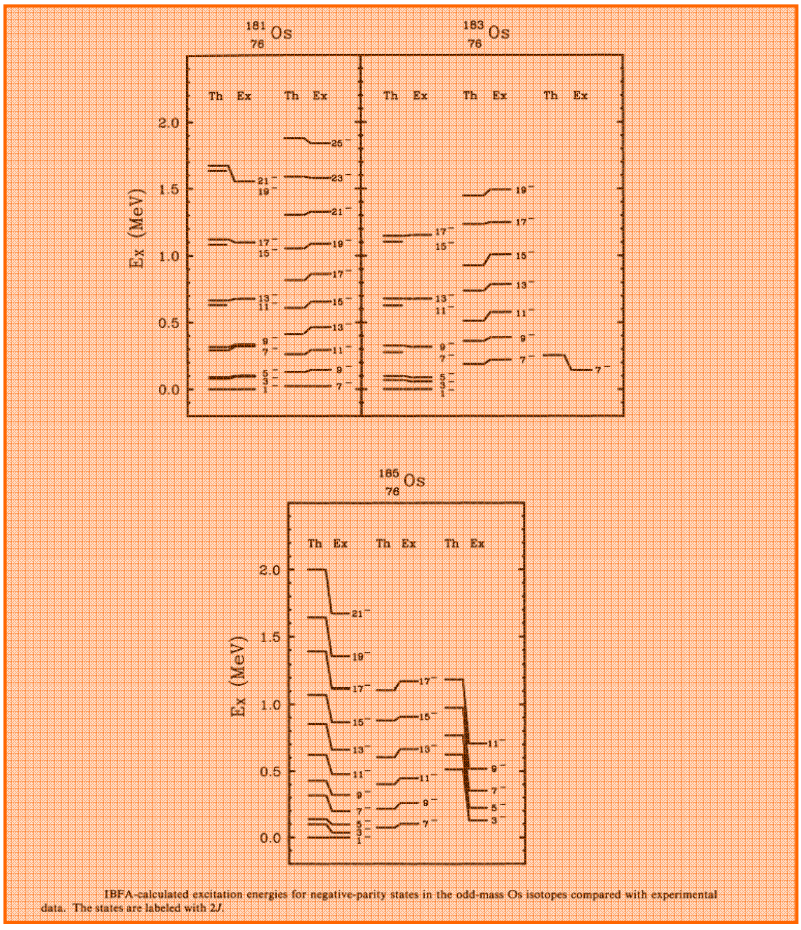

IBFA-calculated excitation energies for negative-parity states in the odd-mass Os isotopes compared with experimental data. The states are labeled with $2J$.

The IBFM states for odd-A Re and Os nuclei are obtained in multi-j calculations.

The choice of the model space has a strong influence on the model parameters. Even if there is a large separation between shells, the mixing due to the strong core-particle quadrupole interaction does not allow for restricting the model space to a single j shell. For example: Levels based on the $g_{9/2}$ particle. Here the $d_{5/2}$ particle from the next major shell has to be included due to the large non-spinflip matrix element $\langle d_{5/2} \parallel Y_2 \parallel g_{9/2} \rangle$. The same situation appears in the case of $h_{11/2}$ ($f_{7/2}$ has to be included in the model space). Restricting the model space requires a renormalization of the interactions. For unique-parity states:

- Strengths of boson-fermion interactions obtained in a single j calculation are effective strengths
- Strengths of boson-fermion interactions obtained in a multi j calculation are real strengths

Intruder deformed bands in odd Ag isotopes

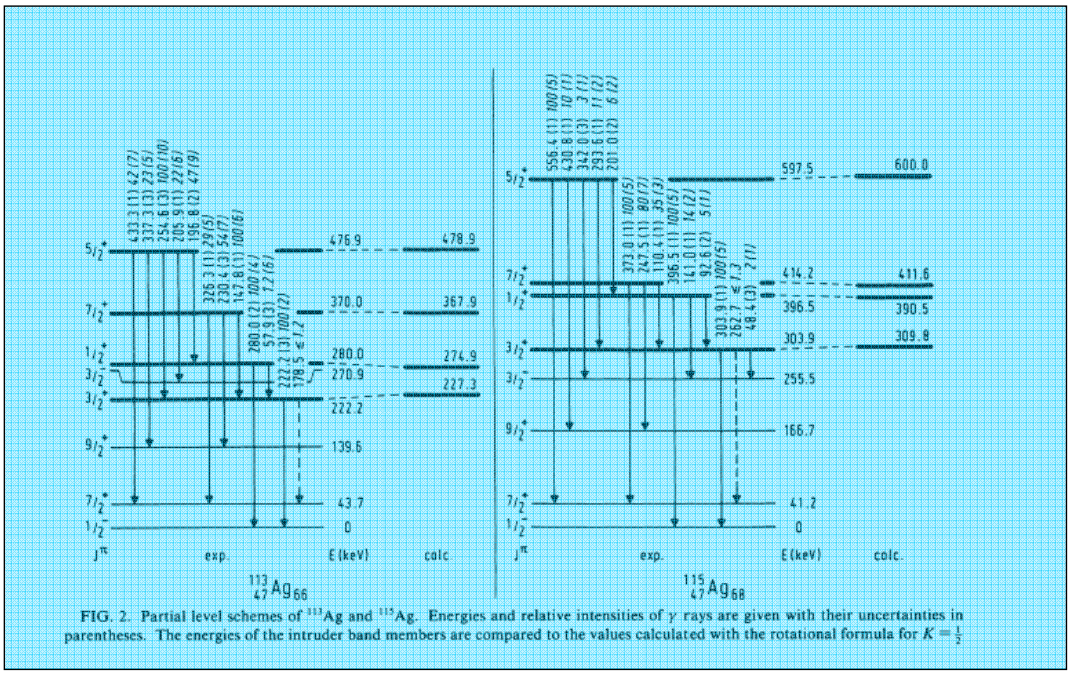

FIG. 2. Partial level schemes of ^{113}Ag and ^{115}Ag. Energies and relative intensities of γ rays are given with their uncertainties in parentheses. The energies of the intruder band members are compared to the values calculated with the rotational formula for $K = \frac{1}{2}$.

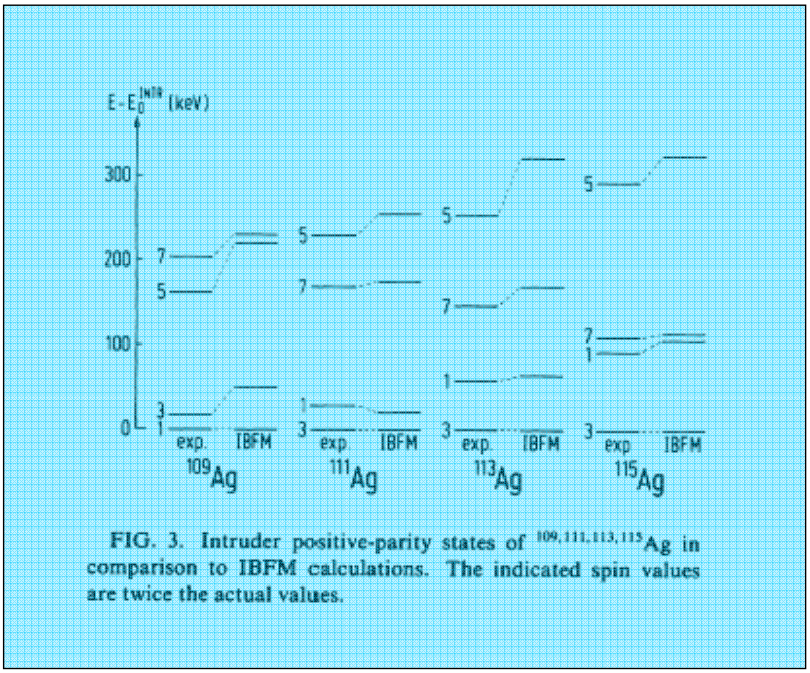

FIG. 3. Intruder positive-parity states of ^{109,111,113,115}Ag in comparison to IBFM calculations. The indicated spin values are twice the actual values.

Only the monopole fermion-boson interaction strength is slightly changed from isotope to isotope. All other interaction strengths and occupation probabilities are the same for all isotopes.

O(6) nuclei

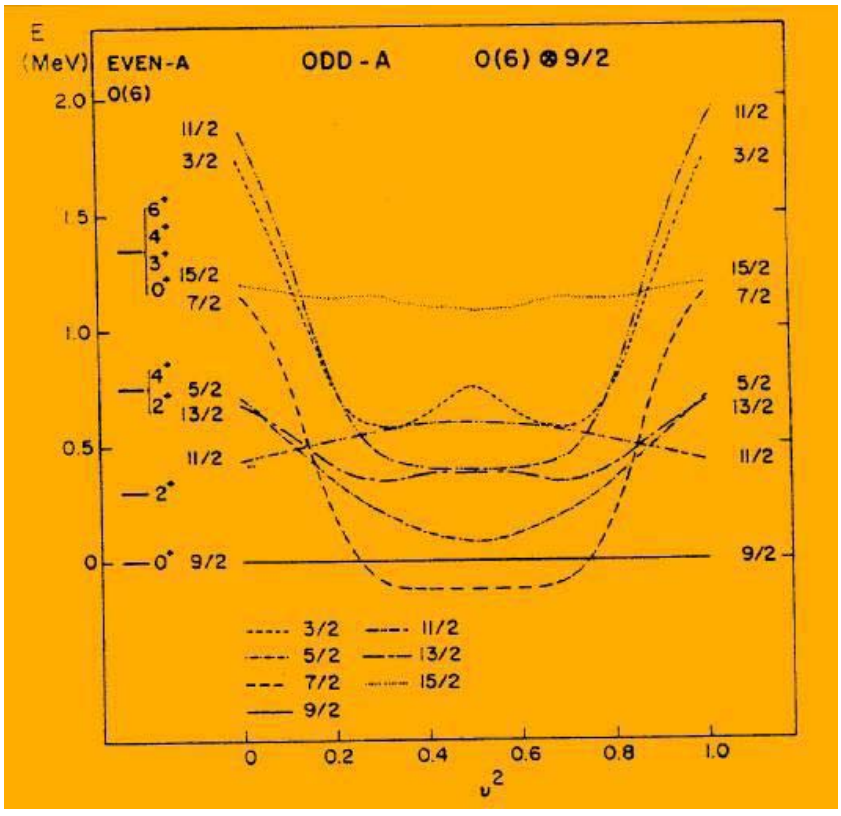

Scholten

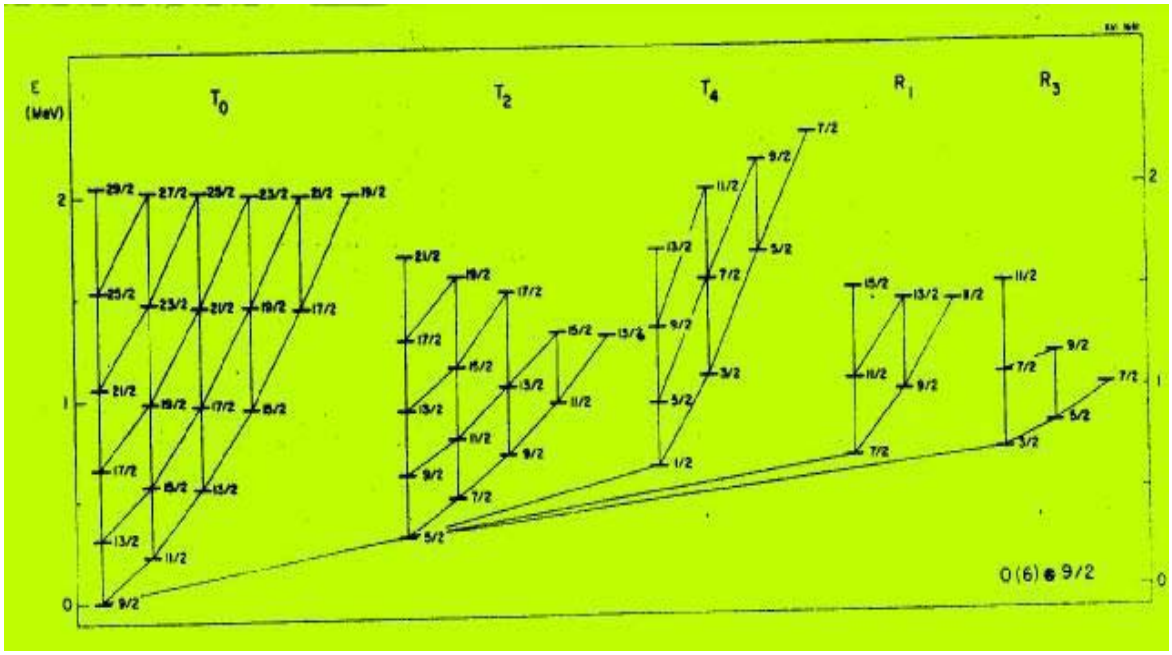

Scholten

Transitional nuclei

^{71}Ge

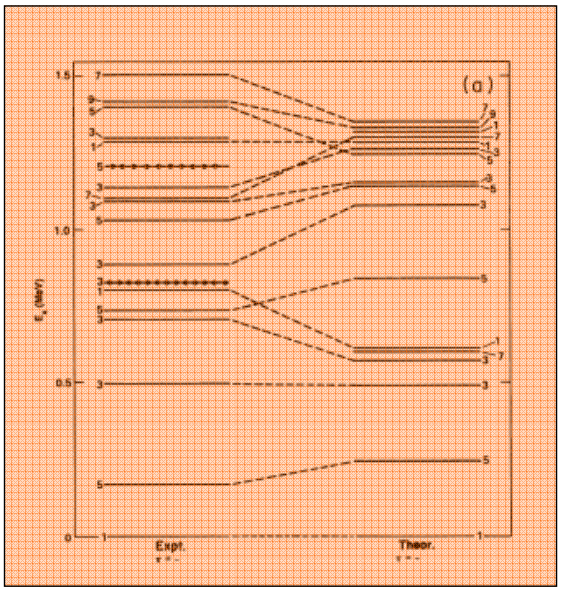

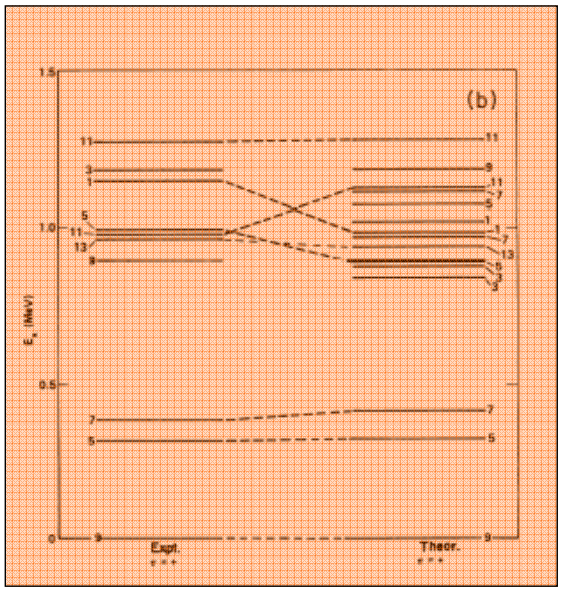

Negative parity levels Positive parity levels

Angular momentum x 2

^{105}Pd

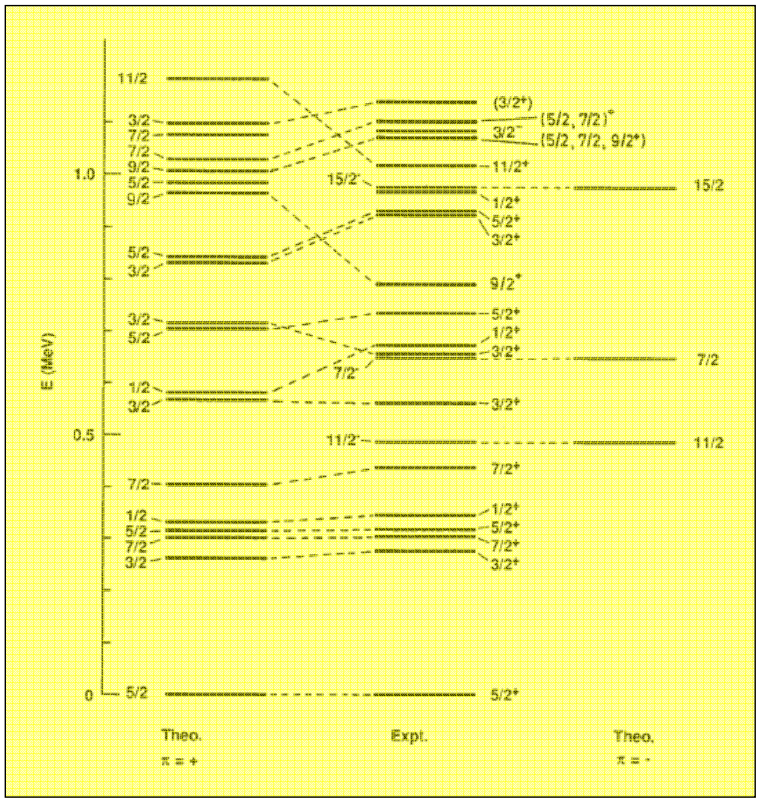

J of Level		I_γ	
From	To	Expt.	Theor.
$3/2_1^+$	$5/2_1^+$	100	100
$7/2_1^+$	$3/2_1^+$		0.0005
	$5/2_1^+$	100	100
$5/2_2^+$	$7/2_1^+$		0.0002
	$3/2_1^+$	0.12	0.7
	$5/2_1^+$	100	100
$1/2_1^+$	$5/2_2^+$		0
	$3/2_1^+$	27	93
	$5/2_1^+$	100	100
$7/2_2^+$	$5/2_2^+$		2
	$7/2_1^+$		0.0006
	$3/2_1^+$		0.03
	$5/2_1^+$	100	100
$3/2_2^+$	$7/2_2^+$		0.0005
	$1/2_1^+$	2.4	1
	$5/2_2^+$		2
	$7/2_1^+$		0.005
	$3/2_1^+$		0.4
	$5/2_1^+$	100	100
$3/2_3^+$	$3/2_2^+$	0.8	0.4
	$7/2_2^+$		0.08

Halflives

J	Expt. [a]	Theor.
$3/2_1^+$	0.067 ns	0.03 ns
$5/2_2^+$	0.04 ns	0.1 ns
$7/2_2^+$	3.8 ps	7.7 ps
$1/2_1^+$	0.88 ns	0.22 ns
$3/2_2^+$	1.9 ps	6.3 ps
$1/2_2^+$	>2 ps	1.6 ps

BOSON-FERMION SYMMETRIES
SUPERSYMMETRIES

If the Hamiltonian can be expressed in terms of Casimir invariants of the chain of subgroups, the energy spectrum can be obtained ANALYTICALLY. Other observables (B(E2), B(M1), static moments, spectroscopic factors, ...) can be expressed in analytical form, too.

The symmetry group related to IBM-1 is $U(6)$. The six dimensions are formed by the s boson and five components of d_μ boson. Since the number of bosons is invariant, the group is unitary. There are three chains of subgroups:

$$\begin{array}{lrll} U(6) & \supset & U(5) \supset O(5) \supset O(3) \supset O(2) & \textit{vibrational limit} \\ U(6) & \supset & SU(3) \quad\quad \supset O(3) \supset O(2) & \textit{rotational limit} \\ U(6) & \supset & O(6) \supset O(5) \supset O(3) \supset O(2) & \gamma - \textit{soft limit} \end{array}$$

For boson-fermion systems many group chains have been investigated. Example:
A $j = 3/2$ particle coupled to an $O(6)$ core ($j = 3/2$ has four different m-states and therefore forms a representation of the $U(4)$ group).

$$U^B(6) \otimes U^F(4) \supset O^B(6) \otimes U^F(4) \supset Spin(6) \supset Spin(5) \supset Spin(3) \supset Spin(2)$$

$$E = -\frac{A}{4}[\sigma_1(\sigma_1+4) + \sigma_2(\sigma_2+2) + \sigma_3^2] + \frac{B}{6}[\tau_1(\tau_1+3) + \tau_2(\tau_2+1)] + CJ(J+1) + D\Sigma(\Sigma+4)$$

$$\begin{array}{rll} U^B(6) & \textit{quantum numbers} & [N] \\ U^F(4) & \textit{quantum numbers} & \{M\} \\ O^B(6) & \textit{quantum numbers} & \Sigma \\ Spin(6) & \textit{quantum numbers} & (\sigma_1, \sigma_2, \sigma_3) \\ Spin(5) & \textit{quantum numbers} & (\tau_1, \tau_2) \\ Spin(3) & \textit{quantum numbers} & J \\ Spin(2) & \textit{quantum numbers} & M_J \end{array}$$

$O^B(6) \otimes U^F(4) \supset Spin(6) \longrightarrow$ Parameters describing the boson system are in a unique relation to the parameters describing the boson-fermion system.

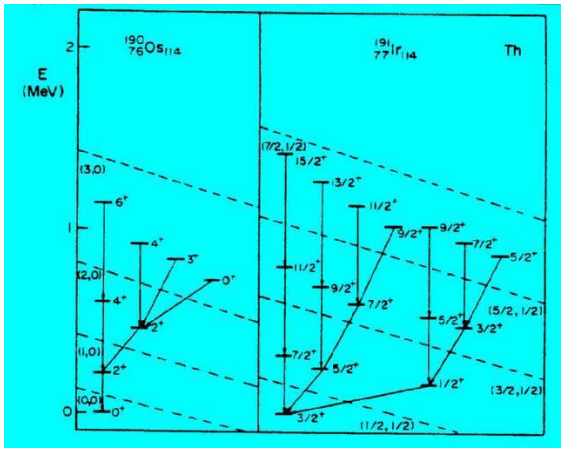

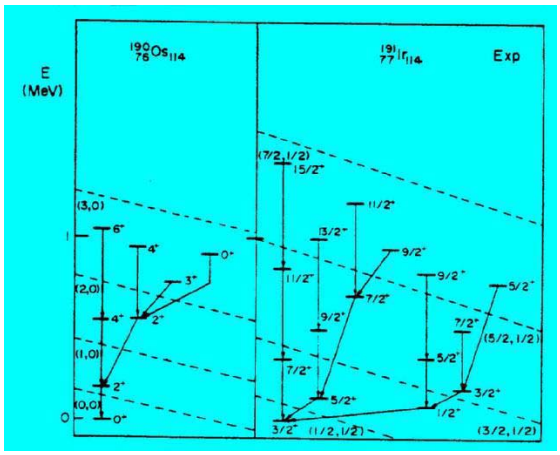

Problems:

- The symmetry approach to boson-fermion systems is more phenomenological in nature
- It can be applyed only in special cases when one or few fermion configurations are coupled to boson cores in one of the symmetry limits of IBM

Advantages:

- This approach was extended to boson-fermion-fermion systems (odd-odd nuclei)
- The spectra of neighboring even-even, odd-even and odd-odd nuclei can be described with the same set of parameters
- Analytical expressions are available
- Evidence that collective and single-particle degrees of freedom are closely related

2.

High spin states in the interacting boson and interacting boson-fermion model

Interacting Boson Model (IBM-1) based models constructed to describe the physics of high-spin states in nuclei ($10\ \hbar \leq J \leq 30\ \hbar$)**:**

- **Interacting boson plus broken pairs model (IBBPM) for even-even nuclei**
- **Interacting boson fermion plus broken pairs model (IBFBPM) for odd-even nuclei**

In the formulation of these models one has to go beyond the boson approximation and include selected non-collective fermion degrees of freedom. By including part of the original shell-model fermion space through successive breaking of correlated S and D pairs, the IBM can describe the structure of high-spin states.

The models are based on the IBM-1; the boson space consists of s and d bosons, with no distinction between protons and neutrons. To generate high-spin states, the models allow one or two bosons to be destroyed and to form non-collective fermion pairs, represented by two- and four-quasiparticle states which recouple to the boson core. High-spin states are described in terms of broken pairs.

Advantages of using models based on the IBM over more traditional approaches based on the cranking approximations:

- No assumption has to be made about the geometrical picture of high-spin bands
- The bands result from a consistent calculation of the complete excitation spectrum, which includes also the ground state band
- Polarization effects directly result from the model fermion-boson interactions
- All calculations are performed in the laboratory frame, and therefore the results can be directly compared with experimental data
- This extension of the model is especially relevant for transitional regions, where single-particle excitations and vibrational collectivity are dominant modes, and the traditional cranking approach to high-spin physics is not adequate

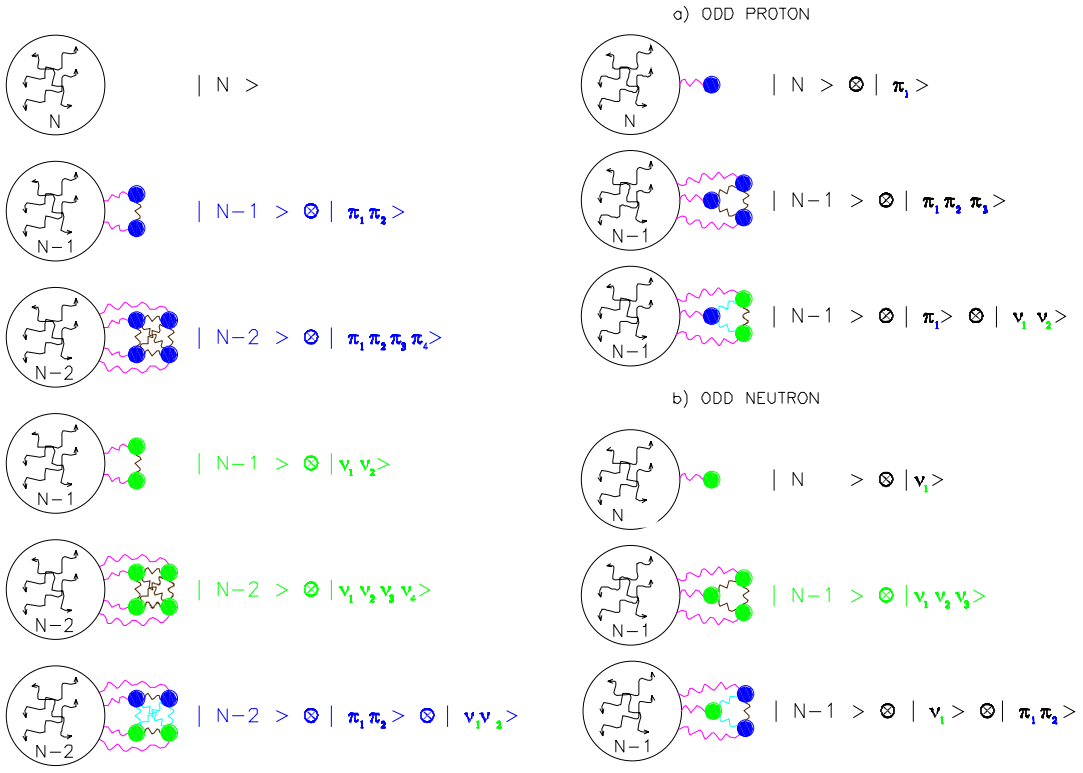

The model space for an even-even nucleus with $2N$ valence nucleons is

$$| \ N \ bosons \ > \oplus | \ (N-1) \ bosons \otimes 1 \ broken \ pair > \oplus | \ (N-2) \ bosons \otimes 2 \ broken \ pairs >$$

This means that the fermion basis can contain two-proton, two-neutron, four-proton, four-neutron and two-proton-two-neutron configurations.

For odd-A nuclei, two-broken pair configurations are not included in the model space. They would generate five-quasiparticle configurations resulting in exhaustive numerical calculations. The IBFBPM can describe one- and three-fermion structures. The two fermions in a broken pair can be of the same type as the unpaired fermion, resulting in a space with three identical fermions. If the fermions in the broken pair are different from the unpaired fermion, the fermion basis contains two protons and one neutron or vice versa.

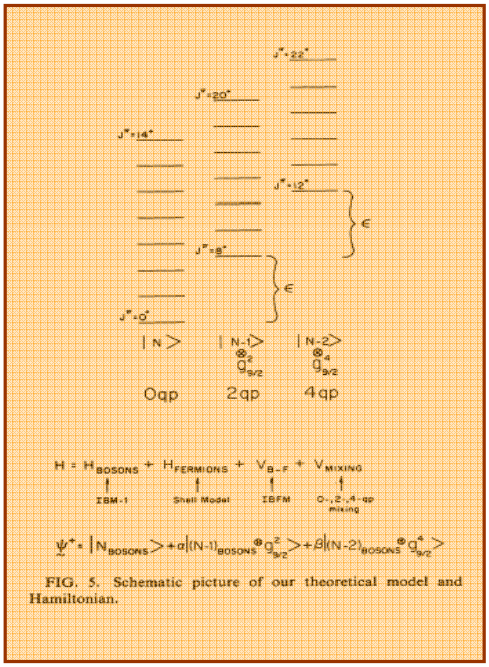

FIG. 5. Schematic picture of our theoretical model and Hamiltonian.

The Interacting boson plus broken pairs model (IBBPM) Hamiltonian for an even-even nucleus:

$$H \ = \ H_B + H_{\nu F} + H_{\pi F} + V_{\nu BF} + V_{\pi BF} + V_{\nu}^{mix} + V_{\pi}^{mix} + V_{\nu\pi}$$

The label π stands for protons and ν for neutrons. If broken pairs contain both protons and neutrons, the full model Hamiltonian is used. Otherwise, when broken pairs contain only protons ($\alpha = \pi$) or neutrons ($\alpha = \nu$), the model Hamiltonian is reduced to:

$$H \ = \ H_B + H_{\alpha F} + V_{\alpha BF} + V_{\alpha}^{mix}$$

In description of high-spin states in odd-even nuclei we employ the Interacting boson fermion plus broken pairs model (IBFBPM).

- When the two fermions in a broken pair are of the same type as the unpaired fermion, the reduced Hamiltonian is used, where α labels the type of fermion (proton or neutron).
- If the fermions in the broken pair are different from the unpaired fermion, the full Hamiltonian is used, without the pair breaking interaction of the unpaired fermion and with the fermion Hamiltonian of the unpaired fermion containing only single-fermion energies.

H_B is the boson Hamiltonian of IBM-1 describing a system of N interacting bosons (correlated S and D pairs) that approximate the valence nucleon pairs:

$$
\begin{aligned}
H_B &= \varepsilon\, \hat{N} + \frac{1}{2}\, v_0\, \left([d^\dagger \times d^\dagger]_{(0)} \times [\tilde{s} \times \tilde{s}]_{(0)} + h.c.\right)_{(0)} \\
&+ \frac{1}{\sqrt{2}}\, v_2\, \left([d^\dagger \times d^\dagger]_{(2)} \times [\tilde{d} \times \tilde{s}]_{(2)} + h.c.\right)_{(0)} \\
&+ \sum_{L=0,2,4} \frac{1}{2}\, C_L\, \sqrt{2L+1}\, \left([d^\dagger \times d^\dagger]_{(L)} \times [\tilde{d} \times \tilde{d}]_{(L)}\right)_{(0)}
\end{aligned}
$$

$$n_s = N - n_d$$

$H_{\alpha F}$ is the fermion Hamiltonian which contains single-fermion (quasiparticle) energies and fermion-fermion interactions. The quasiparticle energies and occupation probabilities contained in the fermion Hamiltonian and other terms, are obtained in a BCS calculation with some standard set of single fermion energies.

$$H_{\alpha F} = \sum_i \varepsilon_{\alpha_i}\, a^\dagger_{\alpha_i} \tilde{a}_{\alpha_i} + \frac{1}{4} \sum_{abcd} \sum_{JM} V^J_{\alpha abcd}\, A^\dagger_{JM}(\alpha_a \alpha_b)\, A_{JM}(\alpha_c \alpha_d)$$

$$A^\dagger_{JM}(\alpha_a \alpha_b) = \frac{1}{\sqrt{1+\delta_{ab}}}\, [a^\dagger_{\alpha_a}\, a^\dagger_{\alpha_b}]^M_J$$

$$V^J_{\alpha abcd} = (u_{\alpha_a} u_{\alpha_b} u_{\alpha_c} u_{\alpha_d} + v_{\alpha_a} v_{\alpha_b} v_{\alpha_c} v_{\alpha_d})\, G(\alpha_a \alpha_b \alpha_c \alpha_d J) + 4\, v_{\alpha_a} u_{\alpha_b} v_{\alpha_c} u_{\alpha_d}\, F(\alpha_a \alpha_b \alpha_c \alpha_d J)$$

$V_{\alpha BF}$ is the interaction between the unpaired fermions and the boson core containing the dynamical, exchange and monopole interactions of the IBFM-1:

$$V_{\alpha BF} = V_{\alpha DYN} + V_{\alpha EXC} + V_{\alpha MON}$$

$$V_{\alpha DYN} = \Gamma_0 \sum_{\alpha j_1 \alpha j_2} \sqrt{5}\,(u_{\alpha j_1}u_{\alpha j_2} - v_{\alpha j_1}v_{\alpha j_2})\,\langle \alpha j_1 \parallel Y_2 \parallel \alpha j_2\rangle \left([a^\dagger_{\alpha j_1} \times \tilde{a}_{\alpha j_2}]^{(2)} \times Q_B^{(2)}\right)^{(0)}$$

$Q_B^{(2)}$ is the standard boson quadrupole operator

$$Q_B^{(2)} = [s^\dagger \times \tilde{d} + d^\dagger \times \tilde{s}]^{(2)} + \chi[d^\dagger \times \tilde{d}]^{(2)}$$

$$V_{\alpha EXC} = \Lambda_0 \sum_{\alpha j_1 \alpha j_2 \alpha j_3} (-2)\sqrt{\frac{5}{2\,\alpha j_3 + 1}}\,(u_{\alpha j_1}v_{\alpha j_3} + v_{\alpha j_1}u_{\alpha j_3})\;(u_{\alpha j_2}v_{\alpha j_3} + v_{\alpha j_2}u_{\alpha j_3})$$
$$\langle \alpha j_3 \parallel Y_2 \parallel \alpha j_1\rangle\,\langle \alpha j_3 \parallel Y_2 \parallel \alpha j_2\rangle\;:\left([a^\dagger_{\alpha j_1} \times \tilde{d}\,]_{\alpha j_3} \times [\tilde{a}_{\alpha j_2} \times d^\dagger\,]_{\alpha j_3}\right)^{(0)}:$$

$$V_{\alpha MON} = A_0 \sum_{\alpha j} \sqrt{5}\,(2\alpha j + 1)\,\left([a^\dagger_{\alpha j} \times \tilde{a}_{\alpha j}]^{(0)} \times [d^\dagger \times \tilde{d}]^{(0)}\right)^{(0)}$$

The pair breaking interaction V_α^{mix} which mixes states with different number of fermions, conserving the total nucleon number only:

$$V_\alpha^{mix} = -U_0\left\{\sum_{\alpha j_1 \alpha j_2} u_{\alpha j_1}u_{\alpha j_2}(u_{\alpha j_1}v_{\alpha j_2} + u_{\alpha j_2}v_{\alpha j_1})\langle \alpha j_1 \parallel Y_2 \parallel \alpha j_2\rangle^2 \frac{1}{\sqrt{2\,\alpha j_2 + 1}}\left([a^\dagger_{\alpha j_2} \times a^\dagger_{\alpha j_2}]^{(0)} \cdot \tilde{s}\right) + hc\right\}$$
$$-U_2\left\{\sum_{\alpha j_1 \alpha j_2} (u_{\alpha j_1}v_{\alpha j_2} + u_{\alpha j_2}v_{\alpha j_1})\langle \alpha j_1 \parallel Y_2 \parallel \alpha j_2\rangle\left([a^\dagger_{\alpha j_1} \times a^\dagger_{\alpha j_2}]^{(2)} \cdot \tilde{d}\right) + hc\right\}$$

The proton-neutron interaction is:

$$V_{\nu\pi} = \sum_{\nu\nu'\pi\pi'} \sum_J h_J(\nu\nu'\pi\pi')(u_\nu u_{\nu'} - v_\nu v_{\nu'})(u_\pi u_{\pi'} - v_\pi v_{\pi'})\left(\left[a^\dagger_\nu \times \tilde{a}_{\nu'}\right]^{(J)} \cdot \left[a^\dagger_\pi \times \tilde{a}_{\pi'}\right]^{(J)}\right)$$

The coefficients $h_J(\nu\nu'\pi\pi')$ are connected to the two-body matrix elements of the residual proton-neutron interaction by:

$$h_J(\nu\nu'\pi'\pi) = (-)^{j_\nu + j_\pi} \sum_{J'} (-)^{J'} \sqrt{2J'+1}\,\langle (j_\nu j_\pi)J' \parallel V(1,2) \parallel (j_{\nu'} j_{\pi'})J'\rangle\, W(j_\nu j_\pi j_{\nu'} j_{\pi'}; J'J$$

The residual proton-neutron interaction is usually taken in the form:

$$H_\delta = 4\pi\, V_\delta\, \delta(\vec{r}_\pi - \vec{r}_\nu)\,\delta(r_\pi - R_0)\,\delta(r_\nu - R_0)$$

The strength parameters of the boson-fermion interactions should be those obtained in the analysis of the neighboring nuclei. For example, the boson-fermion strength parameters for the couplings of two and four-proton configurations to the boson core in an even-even nucleus, have to be the same as for coupling of one-proton configurations to the boson core in the neighboring odd-even nucleus. This is the case for spherical, transitional and γ-soft nuclei. However, approaching the rotational SU(3) limit of IBM, the boson-fermion interaction strengths are not identical for an even-even nucleus and its odd-even neighbor. The effective core for configurations based on broken pairs in a deformed nucleus can be somewhat different from the one obtained by a simple decrease of the boson number by one.

$$T(E2)=\frac{3}{4\pi}e^{\text{vib}}R_0^2[(d^\dagger\times\tilde{s}+s^\dagger\times\tilde{d})^{(2)}+\chi(d^\dagger\times\tilde{d})^{(2)}]$$

$$-e\frac{1}{\sqrt{5}}\sum_{j_1j_2}q_{j_1j_2}[(u_{j_1}u_{j_2}-v_{j_1}v_{j_2})(a_{j_1}^\dagger\times\tilde{a}_{j_2})^{(2)}-\frac{u_{j_1}v_{j_2}}{\sqrt{N}}[(a_{j_1}^+\times a_{j_2}^+)^{(2)}\times\tilde{s}]^{(2)}+\frac{u_{j_2}v_{j_1}}{\sqrt{N}}[(\tilde{a}_{j_1}\times\tilde{a}_{j_2})^{(2)}\times s^\dagger]^{(2)}]$$

where

$$q_{j_1j_2}=\langle j_1\|r^2Y_2\|j_2\rangle\ .$$

We take $\langle r^2\rangle=\frac{3}{5}R_0^2$, and $R_0=0.12A^{1/3}\times10^{-12}$ cm. N is the number of bosons.

$$T(M1)=\sqrt{30/4\pi}\,g_R(d^\dagger\times\tilde{d})^{(1)}$$

$$-\frac{1}{\sqrt{4\pi}}\sum_{j_1j_2}[g_1\langle j_1\|\vec{j}\|j_2\rangle+(g_s-g_1)\langle j_1\|\vec{s}\|j_2\rangle]$$

$$\times\{(u_{j_1}u_{j_2}+v_{j_1}v_{j_2})(a_{j_1}^\dagger\times\tilde{a}_{j_2})^{(1)}-\frac{u_{j_1}v_{j_2}}{\sqrt{N}}[(a_{j_1}^\dagger\times a_{j_2}^\dagger)^{(1)}\times\tilde{s}]^{(1)}+\frac{u_{j_2}v_{j_1}}{\sqrt{N}}[(\tilde{a}_{j_1}\times\tilde{a}_{j_2})^{(1)}\times s^\dagger]^{(1)}]$$

Spherical nuclei

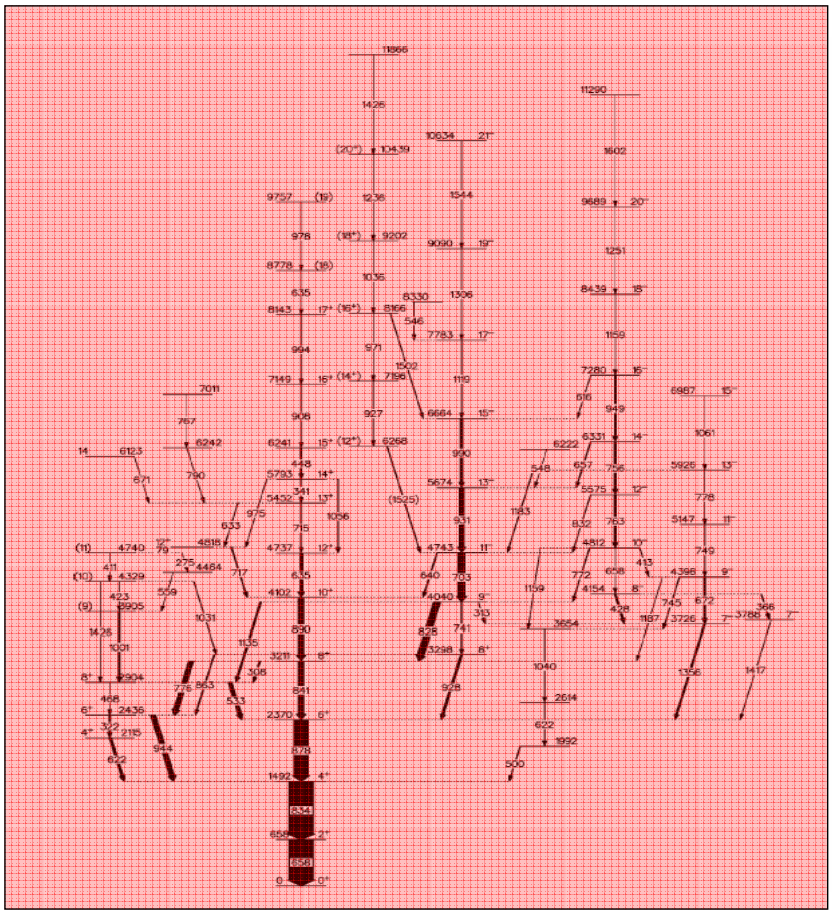

^{104}Cd

Parameterization for neutrons from even-odd Cd nuclei

Parameterization for protons in accordance with odd-even In and Ag nuclei

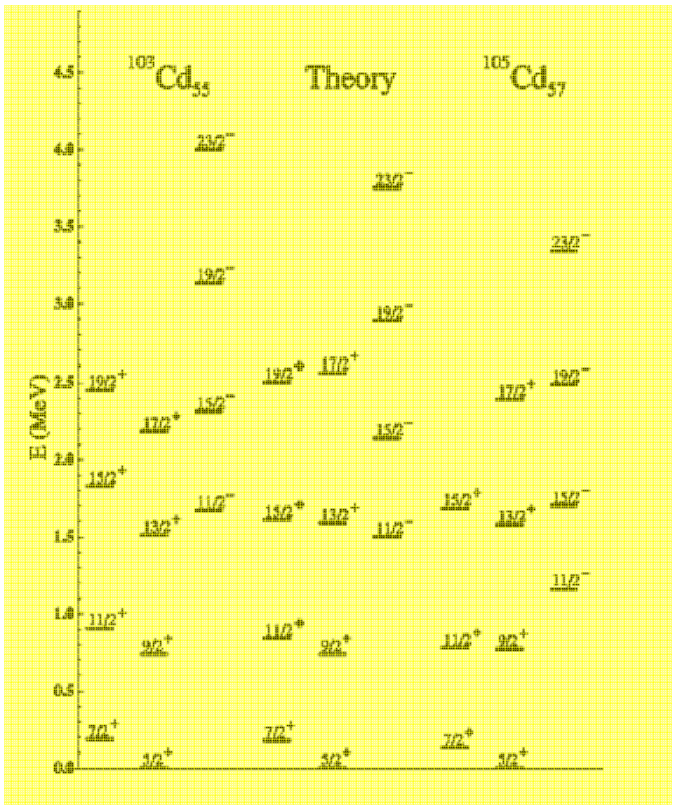

^{104}Cd

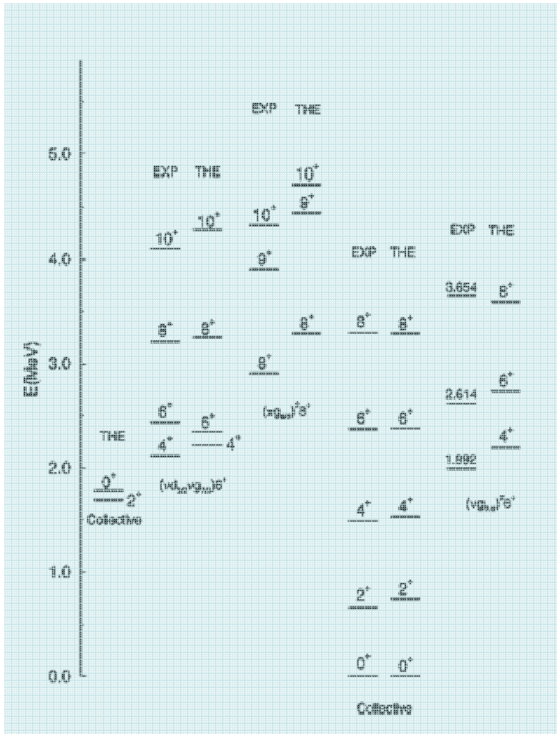

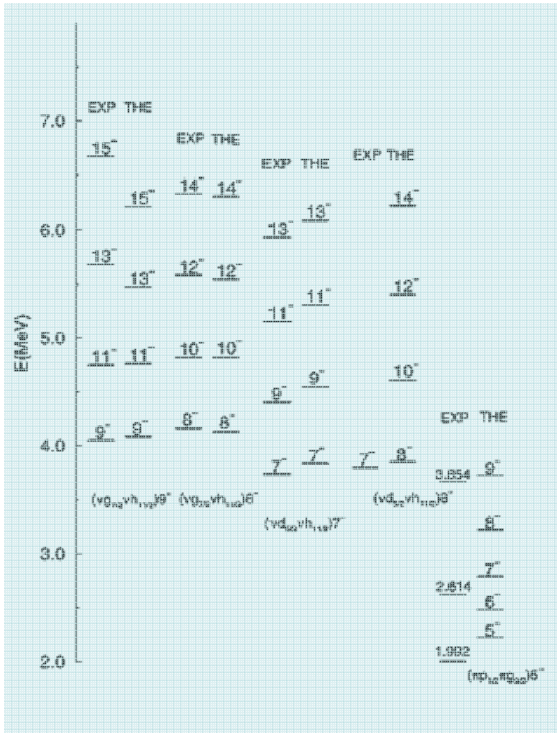

^{101}Ag

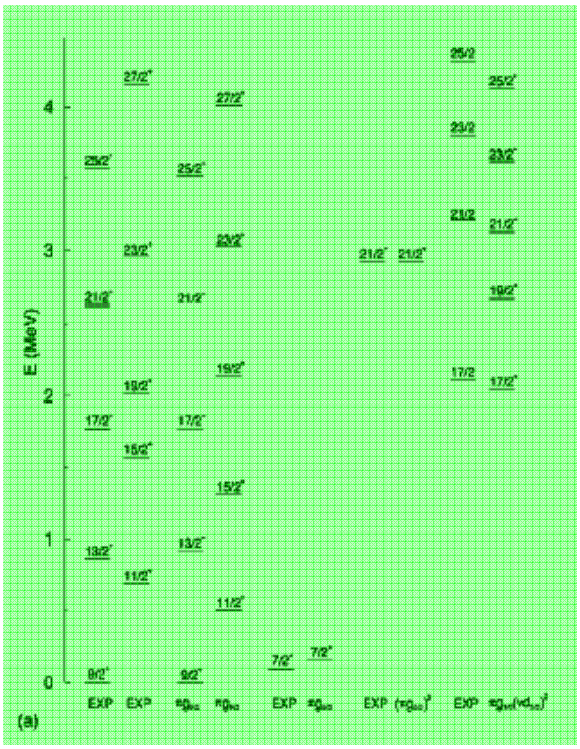

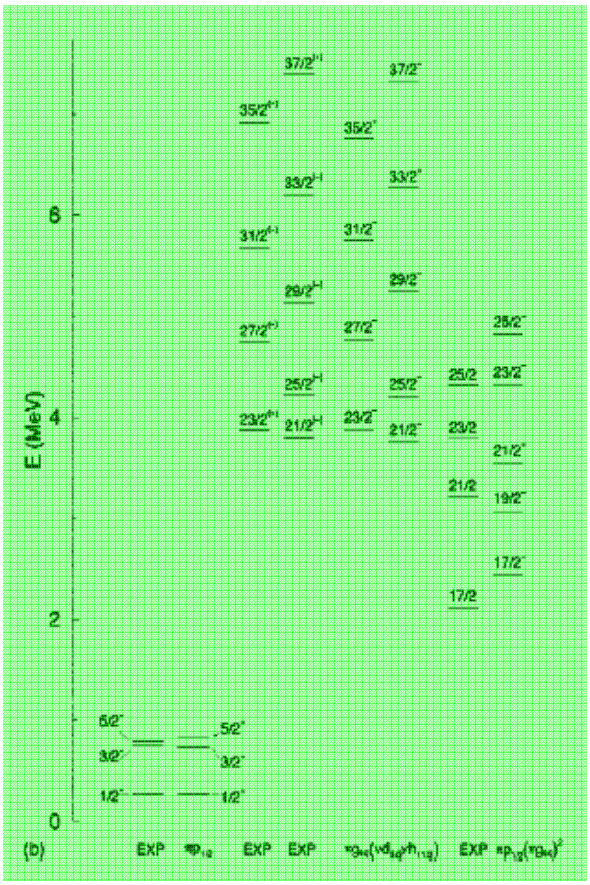

^{101}Ag

State E_x (keV)	I^π	Lifetime (ps) DDCM	RDDS	DSA/NGTB	Adopted	Theory	
Positive parity							
98	$7/2^+$					425	
687	$11/2^+$	2.7(3)			2.7(3)	2.0	
861	$13/2^+$	11.7(10)			11.7(10)	3.4	
1573	$15/2^+$	2.1(5)			2.1(5)	0.4	
1769	$17/2^+$	1.9(2)			1.9(2)	1.9	
2017	$19/2^+$	9(1)			9(1)	5.0	
2621	$21/2^+$	0.6(1)			0.6(1)	0.4	
2922	$21/2_2^+$					1700[a]	
						2.8[b]	
2956	$23/2^+$	1.8(3)			1.8(3)	0.9	
3578	$25/2^+$		<2.0		<2.0	0.4	
4159	$27/2^+$		<2.5		<2.5	0.3	
4572	$(29/2^+)$		14(1)		14(1)		
5300	$(31/2^+)$			≤1.7	≤1.7		
Negative parity							
750	$3/2^{(-)}$					10.2	
797	$5/2^{(-)}$					30.5	
3870	$23/2^{(-)}$	11.4(11)			11.4(11)	8.4	
4217	$25/2^{(-)}$	1.1(2)			1.1(2)	1.2	
4749	$27/2^{(-)}$		1.1(1)		1.1(1)	1.1	
5134	$29/2^{(-)}$			0.83(8)	0.83(8)	0.81	
5678	$31/2^{(-)}$			0.41(5)	0.41(5)	0.45	
6197	$33/2^{(-)}$			0.30(4)	0.30(4)	0.34	
6917	$35/2^{(-)}$			0.18(5)	0.18(5)	0.13	
7393	$37/2^{(-)}$			≤1.3	≤1.3	0.39	
No parity assigned						$\pi=+$	$\pi=-$
2115	17/2		199(7)		199(7)	120	
3210	21/2	1.2(1)			1.2(1)	1.0	2.9
3801	23/2					0.5	0.9
4315	25/2					0.5	0.4

[a]If wave function predominantly $\pi^3(g_{9/2})$.
[b]If wave function predominantly $\pi(g_{9/2})$.

Structure of isomers in spherical nuclei

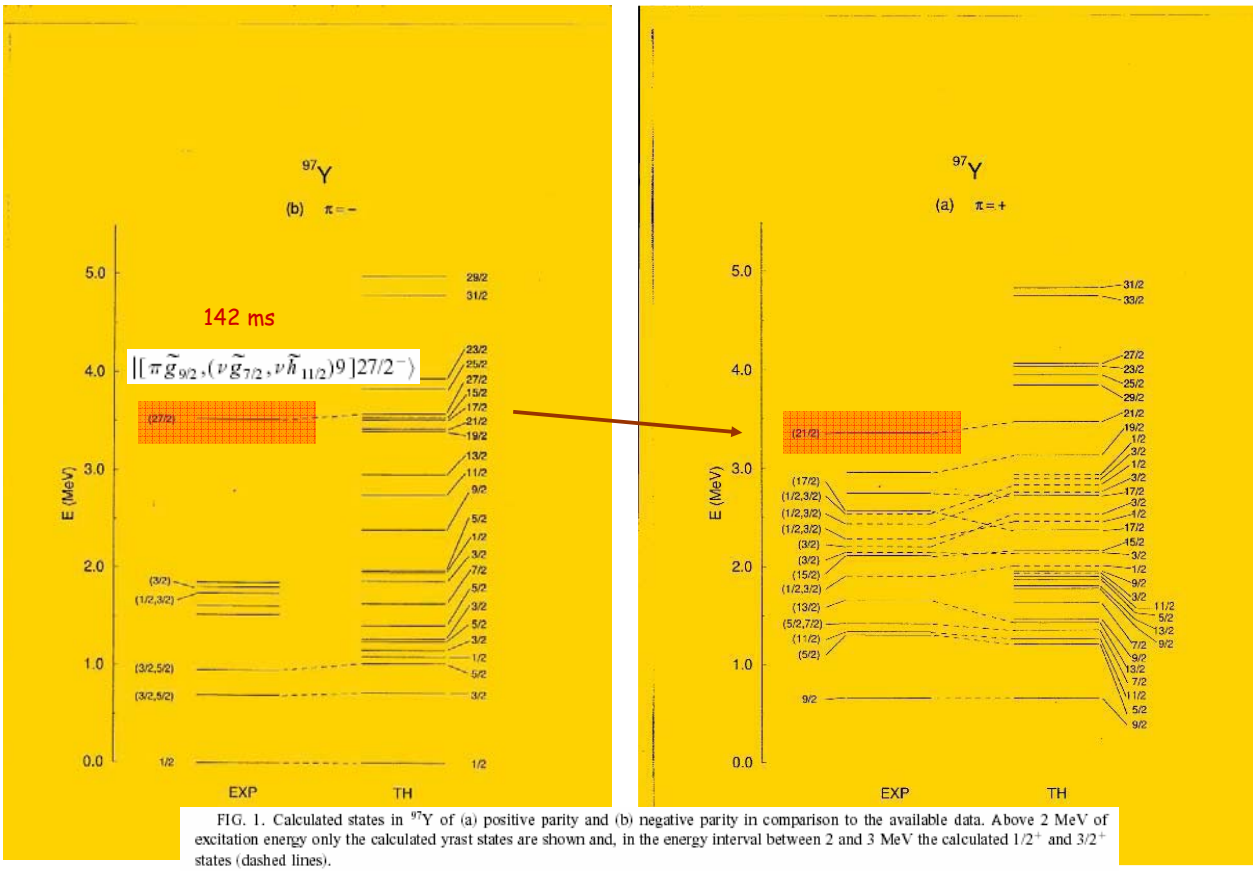

FIG. 1. Calculated states in ^{97}Y of (a) positive parity and (b) negative parity in comparison to the available data. Above 2 MeV of excitation energy only the calculated yrast states are shown and, in the energy interval between 2 and 3 MeV the calculated $1/2^+$ and $3/2^+$ states (dashed lines).

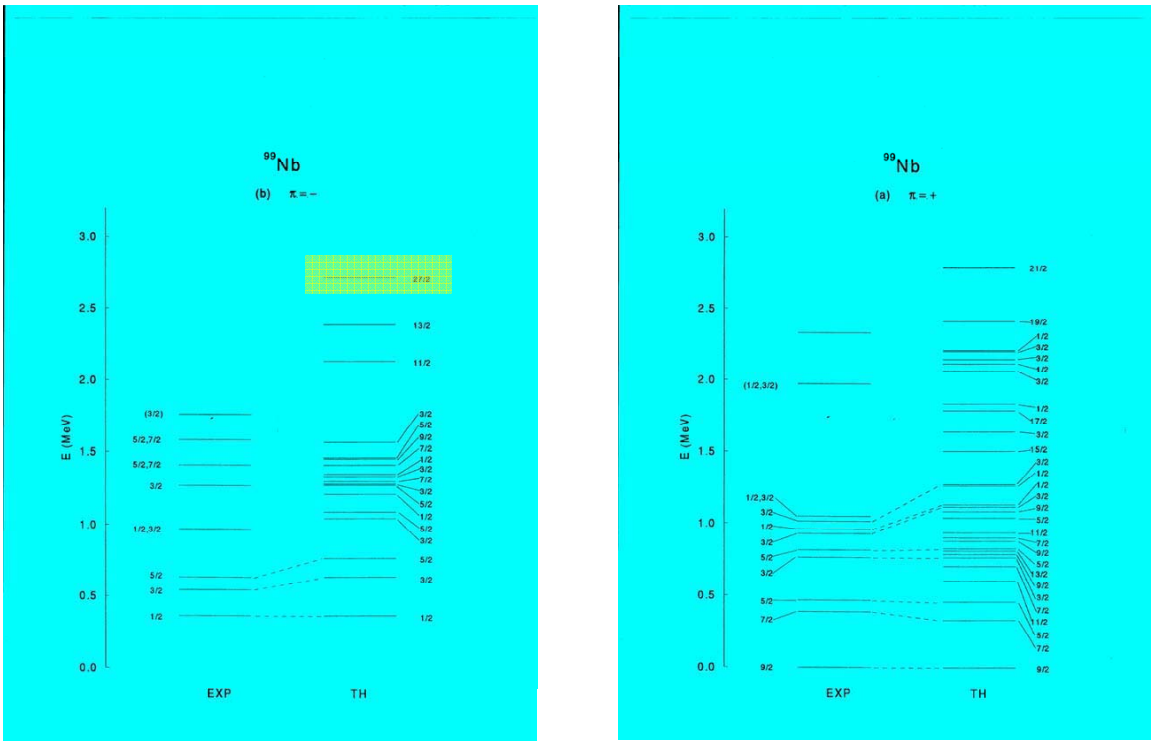

Assuming a possible error of 200 – 300 keV for the predicted energies, a $27/2^-$ isomer with a halflife in the µs - ms range could be found in ^{99}Nb

Deformed nuclei

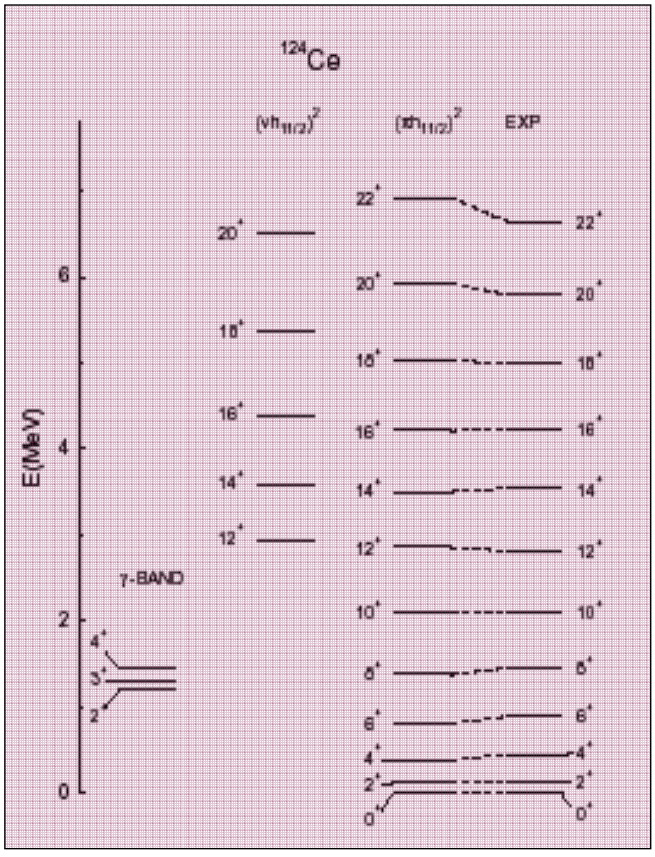

This nucleus displays a transitional structure between deformed nuclei (lighter Ce isotopes) described by the SU(3) limit of the IBM, and γ-soft nuclei (heavier Ce isotopes) which correspond to the O(6) limit of the of the IBM. The SU(3)-O(6) transition can be described by the boson Hamiltonian

$$H_{IBM} = -\frac{\alpha}{10}\, Q\cdot Q \;+\; \frac{\beta}{10}\, L\cdot L$$

and is determined by the value of the parameter χ in the quadrupole boson operator. The limiting cases are: $\chi = 0$ corresponds to the O(6) limit of the IBM-1, and $\chi = -\frac{\sqrt{7}}{2}$ describes a prolate shape in the SU(3) dynamical symmetry limit.

Here: $\alpha = 0.19$ MeV, $\beta = 0.13$ MeV, $\chi = -1.0$ and the boson number $N = 12$.

$v^2(\pi h_{11/2}) = 0.06$
$\varepsilon(\pi h_{11/2}) = 1.70$ MeV
$v^2(\nu h_{11/2}) = 0.40$
$\varepsilon(\nu h_{11/2}) = 1.32$ MeV

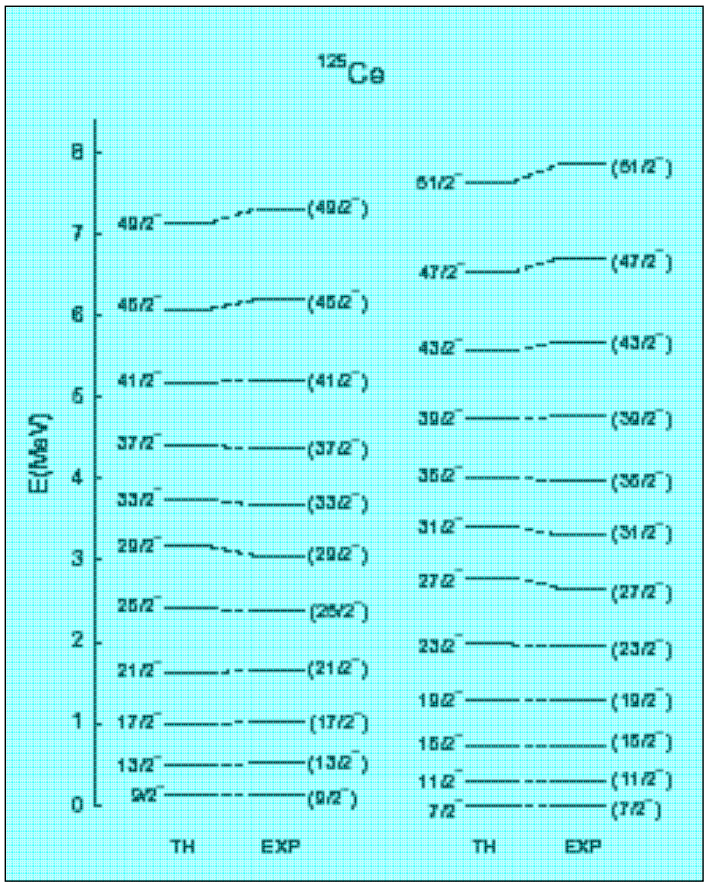

This band is based on the $\nu h_{11/2}$ orbital fo the states with $I \leq 27/2^-$, and on the three fermion configuration $\nu h_{11/2}\,(\pi h_{11/2})^2$ for I $29/2$. The structure of this band is very sim ple. The neutron $\nu h_{11/2}$ orbital couples to th yrast sequence of states in the core nucleu ^{124}Ce.

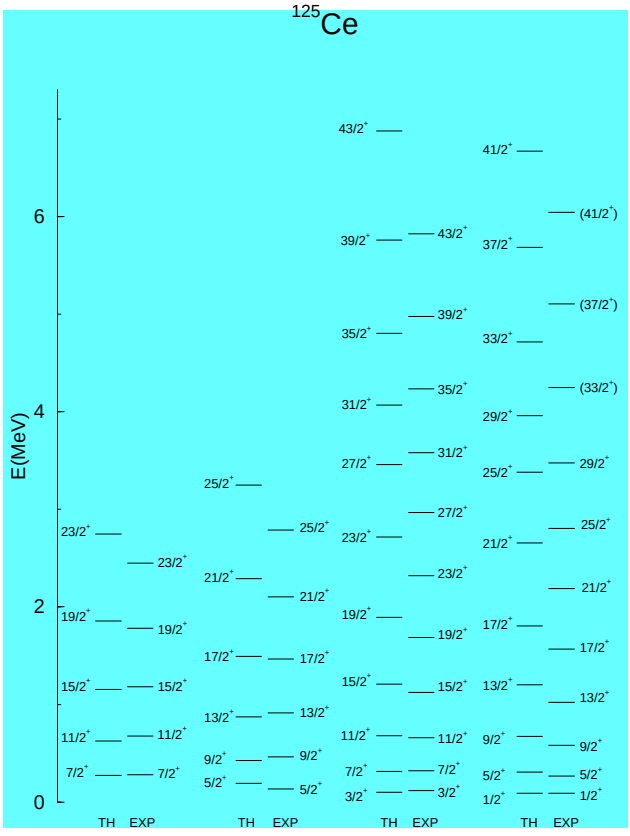

The band 2 is based on the $\nu d_{5/2}$ and $\nu g_{7/2}$ neutron orbitals. The band 3, in addition, contains sizeable components based on the $\nu d_{3/2}$ and $\nu s_{1/2}$ states. While the alignment of a proton pair is not observed in band 2, the states with $I \geq 25/2^+$ of band 3 are based on the one-neutron plus $(\pi h_{11/2})^2$ configuration.

2 2 3 3

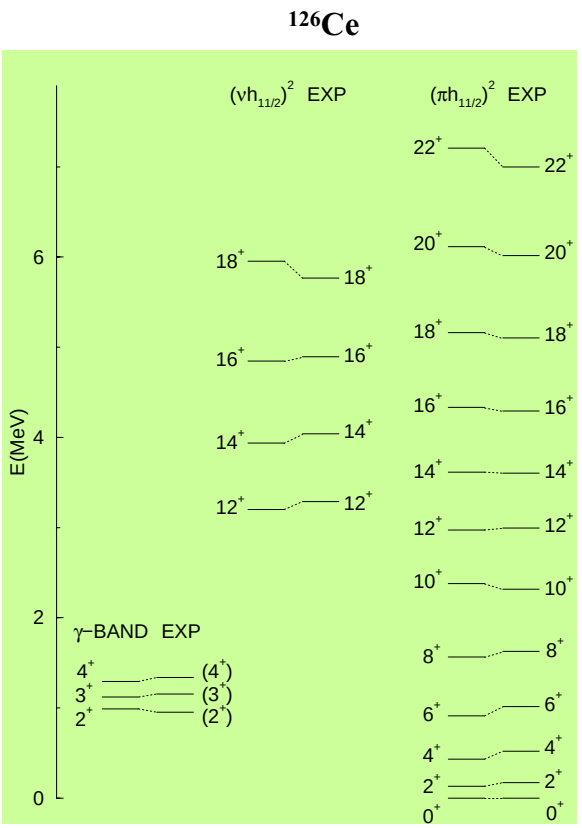

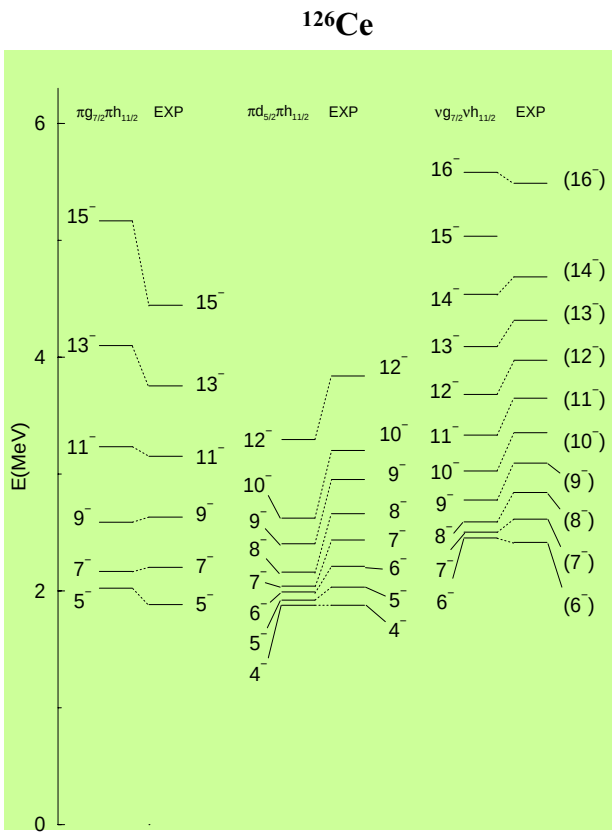

Transitional nuclei

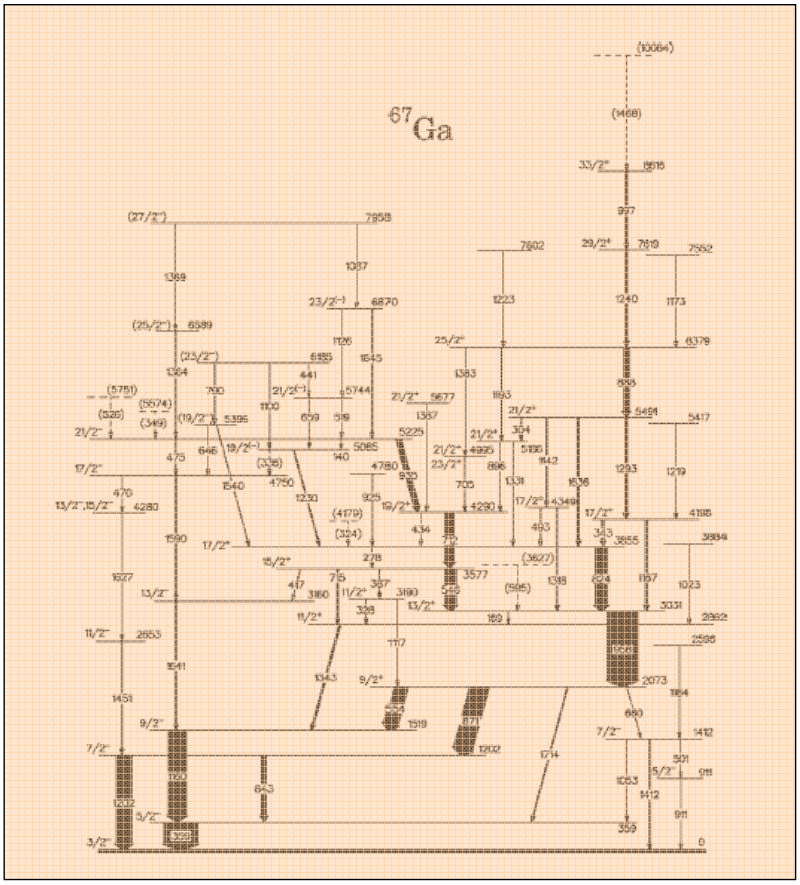

Wave functions

$$|I_k^{\pi}\rangle = \sum_{j n_d \upsilon R} \xi_{j,n_d \upsilon R;I} \; |\pi\tilde{j}, n_d \upsilon R; I\rangle$$

$$+ \sum_{jj'j'' I_{\alpha\alpha} I_{\pi\alpha\alpha} n_d \upsilon R} \eta_{jj'j'' I_{\alpha\alpha} I_{\pi\alpha\alpha}, n_d \upsilon R; I}$$

$$\times |[\pi\tilde{j}, (\alpha\tilde{j}', \alpha\tilde{j}'') I_{\alpha\alpha}] I_{\pi\alpha\alpha}, n_d \upsilon R; I\rangle$$

Here $\pi\tilde{j}$ stands for a proton quasiparticle, and $\alpha\tilde{j}', \alpha\tilde{j}''$ for neutron quasiparticles ($\alpha = \nu$), or proton quasiparticles ($\alpha = \pi$), which are coupled to the angular momentum $I_{\alpha\alpha}$. Angular momenta j and $I_{\alpha\alpha}$ are coupled to the three-quasiparticle angular momentum denoted by $I_{\pi\alpha\alpha}$. In the boson part of the wave function, the $n_d d$ bosons are coupled to the total boson angular momentum R. The additional quantum number υ is used to distinguish between the n_d-boson states having the same angular momentum R. We note that the number of s bosons associated with the boson state $|n_d \upsilon R\rangle$ is $n_s = N - n_d$, where N is the total number of bosons.

To make it easier to follow the origin of states, for the indexing of the theoretical states we use I_{qp_i} for the quasiparticle+phonon states, I_{bp_i} for proton broken pair states and I_{bn_i} for neutron broken pair states. Here the index i denotes the ith state of the denoted type. In the standard notation I_k, the index k is used as total label obtained from the IBFBPM calculation. The indexing I_k is pointed out only for states where $i \neq k$. Otherwise, the indexes i and k are equal.

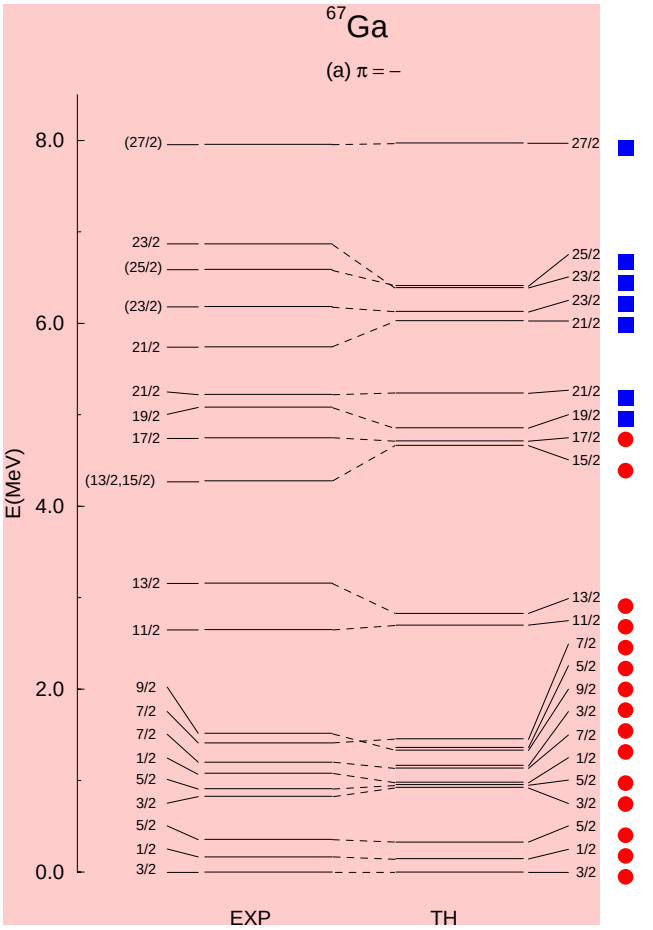

one proton two neutron state

one proton state

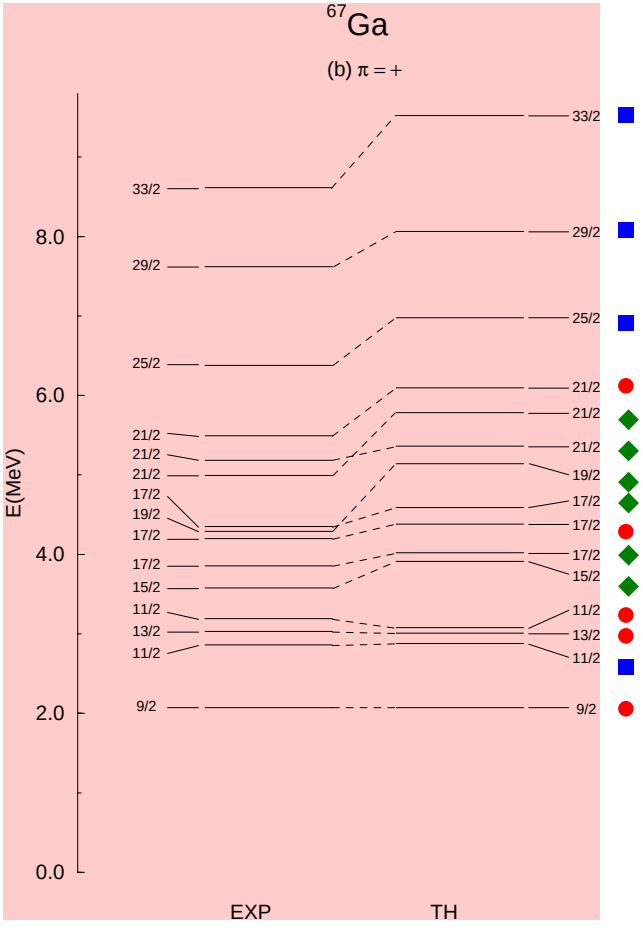

three proton state

one proton two neutron state

one proton state

$I_i^\pi \rightarrow I_f^\pi$ ($\hbar$) ($\hbar$)	$E_i \rightarrow E_f$ Expt. Expt.	$B(E2)(e^2b^2)$ IBFBPM	$B(M1)(\mu_N^2)$ IBFBPM	I_γ Expt.	I_γ IBFBPM
$1/2^-_{qp_1} \rightarrow 3/2^-_{qp_1}$	167→0	0.013	0.058	100	100
$5/2^-_{qp_1} \rightarrow 1/2^-_{qp_1}$	359→167	0.027			1.8
$\rightarrow 3/2^-_{qp_1}$	→0	0.003	0.006	100	100
$3/2^-_{qp_2} \rightarrow 5/2^-_{qp_1}$	828→359	1×10^{-5}	0.013	4	6
$\rightarrow 1/2^-_{qp_1}$	→167	2×10^{-5}	0.022	10	27
$\rightarrow 3/2^-_{qp_1}$	→0	0.027	0.028	100	100
$5/2^-_{qp_2} \rightarrow 3/2^-_{qp_2}$	911→828	0.002	0.306		0.9
$\rightarrow 5/2^-_{qp_1}$	→359	9×10^{-5}	0.0005	2.2	0.5
$\rightarrow 1/2^-_{qp_1}$	→167	0.003		2.2	2.0
$\rightarrow 3/2^-_{qp_1}$	→0	0.029	0.010	100	100
$1/2^-_{qp_2} \rightarrow 5/2^-_{qp_2}$	1082→911	0.0004			0.0002
$\rightarrow 3/2^-_{qp_2}$	→828	0.0003	0.533	12	37
$\rightarrow 5/2^-_{qp_1}$	→359	0.003			1.7
$\rightarrow 1/2^-_{qp_1}$	→167		0.030	100	100
$\rightarrow 3/2^-_{qp_1}$	→0	0.021	0.005	33	122
$7/2^-_{qp_1} \rightarrow 5/2^-_{qp_2}$	1202→911	0.002	0.131		6
$\rightarrow 3/2^-_{qp_2}$	→828	0.0004			0.0004
$\rightarrow 5/2^-_{qp_1}$	→359	0.002	0.012	31	14
$\rightarrow 3/2^-_{qp_1}$	→0	0.033		100	100
$7/2^-_{qp_2} \rightarrow 7/2^-_{qp_1}$	1412→1202	0.002	0.002		0.06
$\rightarrow 5/2^-_{qp_2}$	→911	0.002	0.011	20	5
$\rightarrow 3/2^-_{qp_2}$	→828	0.001			0.2
$\rightarrow 5/2^-_{qp_1}$	→359	0.024	0.008	100	100
$\rightarrow 3/2^-_{qp_1}$	→0	3×10^{-5}		20	0.3
$9/2^-_{qp_1} \rightarrow 7/2^-_{qp_2}$	1519→1412	0.003	0.018		0.03
$\rightarrow 7/2^-_{qp_1}$	→1202	0.0007	0.005		0.2
$\rightarrow 5/2^-_{qp_2}$	→911	0.0003			0.02
$\rightarrow 5/2^-_{qp_1}$	→359	0.049		100	100
$11/2^-_{qp_1} \rightarrow 9/2^-_{qp_1}$	2653→1519	0.001	0.007		5
$\rightarrow 7/2^-_{qp_2}$	→1412	0.0004			0.4
$\rightarrow 7/2^-_{qp_1}$	→1202	0.051		100	100
$13/2^-_{qp_1} \rightarrow 11/2^-_{qp_1}$	3160→2653	0.0003	0.004		0.1
$\rightarrow 9/2^-_{qp_1}$	→1519	0.065		100	100
$15/2^-_{qp_1} \rightarrow 13/2^-_{qp_1}$	4280→3160	0.0009	0.004		1.5
$\rightarrow 11/2^-_{qp_1}$	→2653	0.056		100	100
$17/2^-_{qp_1} \rightarrow 15/2^-_{qp_1}$	4750→4280	8×10^{-5}	0.002	12	0.04
$\rightarrow 13/2^-_{qp_1}$	→3160	0.067		100	100
$21/2^-_{hn_2} \rightarrow 21/2^-_{hn_1}$	5744→5225	2×10^{-6}	0.003	100	100
$\rightarrow 19/2^-_{hn_1}$	→5085	0.0003	0.002	24	161
$23/2^-_{hn_1} \rightarrow 21/2^-_{hn_2}$	6185→5744	0.0004	0.718	30	89
$\rightarrow 21/2^-_{hn_1}$	→5225	0.0007	0.007		10
$\rightarrow 19/2^-_{hn_1}$	→5085	0.025		40	40
$25/2^-_{hn_1} \rightarrow 23/2^-_{hn_1}$	6589→6185	0.0006	0.006		0.4
$\rightarrow 21/2^-_{hn_2}$	→5744	8×10^{-6}			0.002
$\rightarrow 21/2^-_{hn_1}$	→5225	0.036		100	100
$23/2^-_{hn_2} \rightarrow 25/2^-_{hn_1}$	6870→6589	0.007	0.598		20
$\rightarrow 23/2^-_{hn_1}$	→6185	0.0002	0.0004		0.2
$\rightarrow 21/2^-_{hn_2}$	→5744	4×10^{-5}	0.003	36	6
$\rightarrow 21/2^-_{hn_1}$	→5225	0.008	0.0003	100	100
$\rightarrow 19/2^-_{hn_1}$	→5085	3×10^{-7}			0.005

^{67}Ga

$I_i^\pi \rightarrow I_f^\pi$ ($\hbar$) ($\hbar$)	$E_i \rightarrow E_f$ Expt. Expt.	$B(E2)(e^2b^2)$ IBFBPM	$B(M1)(\mu_N^2)$ IBFBPM	I_γ Expt.	I_γ IBFBPM
$27/2^-_{hn_2} \rightarrow 23/2^-_{hn_2}$	7958→6870	0.041		50	259
$\rightarrow 25/2^-_{hn_1}$	→6589	0.005	0.0001	100	100
$\rightarrow 23/2^-_{hn_1}$	→6185	9×10^{-6}			0.6
$13/2^+_{qp_1} \rightarrow 9/2^+_{qp_1}$	3031→2073	0.037		100	100
$11/2^+_{qp_1} \rightarrow 13/2^+_{qp_1}$	3190→3031	0.001	0.119		0.4
$\rightarrow 9/2^+_{qp_1}$	→2073	0.041	0.058	100	100
$15/2^+_{hp_1} \rightarrow 11/2^+_{qp_1}$	3577→3190	0.002		3.4	33
$\rightarrow 13/2^+_{qp_1}$	→3031	0.0009	4×10^{-5}	100	100
$17/2^+_{hp_1} \rightarrow 15/2^+_{hp_1}$	3855→3577	0.006	0.039	1.2	22
$\rightarrow 13/2^+_{qp_1}$	→3031	0.015		100	100
$17/2^+_{qp_1} \rightarrow 17/2^+_{hp_1}$	4198→3855	6×10^{-5}	0.095	90	6
$\rightarrow 15/2^+_{hp_1}$	→3577	0.001	0.028		11
$\rightarrow 13/2^+_{qp_1}$	→3031	0.043		100	100
$19/2^+_{hp_1} \rightarrow 17/2^+_{qp_1}$	4290→4198	0.002	0.001		0.02
$\rightarrow 17/2^+_{hp_1}$	→3855	0.004	9×10^{-5}	1.6	1.2
$\rightarrow 15/2^+_{hp_1}$	→3577	0.029		100	100
$17/2^+_{hp_2} \rightarrow 19/2^+_{hp_1}$	4349→4290	6×10^{-5}	0.004		0.02
$\rightarrow 17/2^+_{qp_1}$	→4198	3×10^{-5}	0.008		0.8
$\rightarrow 17/2^+_{hp_1}$	→3855	0.0004	0.001	52	5
$\rightarrow 15/2^+_{hp_1}$	→3577	0.0001	0.012	<10	146
$\rightarrow 13/2^+_{qp_1}$	→3031	0.0014		100	100
$21/2^+_{hp_2} \rightarrow 17/2^+_{hp_2}$	4995→4349	0.035			24
$\rightarrow 19/2^+_{hp_1}$	→4290	2×10^{-5}	0.033	100	100
$\rightarrow 17/2^+_{qp_1}$	→4198	0.009			17
$\rightarrow 17/2^+_{hp_1}$	→3855	0.0002			2.7
$21/2^+_{hp_1} \rightarrow 21/2^+_{hp_2}$	5186→4995	0.0002	0.005		0.03
$\rightarrow 17/2^+_{hp_2}$	→4349	0.0002			0.04
$\rightarrow 19/2^+_{hp_1}$	→4290	0.003	0.106	31	67
$\rightarrow 17/2^+_{qp_1}$	→4198	0.0003			0.2
$\rightarrow 17/2^+_{hp_1}$	→3855	0.040		100	100
$21/2^+_{qp_1} \rightarrow 21/2^+_{hp_1}$	5491→5186	0.0002	0.029	2.1	0.7
$\rightarrow 21/2^+_{hp_2}$	→4995	1×10^{-5}	0.001		0.1
$\rightarrow 17/2^+_{hp_2}$	→4349	0.008		27	9
$\rightarrow 19/2^+_{hp_1}$	→4290	0.0004	0.004		7
$\rightarrow 17/2^+_{qp_1}$	→4198	0.048		100	100
$\rightarrow 17/2^+_{hp_1}$	→3855	0.002		67	14

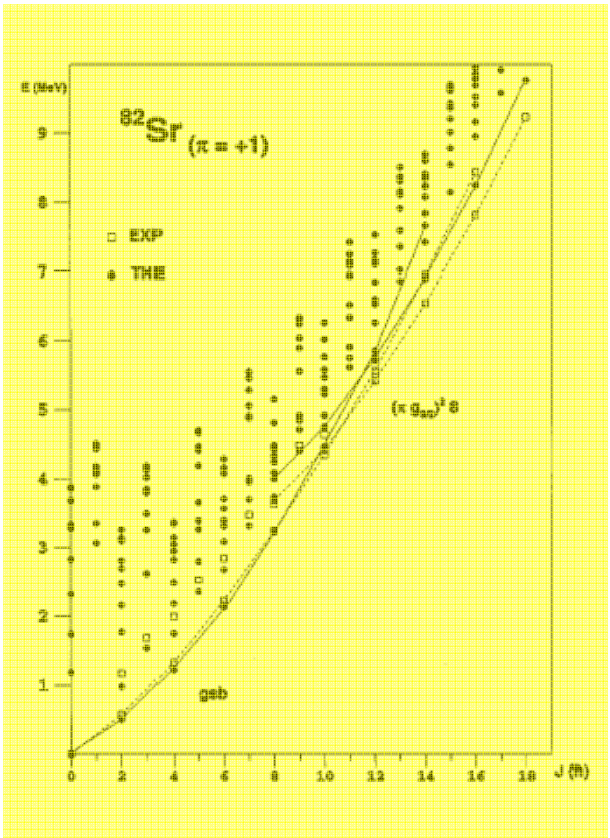

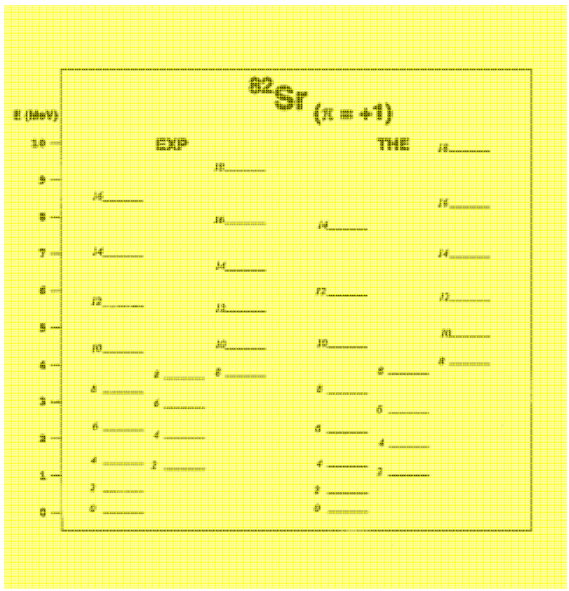

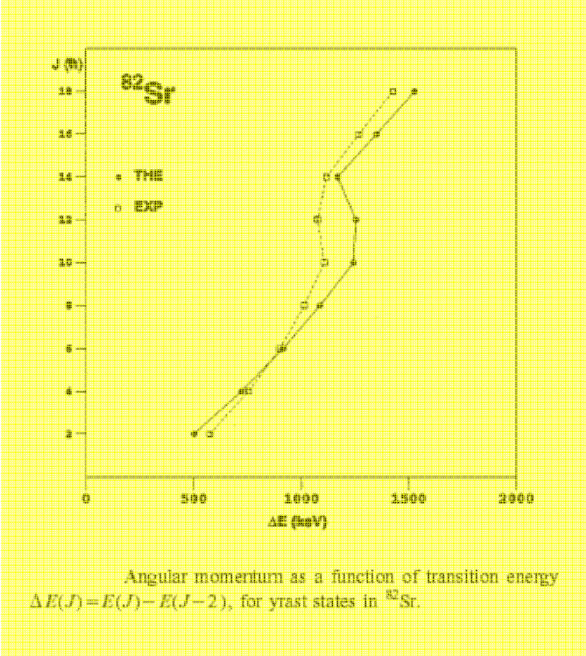

Angular momentum as a function of transition energy $\Delta E(J) = E(J) - E(J-2)$, for yrast states in ^{82}Sr.

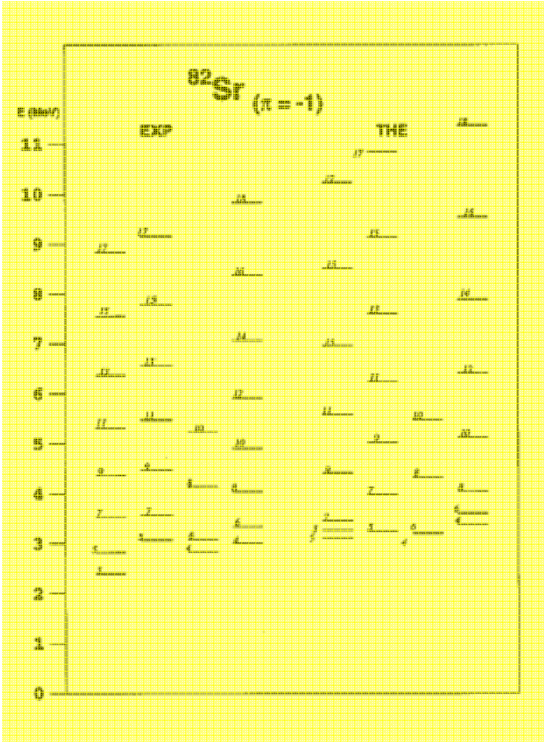

Interactions ?

The strength of the exchange interaction is adjusted to reproduce the energy spacings of negative-parity states in ^{82}Sr. It differs considerably from that used for odd-even isotopes In order to understand the origin of this anomaly, one may consider the coupling of unpaired protons to proton bosons in the ^{82}Sr. To create multiproton states in the even-even nucleus we destroy proton bosons and the effective coupling of the exchange interaction is reduced. In the IBM-2 framework this reduction would be implicit and no adjustment of strength parameters should be needed. However, in our model based on IBM-1, we couple to all the core bosons, irrespective of their nature and the suppression of coupling is greatly diminished. Thus, the need to empirically reduce the strength of coupling parameter. This effect should be especially pronounced near closed shells, and in our case the reduction of the exchange interaction might be due to the subshell closure at $Z = 40$.

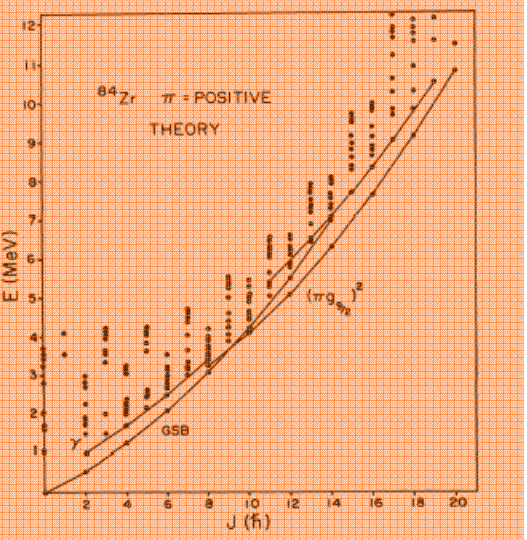

Some of the positive-parity states calculated for ^{84}Zr. The first ten states of each spin, for configurations involving core vibrations coupled to quasiproton states, are shown.

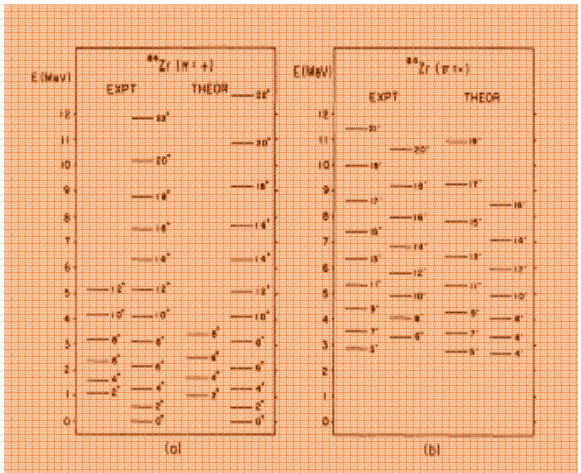

A detailed comparison of states calculated for ^{84}Zr (a) in the positive-parity sequence (b) in the negative-parity sequence.

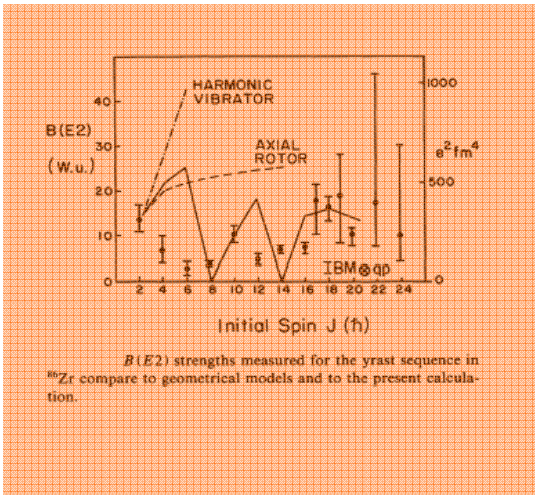

$B(E2)$ strengths measured for the yrast sequence in ^{86}Zr compare to geometrical models and to the present calculation.

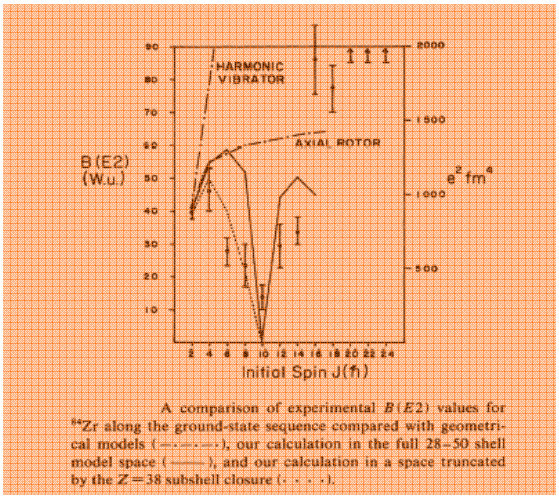

A comparison of experimental $B(E2)$ values for ^{84}Zr along the ground-state sequence compared with geometrical models (– · – · –), our calculation in the full 28–50 shell model space (——), and our calculation in a space truncated by the $Z=38$ subshell closure (· · · ·).

The pair breaking interaction V^{mix}, which mixes states with different number of fermions, and conservs only the total number of valence nucleons, in general does not induce sufficient mixing as can be deduced, for example, from observed transition strengths. It is the lowest order contribution to a pair-breaking interaction. Since the interaction contains only fermion operators of rank 0 and 2, it cannot connect in first order the ground state band with two-fermion states of higher fermion angular momenta. In order to enhance the mixing, interactions that contain fermion operators of higher rank could be included in the model Hamiltonian. However, such an interaction would also require higher order boson operators, with parameters that cannot be determined from available experimental data, or from the intrinsic structure of the model.

^{138}Nd

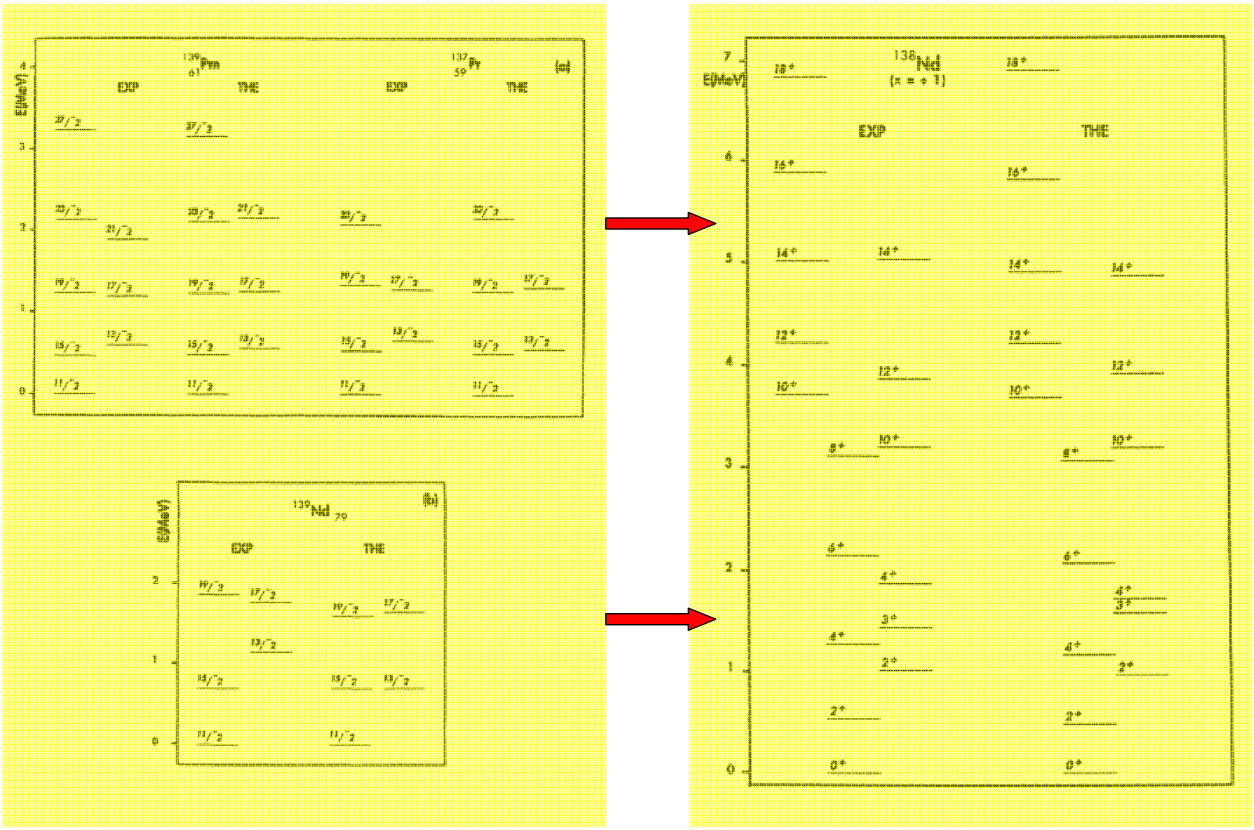

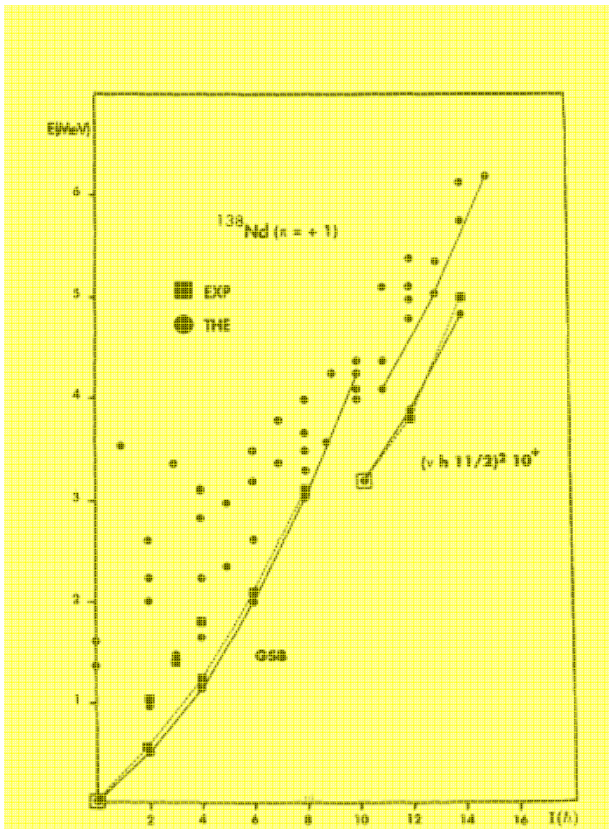

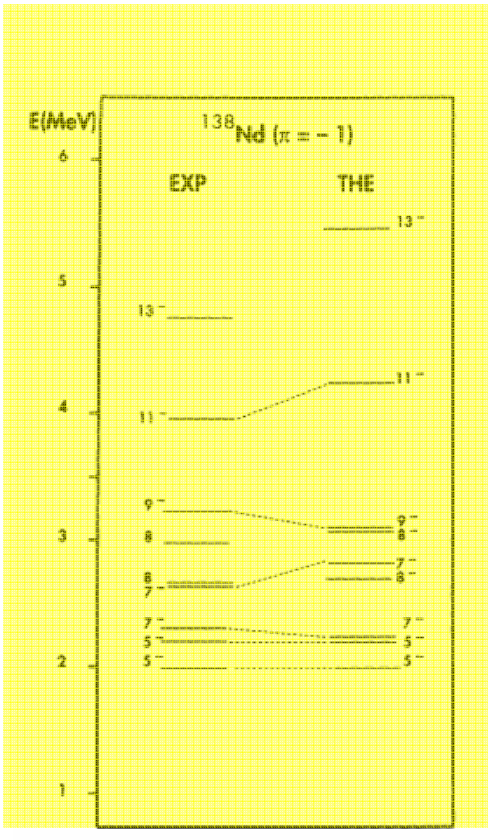

h11/2 d3/2 neutron pair

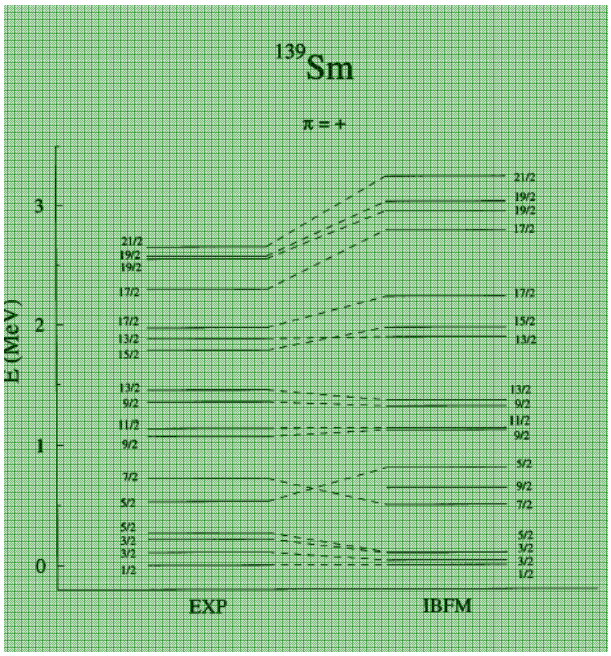

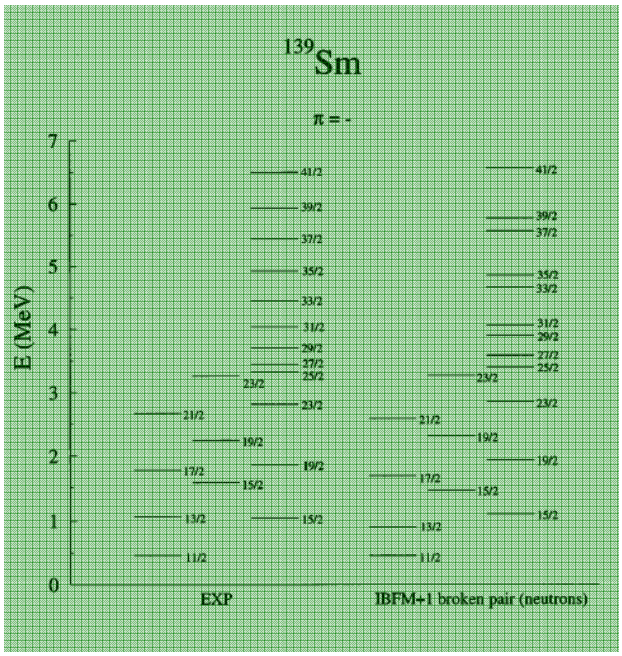

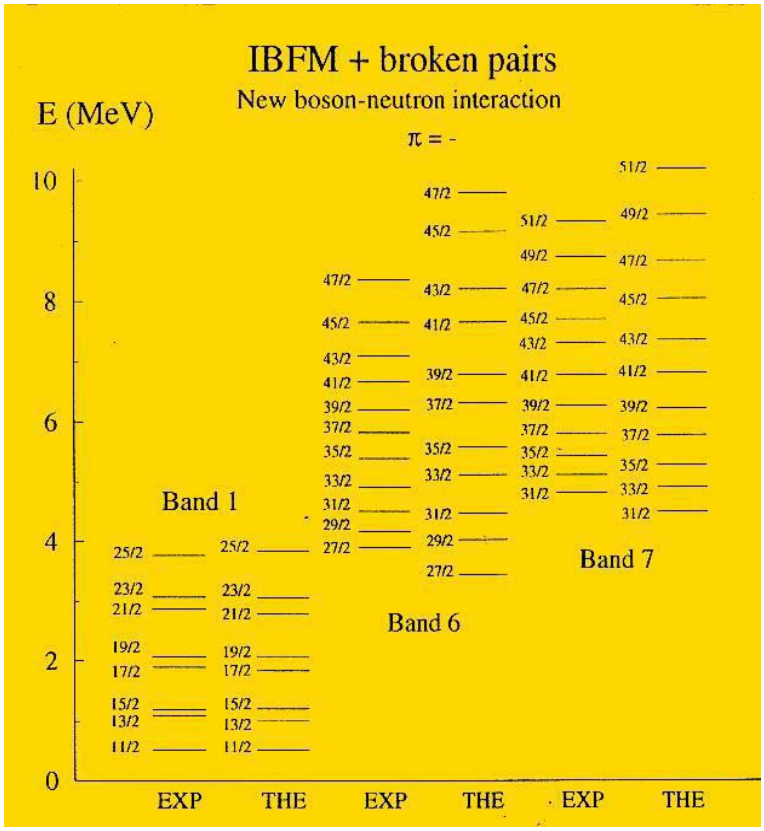

$^{137}Nd_{77}$

Band 1 (ν h11/2)

Band 6 $(\nu\ h11/2)^3$

Band 7 $(\nu\ h11/2)\ (\pi\ h11/2)^2$

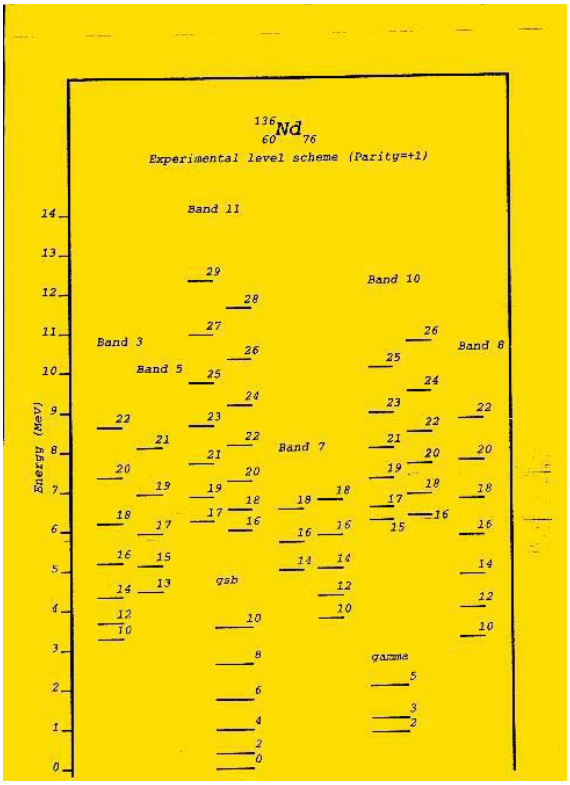

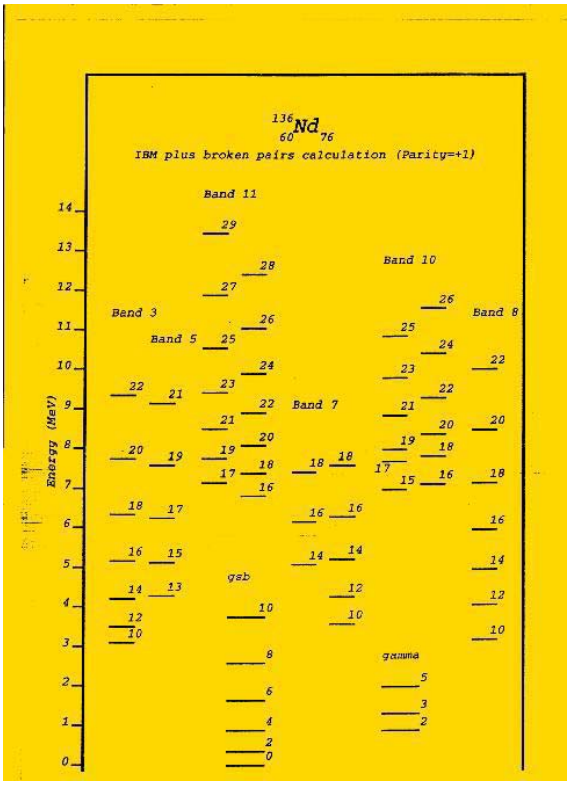

Bands 3, 5, 7 $(\pi\ h11/2)^2$

Band 8 $(\nu\ h11/2)^2$

Bands 10, 11 $(\pi\ h11/2)^2\ (\nu\ h11/2)^2$!!!

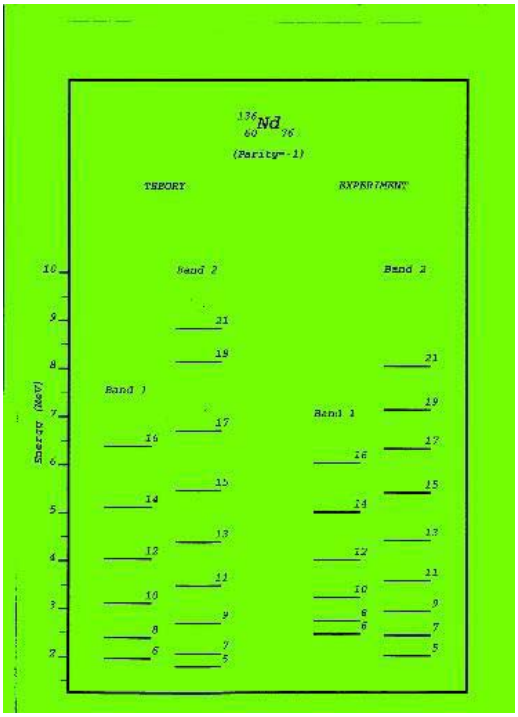

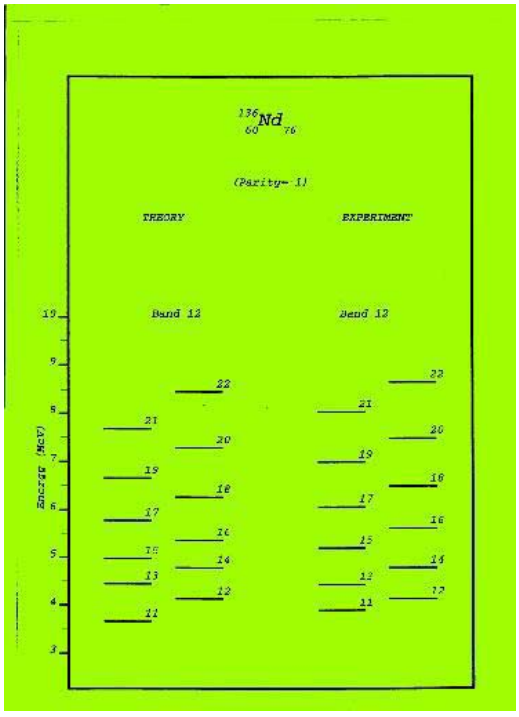

Bands 1, 2 $(\nu\ d3/2\ \ \nu\ h11/2)$

Band 12 $(\nu\ d3/2\ \ (\nu\ h11/2)^3)$

^{101}Rh

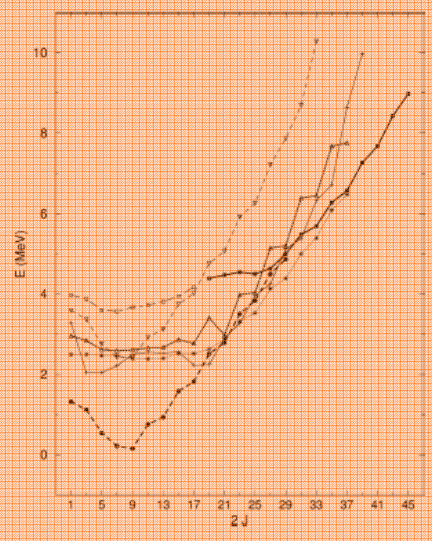

Fig. 4. Positive-parity levels calculated with the IBFBPM model for the following configurations: •: $\pi g_{9/2}$, □: $\pi g_{9/2}\nu(h^2_{11/2})_{\text{small } I}$, ■: $\pi g_{9/2}\nu(h^2_{11/2})_{I=10}$, *: $\pi g_{9/2}\nu(d_{5/2}$ and/or $g_{7/2})$, +: $(\pi p_{1/2}$ and/or $\pi p_{3/2}$ and/or $\pi f_{5/2})\ \nu h_{11/2}\nu(d_{5/2}$ or $g_{7/2})$, Δ: $\pi g^3_{9/2}$, ▽: $\pi g_{9/2}(\pi p_{1/2}$ and/or $\pi p_{3/2}$ and/or $\pi f_{5/2})$.

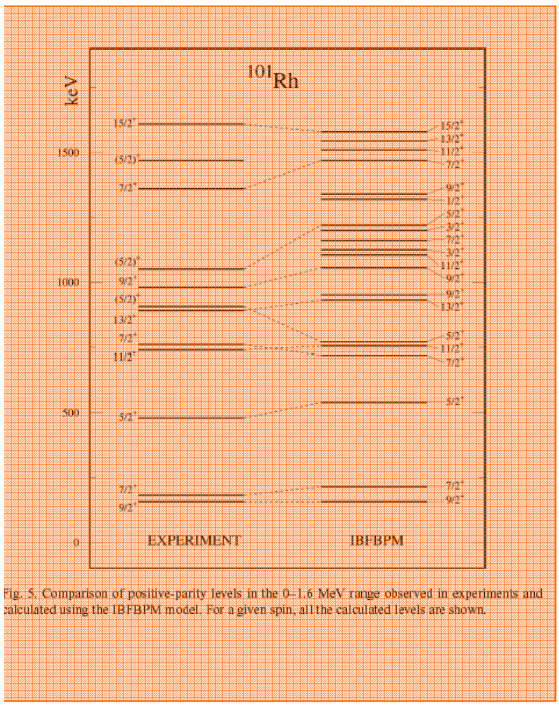

Fig. 5. Comparison of positive-parity levels in the 0–1.6 MeV range observed in experiments and calculated using the IBFBPM model. For a given spin, all the calculated levels are shown.

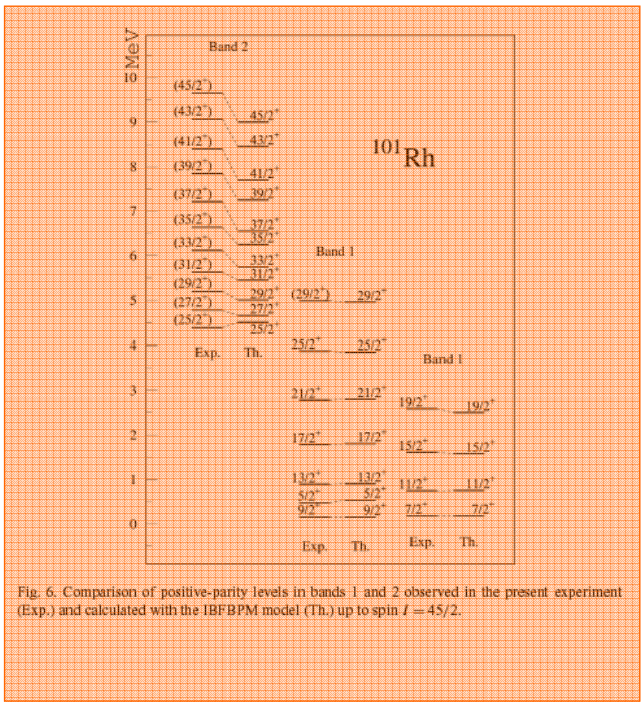

Fig. 6. Comparison of positive-parity levels in bands 1 and 2 observed in the present experiment (Exp.) and calculated with the IBFBPM model (Th.) up to spin $I = 45/2$.

Band 1 π g9/2

Band 2 π g9/2 (ν h11/2)^2

^{101}Rh

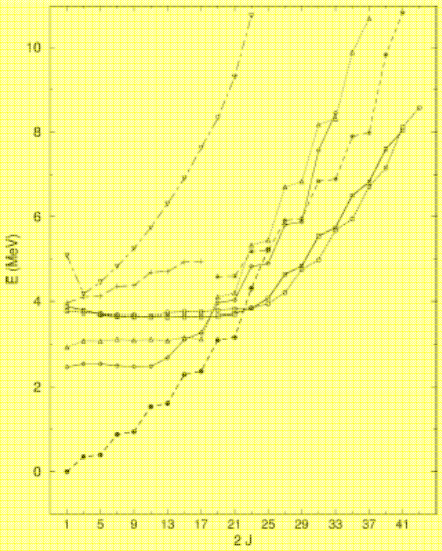

Fig. 7. Negative-parity levels calculated with the IBFBPM model for the following configurations: •: $\pi p_{1/2}$ from $1/2^-$ to $21/2^-$ and $\pi f_{5/2}$ for $23/2^-$ and $25/2^-$, □: $\pi g_{9/2}\nu(d_{5/2}h_{11/2})$, ○: $\pi g_{9/2}\nu(g_{7/2}h_{11/2})$, ∗: $\pi p_{1/2}\nu(h^2_{11/2})_{10}$ from $I = 19/2^-$ to $37/2^-$ and $\pi f_{5/2}\nu(h^2_{11/2})_{10}$ from $I = 39/2^-$ to $41/2^-$, +: $\pi(p_{1/2}$ and/or $p_{3/2}$ and/or $f_{5/2})\nu(h^2_{11/2})_{\text{small } I}$, ▽: $\pi(p_{1/2}$ and/or $p_{3/2}$ and/or $f_{5/2})^3$, △: $\pi(p_{1/2}$ and/or $p_{3/2}$ and/or $f_{5/2})\pi g^2_{9/2}$, ◇: $\pi(p_{1/2}$ and/or $p_{3/2}$ and/or $f_{5/2})\nu(d_{5/2}$ and/or $g_{7/2})$.

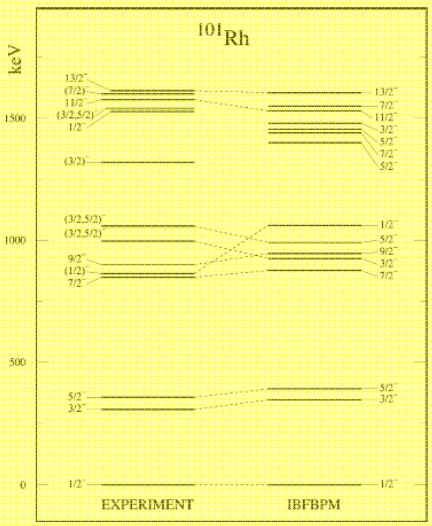

Fig. 8. Comparison of negative-parity levels in the 0–1.6 MeV range observed in experiments and calculated using the IBFBPM model. For a given spin, all the calculated levels are shown.

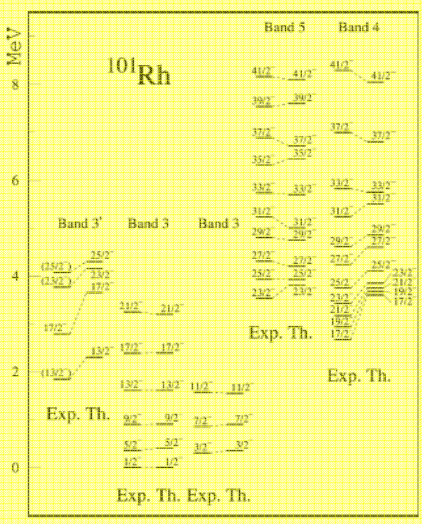

Fig. 9. Comparison of negative-parity levels in bands 3, 4, 5 observed in the present experiment (Exp.) and calculated with the IBFBPM model (Th.) up to spin $I = 41/2$.

Band 3 π p1/2

Bands 4, 5 (π g9/2) (ν d5/2 ν h11/2) or (π g9/2) (ν g7/2 ν h11/2)

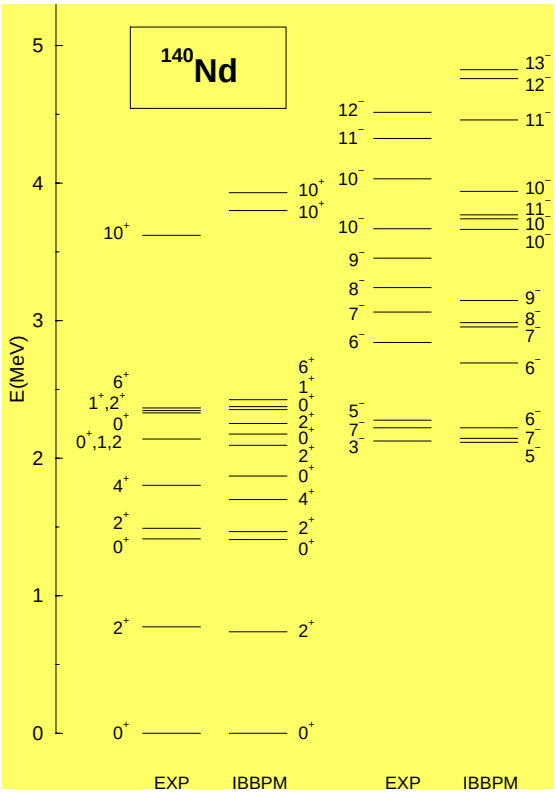
140Nd
E(MeV)
EXP
IBBPM
EXP
IBBPM

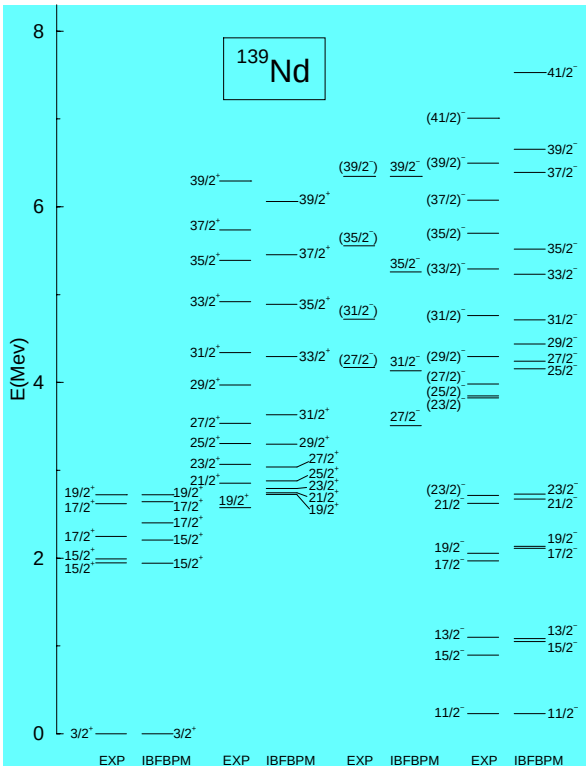
139Nd
E(Mev)
EXP
IBFBPM
EXP
IBFBPM
EXP
IBFBPM
EXP
IBFBPM

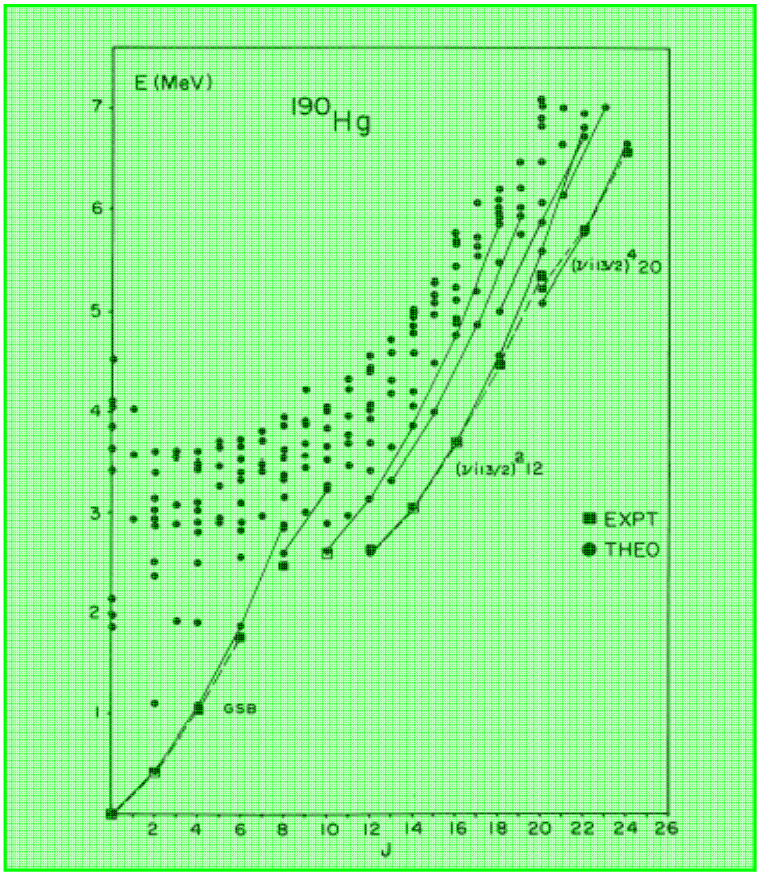

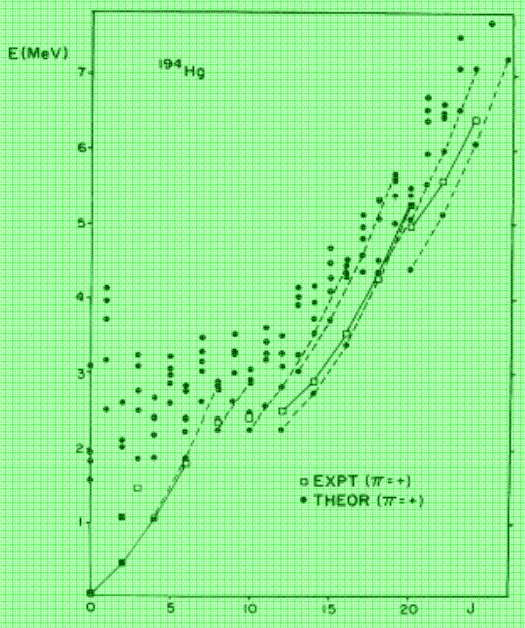

Comparison between calculated (0, 2, and 4qp) (circles) and experimental (squares) positive-parity states in ^{194}Hg. Only the first five calculated levels of each angular momentum J are shown. Sets of states with similar structure (bands) are joined together: dashed lines (calculated bands), solid lines (experimental bands).

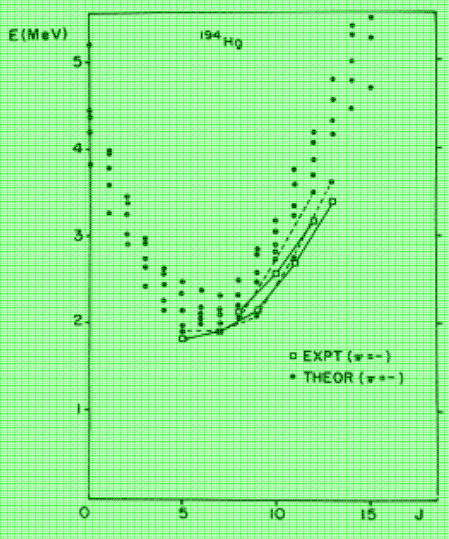

Comparison between calculated (0 and 2qp) (circles) and experimental (squares) negative-parity states in ^{194}Hg. Only the first five calculated levels of each angular momentum J are shown. Sets of states with similar structure (bands) are joined together a

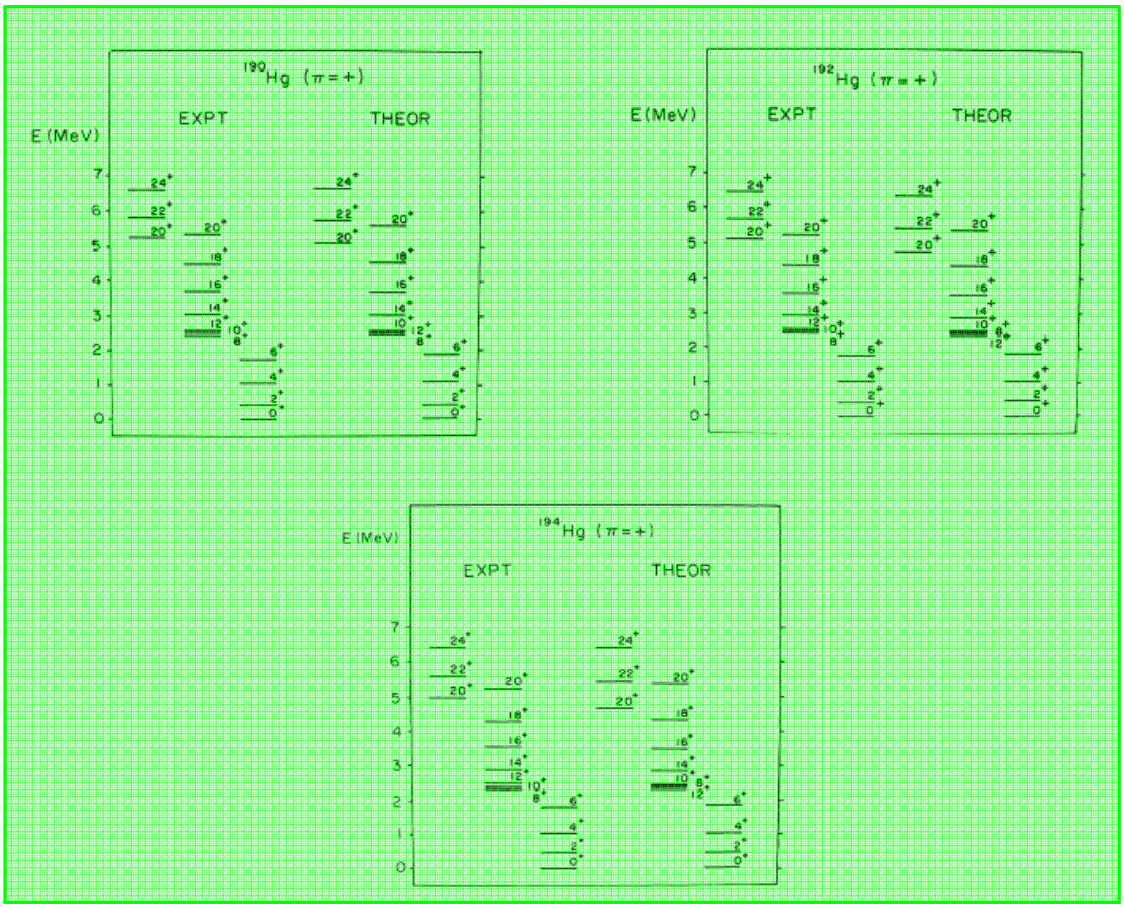

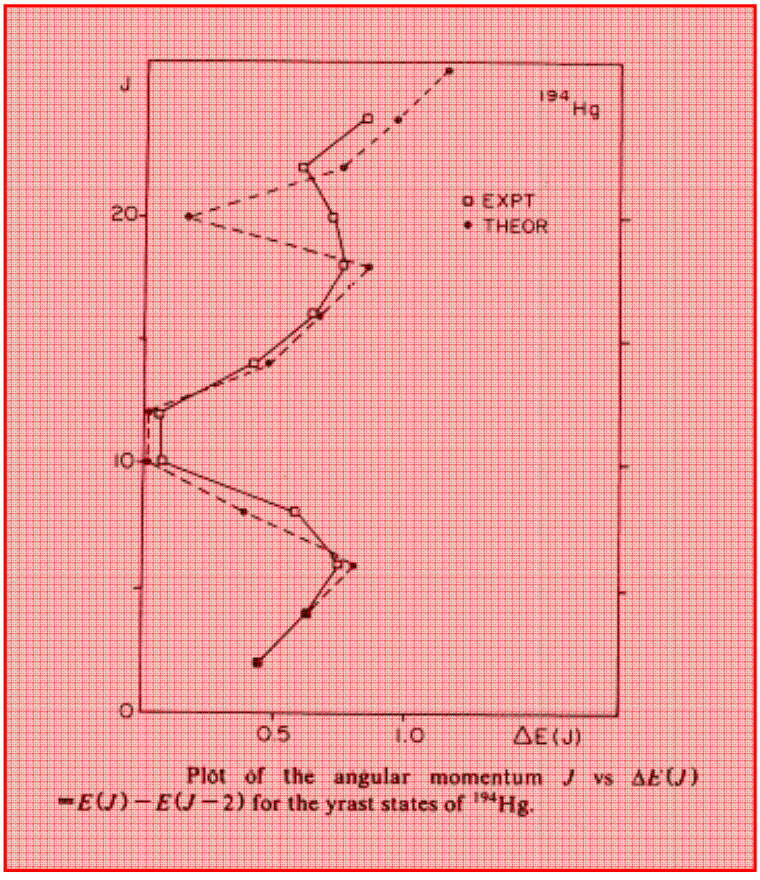

Plot of the angular momentum J vs $\Delta E(J) = E(J) - E(J-2)$ for the yrast states of ^{194}Hg.

3.

Structure of odd-odd nuclei in the interacting boson fermion-fermion model

The IBFFM is able to give an accurate description of the structure of odd-odd nuclei. Odd-odd nuclei constitute a very stringent test of the model:

- A detailed knowledge of even-even cores and odd-mass neighbours is required
- Odd-odd nuclei do not provide the same sort of smoothly varying systematics as do other types of nuclei

IBFFM vs other models ?

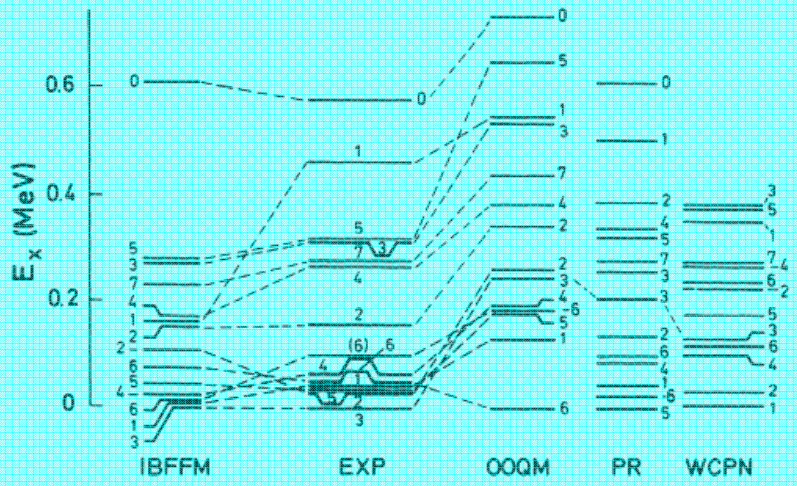

FIG. 7. IBFFM negative-parity energy spectrum of ^{140}La compared with the experimentally known energy spectrum and with the three previous calculations performed using the odd-odd quasiparticle model (OOQM) (Ref. 10), the parabolic rule (PR) (Ref. 2), and the weak-coupling shell model in the proton-neutron formalism (WCPN) (Ref. 11).

IBFFM is successful in describing and predicting

- Level energies
- Electromagnetic properties
- Transfer properties
- Isomers

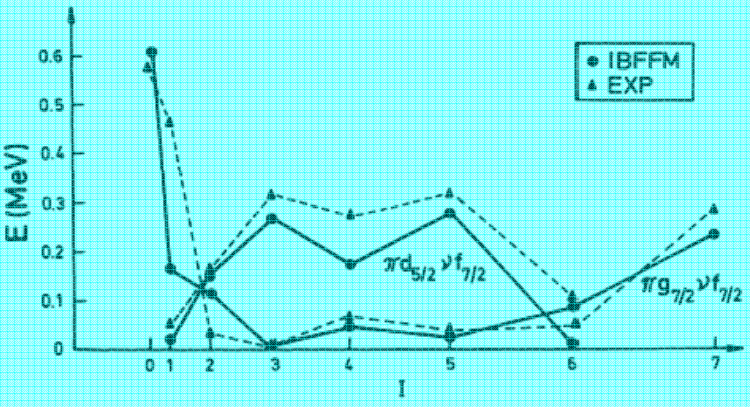

FIG. 8. Classification of the IBFFM levels into multiplets on the basis of largest components in the wave functions. The experimental levels of ^{140}La are compared with the theoretical spectra on the basis of level energies, electromagnetic deexcitation, and transfer properties. IBFFM and experimental levels are presented by solid circles and triangles, respectively.

The IBFFM Hamiltonian for an odd-odd nucleus is:

$$H = H_B + H_{\nu F} + H_{\pi F} + V_{\nu BF} + V_{\pi BF} + V_{\pi\nu}$$

H_B is the boson Hamiltonian of IBM-1 describing a system of N interacting bosons (correlated S and D pairs) that approximate the valence nucleon pairs:

$$\begin{aligned} H_B &= \varepsilon\, \hat{N} + \frac{1}{2}\, v_0\, \left([d^\dagger \times d^\dagger]_{(0)} \times [\tilde{s} \times \tilde{s}]_{(0)} + h.c.\right)_{(0)} \\ &+ \frac{1}{\sqrt{2}}\, v_2\, \left([d^\dagger \times d^\dagger]_{(2)} \times [\tilde{d} \times \tilde{s}]_{(2)} + h.c.\right)_{(0)} \\ &+ \sum_{L=0,2,4} \frac{1}{2}\, C_L\, \sqrt{2L+1}\, \left([d^\dagger \times d^\dagger]_{(L)} \times [\tilde{d} \times \tilde{d}]_{(L)}\right)_{(0)} \end{aligned}$$

$$n_s = N - n_d$$

$H_{\pi F}$ and $H_{\nu F}$ are the fermion Hamiltonians containing quasiparticle energies of protons and neutrons, respectively. The quasiparticle energies and occupation probabilities contained in the fermion Hamiltonian, and other terms, are obtained in a BCS calculation with some standard set of single fermion energies. For protons ($\alpha = \pi$) and for neutrons ($\alpha = \nu$).

$$H_{\alpha F} = \sum_i \varepsilon_{\alpha_i}\, a^\dagger_{\alpha_i} \tilde{a}_{\alpha_i}$$

$V_{\nu BF}$ and $V_{\pi BF}$ are the IBFM-1 boson-fermion interactions containing the dynamical, exchange and monopole interactions. For protons ($\alpha = \pi$) and for neutrons ($\alpha = \nu$).

$$V_{\alpha BF} = V_{\alpha DYN} + V_{\alpha EXC} + V_{\alpha MON}$$

$$V_{\alpha DYN} = \Gamma_0 \sum_{\alpha j_1 \alpha j_2} \sqrt{5}\, (u_{\alpha j_1} u_{\alpha j_2} - v_{\alpha j_1} v_{\alpha j_2})\, \langle \alpha j_1 \parallel Y_2 \parallel \alpha j_2 \rangle\, \left([a^\dagger_{\alpha j_1} \times \tilde{a}_{\alpha j_2}]^{(2)} \times Q_B^{(2)}\right)^{(0)}$$

$Q_B^{(2)}$ is the standard boson quadrupole operator

$$Q_B^{(2)} = [s^\dagger \times \tilde{d} + d^\dagger \times \tilde{s}]^{(2)} + \chi [d^\dagger \times \tilde{d}]^{(2)}$$

$$V_{\alpha EXC} = \Lambda_0 \sum_{\alpha j_1 \alpha j_2 \alpha j_3} (-2) \sqrt{\frac{5}{2\ \alpha j_3 + 1}}\ (u_{\alpha j_1} v_{\alpha j_3} + v_{\alpha j_1} u_{\alpha j_3})\ \ (u_{\alpha j_2} v_{\alpha j_3} + v_{\alpha j_2} u_{\alpha j_3})$$

$$\langle \alpha j_3 \parallel Y_2 \parallel \alpha j_1 \rangle\ \langle \alpha j_3 \parallel Y_2 \parallel \alpha j_2 \rangle\ : \left([a^\dagger_{\alpha j_1} \times \tilde{d}\ ]_{\alpha j_3} \times [\tilde{a}_{\alpha j_2} \times d^\dagger\ ]_{\alpha j_3} \right)^{(0)} :$$

$$V_{\alpha MON} = A_0 \sum_{\alpha j} \sqrt{5}\ (2\alpha j + 1)\ \left([a^\dagger_{\alpha j} \times \tilde{a}_{\alpha j}]^{(0)} \times [d^\dagger \times \tilde{d}]^{(0)} \right)^{(0)}$$

$V_{\pi\nu}$ is the residual proton-neutron interaction taken in the form of spin-spin, surface-delta, spin-spin-delta, tensor or multipole-multipole interaction.

$$H_{\sigma\sigma} = -\sqrt{3}\ V_{\sigma\sigma}\ [\vec{\sigma}_\pi \cdot \vec{\sigma}_\nu]$$

$$H_\delta = 4\pi\ V_\delta\ \delta(\vec{r}_\pi - \vec{r}_\nu)\ \delta(r_\pi - R_0)\ \delta(r_\nu - R_0)$$

$$H_{\sigma\sigma\delta} = 4\pi\ V_{\sigma\sigma\delta}\ [\vec{\sigma}_\pi \cdot \vec{\sigma}_\nu]\ \delta(\vec{r}_\pi - \vec{r}_\nu)\ \delta(r_\pi - R_0)\ \delta(r_\nu - R_0)$$

$$H_T = V_T \left(3\ \frac{[\vec{\sigma}_\pi \cdot \vec{r}_{\pi\nu}]\ [\vec{\sigma}_\nu \cdot \vec{r}_{\pi\nu}]}{r^2_{\pi\nu}} - [\vec{\sigma}_\pi \cdot \vec{\sigma}_\nu] \right)$$

$$H_{MM} = 4\pi\ \frac{\delta(r_\pi - r_\nu)}{r_\pi r_\nu} \sum_{\kappa\mu}\ V_\kappa\ Y^*_{\kappa\mu}(\pi)\ Y_{\kappa\mu}(\nu)$$

$$\vec{r}_{\pi\nu} = \vec{r}_\pi - \vec{r}_\nu \qquad R_0 = 1.2\ A^{\frac{1}{3}}\ \ fm$$

The electromagnetic operators have the form (for protons ($\alpha = \pi$) and for neutrons ($\alpha = \nu$)):

$$M(E2) = M_B(E2) + M_\pi(E2) + M_\nu(E2)$$

$$M_B(E2) = \frac{3}{4\pi} R_0^2 \, e^{VIB} \left([s^\dagger \times \tilde{d} + d^\dagger \times \tilde{s}]^{(2)} + \chi [d^\dagger \times \tilde{d}]^{(2)} \right)$$

$$R_0^2 = 0.0144 \; A^{\frac{2}{3}} \qquad barn$$

$$M_\alpha(E2) = \frac{3}{5} R_0^2 \, e_\alpha \, Y_2(\alpha)$$

$$\vec{M}(M1) = \vec{M}_B(M1) + \vec{M}_\pi(M1) + \vec{M}_\nu(M1)$$

$$\vec{M}_B(M1) = \sqrt{\frac{3}{4\pi}} \sqrt{10} \, g_R \, [d^\dagger \times \tilde{d}]^{(1)}$$

$$\vec{M}_\alpha(M1) = \sqrt{\frac{3}{4\pi}} \left[g_l(\alpha) \, \vec{l}(\alpha) + g_s(\alpha) \, \vec{s}(\alpha) + g_T(\alpha) \, (Y_2(\alpha) \times \vec{s}(\alpha))_1 \right]$$

Spherical nuclei

Parabolic rule for proton-neutron multiplets in the particle-vibration model

Exchange of the quadrupole phonon

The particle-quadrupole vibration interaction is

$$H_2 = \sqrt{20\pi}a_2|Y_2(b_2^\dagger + b_2)|_0$$

$$a_2 = \tfrac{1}{3}(4\pi)^{\ddagger}\frac{1}{ZR_0^2}\langle k\rangle[B(\mathrm{E2};2_1^+ \to 0_1^+)_{\mathrm{vib}}]^{\ddagger}$$

For the quasiparticle, we also include the usual blocking factors U and V in the interaction strength a_2. The symbol $b_2^\dagger$ denotes the creation operator of the quadrupole phonon.

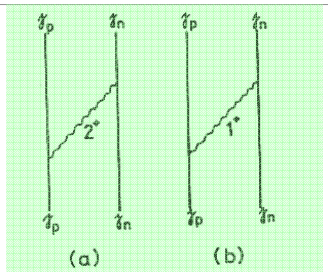

Second-order diagrams for exchange of the quadrupole (fig. a) and spin-vibrational phonons (fig. b).

The contribution to the splitting of the multiplet $|(j_p, j_n)I = |j_p - j_n|, \ldots, j_p + j_n\rangle$ coming from the exchange of quadrupole phonons (fig. a) is

$$\delta E_2 = -\alpha_2 \mathscr{V}\cdot\frac{[I(I+1)-j_n(j_n+1)-j_p(j_p+1)]^2+[I(I+1)-j_n(j_n+1)-j_p(j_p+1)]}{2j_n(2j_n+2)2j_p(2j_p+2)}$$

$$+\frac{\alpha_2\mathscr{V}}{12},$$

$$\alpha_2 = 15a_2^2/\hbar\omega_2$$

Here $\hbar\omega_2$ is the energy of the quadrupole phonon. We assume the coupling strength a_2 to be equal both for protons and for neutrons.

We rewrite the I-dependent terms

$$\delta E_2(I) = A[I(I+1)]^2 + BI(I+1)$$

where A and B stand for the factors which multiply $[I(I+1)]^2$ and $I(I+1)$ respectively.

The quantity $\mathscr{V}$ is the occupation number defined as $\mathscr{V} = 1$ if $|j_p\rangle$ and $|j_n\rangle$ are both particle-like or both hole-like: $\mathscr{V} = -1$ if $|j_n\rangle$ is particle-like and $|j_n\rangle$ is hole-like, or vice versa.

Inclusion of the spin-vibrational 1^+ phonon

The particle-spin-vibration interaction reads

$$H_1 = \sqrt{3}a_1[\sigma_1 \times (b_1^\dagger + b_1)]_0$$

Here a_1 is the coupling strength defined as $a_1 = \kappa_1(\hbar\omega_1/2c_1)^{\frac{1}{2}}$, σ_1 is the spin operator and $b_1^\dagger$ the creation operator of the $\lambda = 1^+$ spin vibration

We derive the expression for the contribution to the energy shift of the $|(j_p j_n)I\rangle$ states due to the exchange of the 1^+ phonon

$$\delta E_1(I) = B_1 I(I+1) + \alpha_1 \frac{j_n(j_n+1)+j_p(j_p+1)}{(2j_n+2)(2j_p+2)}$$

$$B_1 = -\alpha_1 \frac{\xi}{(2j_p+2)(2j_n+2)} \qquad \alpha_1 = 4\frac{a_1^2}{\hbar\omega_1}$$

$$\xi = \begin{cases} 1 & \text{if } \mathcal{N} = -1, \quad \dfrac{(2j_p+2)(2j_n+2)}{2j_p 2j_n} \quad \text{if } \mathcal{N} = 1, \\ -\dfrac{2j_p+2}{2j_p} & \text{if } \mathcal{N} = 0^-, \quad -\dfrac{2j_n+2}{2j_n} \quad \text{if } \mathcal{N} = 0^+. \end{cases}$$

$\mathcal{N}$ is the Nordheim number defined as

$$\mathcal{N} = j_p - l_p + j_n - l_n$$

For $\mathcal{N} = 0$, we use the labels $-$ and $+$. The symbols $\mathcal{N} = 0^-$ and $\mathcal{N} = 0^+$ denote the situations $j_n - l_n = -\frac{1}{2}$, $j_p - l_p = \frac{1}{2}$ and $j_n - l_n = \frac{1}{2}$, $j_p - l_p = -\frac{1}{2}$, respectively.

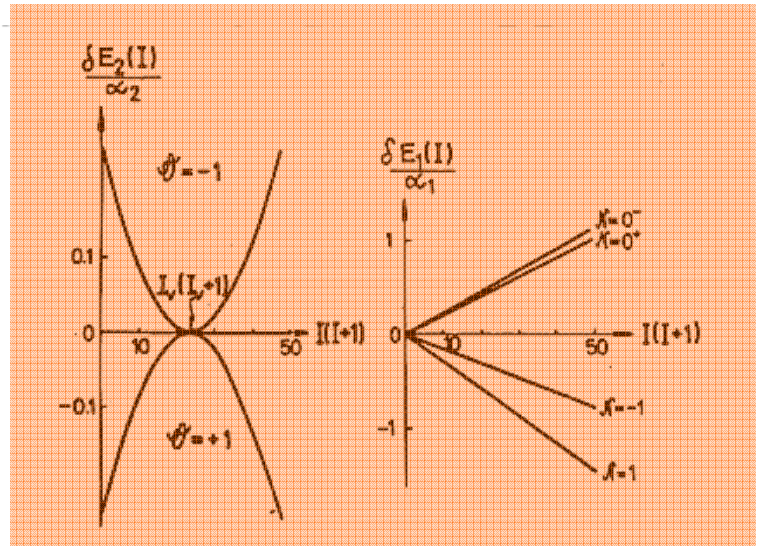

Illustration of energy contributions coming from the exchange of the quadrupole phonon (a) and the spin-vibrational phonon (b) for the multiplet ($j_p = \frac{5}{2}, j_n = \frac{7}{2}$), for four possible combinations of the pair ($\mathcal{N}$, $\mathcal{N}$).

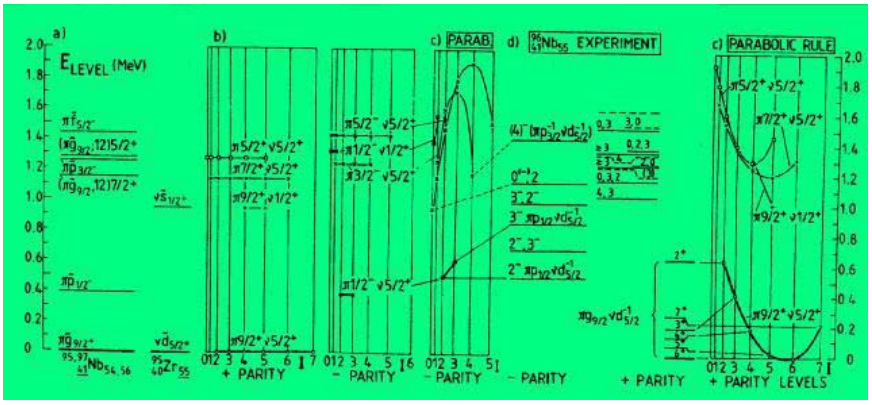
a)
b)
c) PARAB.
d) EXPERIMENT
c) PARABOLIC RULE
+ PARITY
- PARITY
- PARITY
- PARITY
+ PARITY
+ PARITY LEVELS

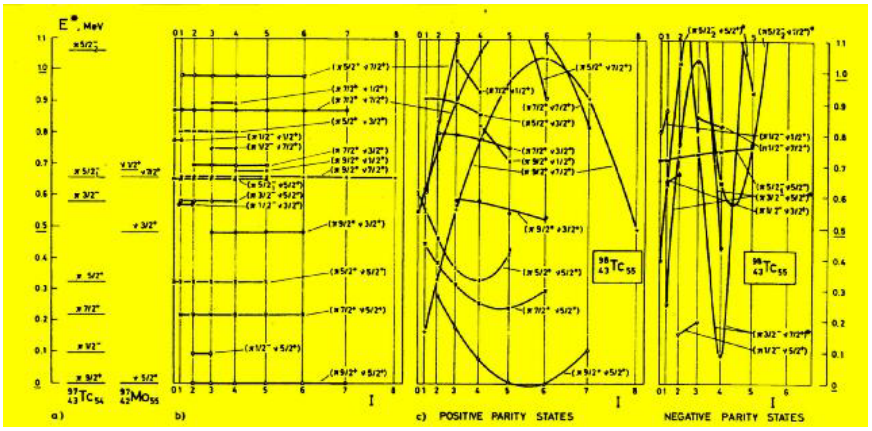
E*, MeV
a)
b)
c) POSITIVE PARITY STATES
NEGATIVE PARITY STATES

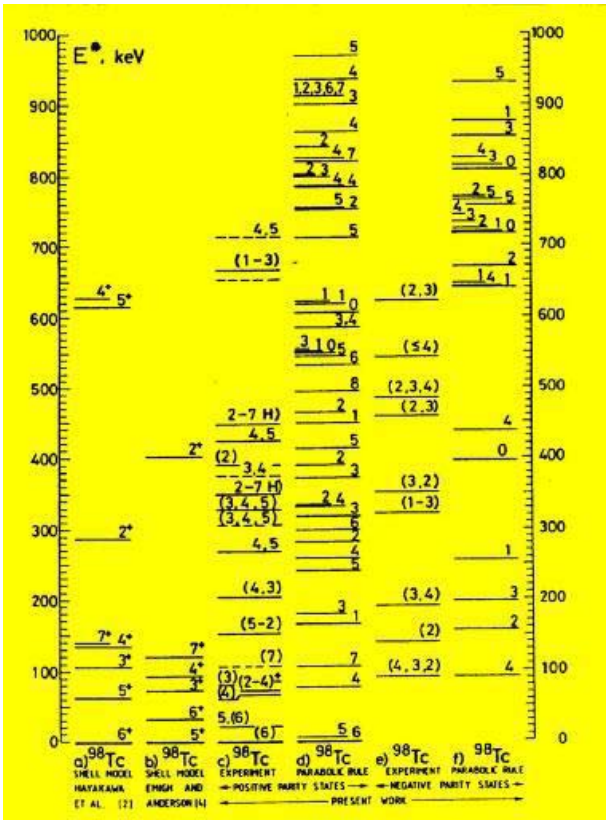
E*, keV
a) 98Tc SHELL MODEL HAYAKAWA ET AL. [2]
b) 98Tc SHELL MODEL EMGH AND ANDERSON [4]
c) 98Tc EXPERIMENT
d) 98Tc PARABOLIC RULE
e) 98Tc EXPERIMENT
f) 98Tc PARABOLIC RULE
POSITIVE PARITY STATES
NEGATIVE PARITY STATES
PRESENT WORK

For spherical nuclei, with only the dynamical interaction and $\chi = 0$ → $r_0 = a\sqrt{\frac{4\pi}{5N}}$

^{96}Y

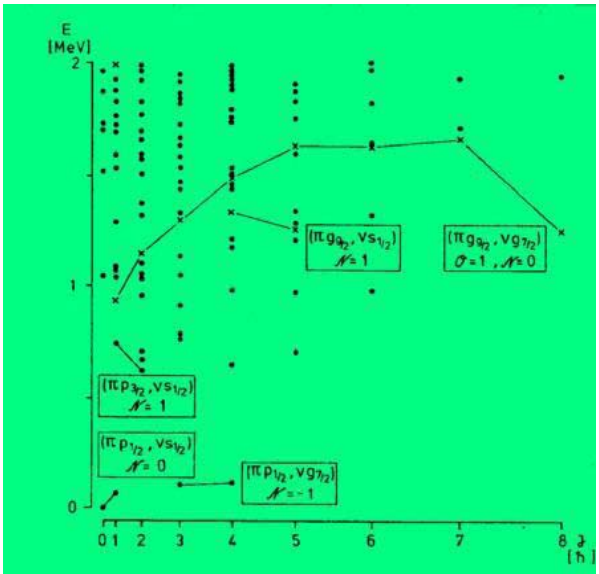

Fig. 4. Negative- and positive-parity levels of ^{96}Y calculated in IBFFM. Negative parity levels are denoted by full circles and positive-parity by crosses. The states classified into the same multiplet on the basis of largest components in the wave functions, are connected by full line

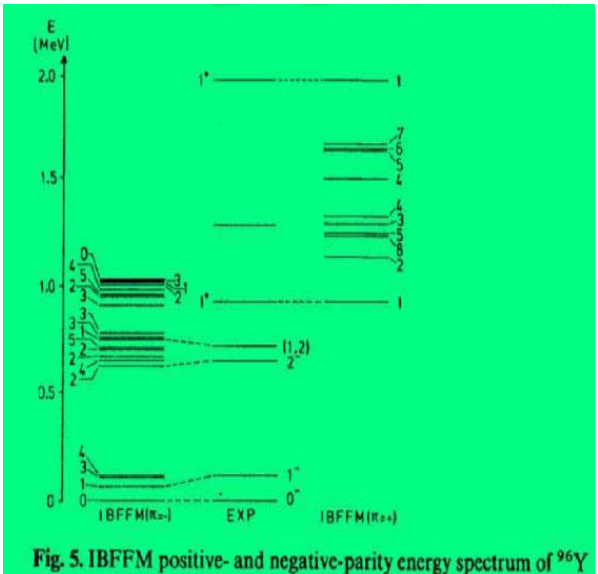

Fig. 5. IBFFM positive- and negative-parity energy spectrum of ^{96}Y in comparison to the available experimental data. The excitation energy of the 8^+ level is not known, but it should amount to ≥ 1 MeV, see text

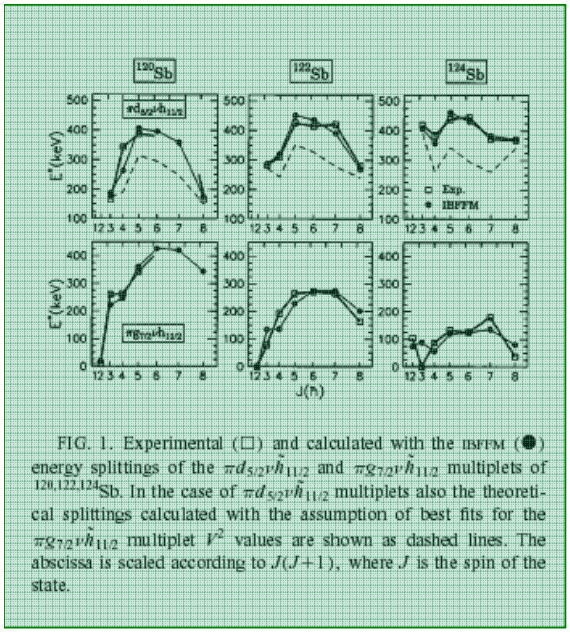

FIG. 1. Experimental (□) and calculated with the IBFFM (●) energy splittings of the $\pi d_{5/2}\nu h_{11/2}$ and $\pi g_{7/2}\nu h_{11/2}$ multiplets of ^{120,122,124}Sb. In the case of $\pi d_{5/2}\nu h_{11/2}$ multiplets also the theoretical splittings calculated with the assumption of best fits for the $\pi g_{7/2}\nu h_{11/2}$ multiplet V^2 values are shown as dashed lines. The abscissa is scaled according to $J(J+1)$, where J is the spin of the state.

In the whole sequence of nuclei it have been used the same:

Cores

Dynamical, exchange and monopole interactions for protons

Dynamical, exchange and monopole interactions for neutrons

Occupation probabilities for protons

Residual proton-neutron delta interaction

Occupation probabilities for neutrons depend on the isotope

Parabolic like structures are present in spherical nuclei even in cases when other interactions (not the dynamical) dominate.

Sb isotopes

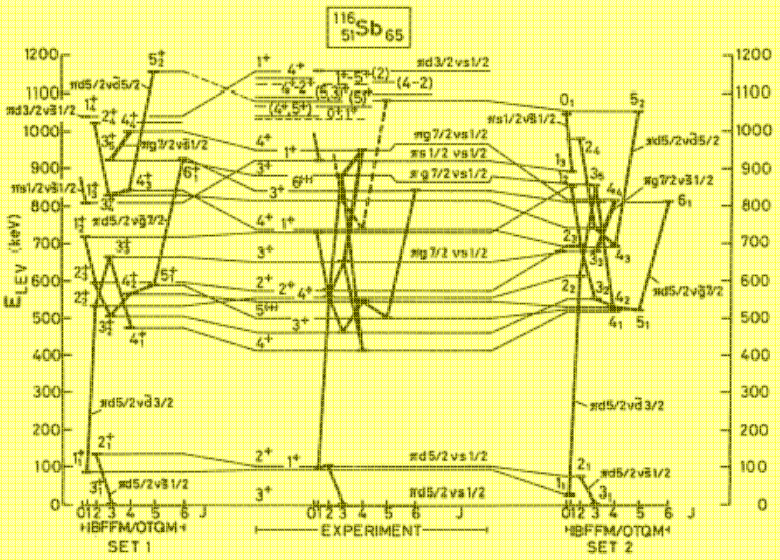

FIG. 6. IBFFM energy spectrum of ^{116}Sb in comparison with experimental data. The solid lines connect the members of the given multiplet. The leading proton-neutron configurations for several multiplets were identified on the basis of the $(^3He,d)$ proton transfer results [4].

TABLE III. Comparison of measured and calculated in IBFFM spectroscopic factors for the ^{121}Sb$(p,d)^{120}$Sb one-neutron transfer reaction. The first two columns contain the energy, spin, and parity of the final states involved in the reaction taken from Ref. [8].

Energy (keV)	J^π	ℓ_n	$S_{(p,d)}$ [a]	$S_{\rm IBFFM}$ [b]
0	1^+	2	0.11	0.15
78	3^+	0	0.19	0.12
149	3^+	0	0.05	0.03
166	3^-	5	0.63	0.44
193	2^+	0	0.11	0.08
		2	0.07	0.05
233	2^+	0	0.06	0.03
		2	0.12	0.05
334	$4^{(+)}$	2	0.10	0.19
343	$4^{(-)}$	5	0.54	0.39
387	$(3-5)$	5	0.44	0.61
390	$(2,3)^+$	2	0.06	0.07
438	(2)	0	0.01	0.02
		2	0.02	0.13

[a] Reference [9].
[b] $S/(2j_{\rm target}+1)$.

TABLE IV. Comparison of measured and calculated in IBFFM spectroscopic factors for the one-neutron transfer reactions leading to ^{122}Sb. The first two columns contain the energy, spin, and parity of the final states involved in the reaction taken from Ref. [13].

Energy (keV)	J^π	ℓ_n	$S_{(p,d)}$ [a]	ℓ_n	$S_{(d,t)}$ [b]	$S_{\rm IBFFM}$ [d]	ℓ_n	$S_{(d,p)}$ [c]	$S_{\rm IBFFM}$
0	2^-	5	0.20		0.46	0.46			
61	3^+	0	0.23	(0)	0.45	0.13	(2)	0.05	0.00
78	3^-	5	0.46			0.52			
121	1^+						(2)	0.30	0.47
137	5^+	2	0.38	(2)	0.37	0.20			
164	8^-	5	0.50			0.53			
167	2^+	2	0.10			0.14	(2)	0.09	0.09
193	4^-	5	0.41			0.58			
210	4^+	0	0.30	(0)	0.34	0.11			
255	3^+						0	0.34	0.44
264	5^-					0.66			
265	7^-	5	0.62			0.57			
272	6^-					0.68			
283	3^-						(5)	2.40	0.40
311	4^-						(5)	0.80	0.43
323	2^+						0	0.30	0.40
334	3^+	2	0.07		0.09	0.22	2	0.16	0.01
394	4^+						2	0.45	0.46
397	2^+	2	0.03		0.10		2	0.45	0.38
414	6^-								0.55
$\approx$ 420	7^-	5	0.03			0.16	(5)	1.70	0.43
425	5^-								0.49
481	4^+	2	0.19	(2)	0.30	0.22			
484	3^+						2	0.51	0.60

[a] Reference [9].
[b] Reference [7].
[c] Reference [13].
[d] $S/(2j_{\rm target}+1)$.

TABLE VI. Magnetic dipole (μ in μ_N) and electric quadrupole (Q in e b) moments of some $^{120-124}$Sb states.

Nucleus	E^*	J^π	μ_{expt} [a]	μ_{IBFFM}	Q_{expt} [a]	Q_{IBFFM}
^{120}Sb	0 keV	1^+	$\pm 2.34(22)$	$+2.25$		-0.10
	78 keV	3^+	$+2.584(6)$	$+2.67$	$\pm 0.41(4)$	-0.47
		8^-	$\pm 2.34(4)$	$+2.45$		-0.51
^{122}Sb	0 keV	2^-	$-1.905(20)$	-2.33	$+0.85(11)$	-0.08
	61 keV	3^+	$+2.983(12)$	$+3.07$	$\pm 0.41(4)$	-0.48
	137 keV	5^+	$+3.05(10)$	$+3.07$		-0.62
^{124}Sb	0 keV	3^-	$\pm 1.20(2)$	-1.23	$+1.87(38)$	$+0.35$
	41 keV	3^+	$+2.970(33)$	$+3.01$		-0.46
	125 keV	6^-	$+0.384(12)$	$+0.36$		$+0.16$

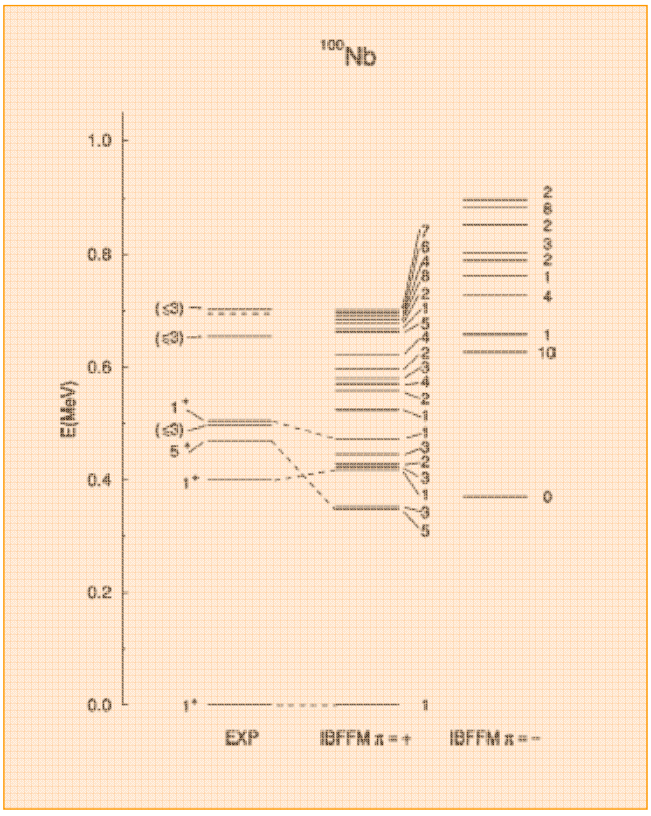

1^+ π g9/2 ν g7/2

5^+ π g9/2 ν s1/2

8^+ π g9/2 ν g7/2

10^- π g9/2 ν h11/2

5^+ 1.5 s isomer

10^- possibly 100 – 150 keV higher

10^- or 8^+ candidates for the 12 µs isomer

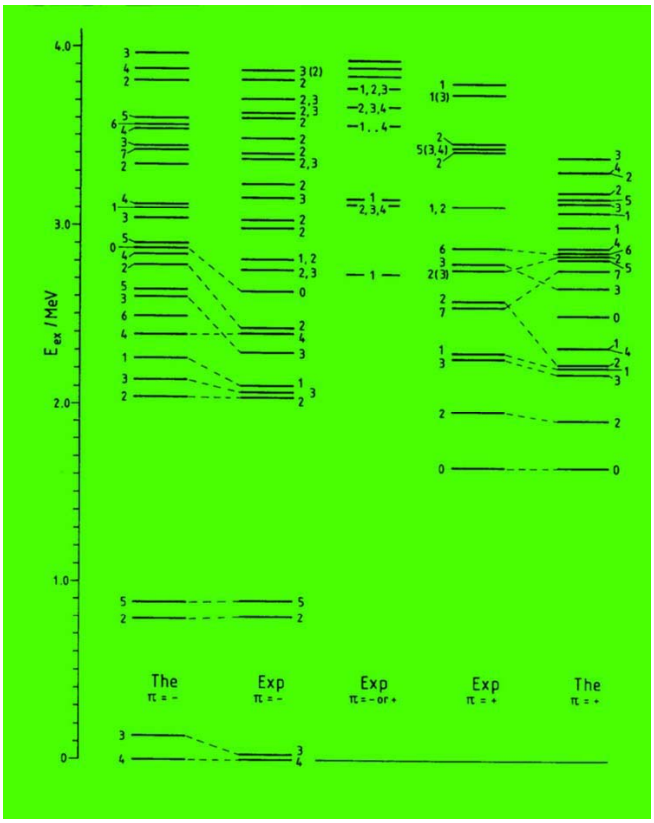

^{40}K

State (keV)	$T_{1/2}$	
	Exp	The
3_1^- (30)	4.24(8) ns	5.2 ns
2_1^- (800)	0.28(4) ps	0.23 ps
5_1^- (891)	0.87(14) ps	0.6 ps
2_2^- (2047)	0.34(4) ps	0.3 ps
3_2^- (2070)	0.47(10) ps	0.1 ps
1_1^- (2104)	0.52(10) ps	0.14 ps
4_2^- (2397)	0.035(14) ps	0.03 ps
0_1^- (2626)	0.21(4) ps	0.2 ps
1_1^+ (2290)	0.083(14) ps	0.25 ps
3_2^+ (2787)	<0.04 ps	0.07 ps
6_1^+ (2879)	0.27(10) ps	0.6 ps

^{40}K

Transition[a]	E_γ/keV	Gamma-branching	
		Exp[b]	The[c]
2_1^- (800) → 4_1^- (0)	800	0.15	0.17
→ 3_1^- (30)	770	100	100
5_1^- (891) → 4_1^- (0)	891	99	99
→ 3_1^- (30)	862	1	0.1
2_2^- (2047) → 4_1^- (0)	2047	29	128
→ 3_1^- (30)	2018	29	100
→ 2_1^- (800)	1247	41	41
3_2^- (2070) → 4_1^- (0)	2070	36	56
→ 3_1^- (30)	2040	49	49
→ 2_1^- (800)	1270	9	6
→ 5_1^- (891)	1178	7	3
1_1^- (2104) → 3_1^- (30)	2074	70	70
→ 2_1^- (800)	1304	29	96
→ 2_2^- (2047)	57	–	0.1
→ 3_2^- (2070)	34	–	0.0
4_2^- (2397) → 4_1^- (0)	2397	26	7
→ 3_1^- (30)	2367	67	67
→ 2_1^- (800)	1597	–	0.4
→ 5_1^- (891)	1506	–	0.1
→ 2_2^- (2047)	350	–	0.0
→ 3_2^- (2070)	327	7	1
→ 3_3^- (2291)	106	–	0.01
0_1^- (2626) → 2_1^- (800)	1826	30	41
→ 2_2^- (2047)	579	–	0.001
→ 1_1^- (2104)	522	70	70
→ 2_3^- (2419)	207	–	0.0
1_1^+ (2290) → 0_1^+ (1644)	646	56	56
→ 2_1^+ (1959)	331	9	10
→ 3_1^+ (2260)	30	–	0.0
3_2^+ (2787) → 2_1^+ (1959)	828	17.4	17.4
→ 3_1^+ (2260)	527	–	0.5
→ 1_1^+ (2290)	497	–	0.0
→ 2_2^+ (2576)	211	–	0.0
→ 2_3^+ (2757)	30	–	0.0

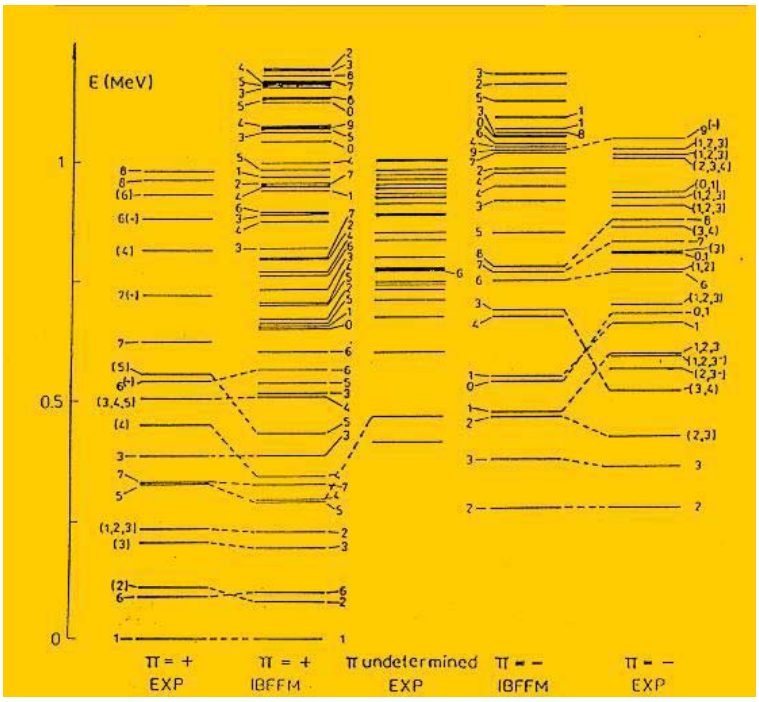

The structure of ^{106}Ag is very complex. The ground states of odd-mass Ag nuclei are $7/2^+$ states based on the proton g9/2 configuration. The IBFFM is successful in the description even of such nuclei.

Deformed nuclei

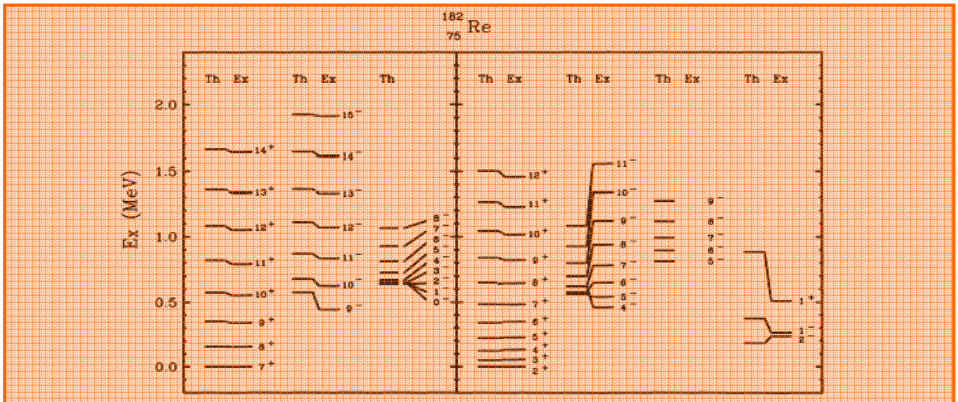

IBFFA-calculated excitation energies for states in odd-odd ^{182}Re compared with experimental data. Because the experimental separation between the 7^+ triplet and 2^+ singlet couplings is not known, the figure is divided into two parts, using each coupling as the reference point. Otherwise, the triplet coupling is shown on the left of a pair of bands, the singlet coupling on the right. For example; 9^- triplet, 0^- singlet.

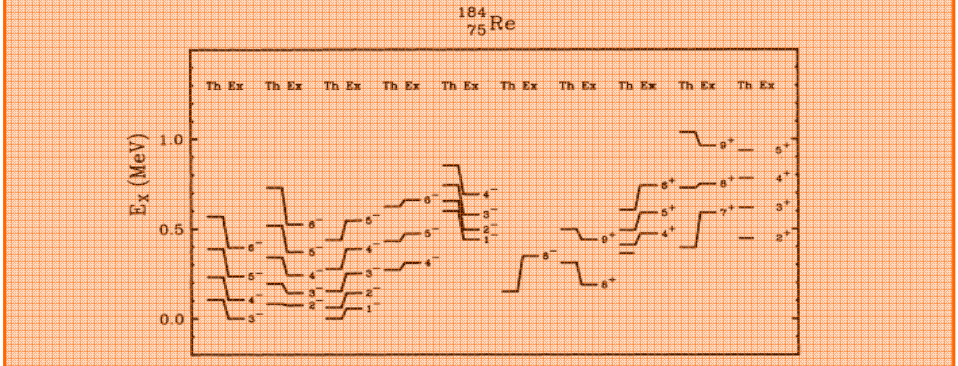

IBFFA-calculated excitation energies for states in odd-odd ^{184}Re compared with experimental data. The bands are plotted in pairs, with the triplet coupling on the left, the singlet coupling on the right of each pair.

Scholten
PRC 37

Quadrupole moments for odd-odd Re isotopes.

Isotope	J^π	Q_{IBA} (e b)	Q_{exp} (e b)
^{180}Re	6^-	6.50	
	1^-	6.45	
^{182}Re	7^+	5.66	<6.4
	2^+	5.40	>6.6
^{184}Re	3^-	5.06	7.9±0.7
	8^+	4.83	

Magnetic moments for odd-odd Re isotopes.

Isotope	J^π	μ_{IBA} (μ_N)	μ_{exp} (μ_N)
^{180}Re	6^-	2.41	
	1^-	2.35	
^{182}Re	7^+	2.33	2.76±0.07
	2^+	3.28	3.07±0.24
^{184}Re	3^-	3.19	2.50±0.19
	8^+	2.09	2.89±0.13

The investigations of odd-A nuclei have revealed the following decoupled–strongly coupled rule:

(i) The strongly coupled band pattern arises if the odd fermion is a particle coupled to an oblate core, or a hole coupled to a prolate core.

(ii) The decoupled band pattern arises if the odd particle is coupled to a prolate core or a hole to the oblate core.

This rule was extended to odd-odd nuclei in the case of coupling two quasiparticles to the asymmetric rotor.

Rules (i) and (ii) can be expressed in terms of quadrupole moments of the odd particle and the core Taking into account the signs of quadrupole moments $Q(j)<0$, $Q(j^{-1})>0$, $Q(2_1^{\text{prolate}})<0$, and $Q(2_1^{\text{oblate}})>0$, the rule reads

$$\text{if } Q(\bar{j})\cdot Q(2_1^{\text{core}}) \begin{cases} <0, & \text{the band is strongly coupled} \\ >0, & \text{the band is decoupled} , \end{cases}$$

where $\bar{j}$ denotes the odd quasiparticle coupled to the core.

This rule is of more general character, independent of the particular nature of the core. It applies as well to the IBFM and IBFFM.

We note that the case of two particles or holes coupled to the core, referred to as the "peaceful" case in the particle–plus–asymmetric rotor model, corresponds to the inverted parabola of the parabolic rule for odd-odd nuclei;[2] this yields the bandheads with angular momenta $J=j_p+j_n$ and $J=|j_p-j_n|$ as the lowest states on two branches of the parabola.

By coupling the proton particle j_1 and the neutron particle j_2 to the SU(3) boson core, there arise $2(j_1+\frac{1}{2})(j_2+\frac{1}{2})$ bands, based on the states of angular momenta $J=J_1\pm J_2$, with $J_1=j_1, j_1-1, \ldots, \frac{1}{2}$ and $J_2=j_2, j_2-1, \ldots, \frac{1}{2}$. For the particular interaction strengths Γ_1^{SUSY} and Γ_2^{SUSY} the band based on the lowest $J=j_1+j_2$ state exhibits an exact $J(J+1)$ energy rule, with the same moment of inertia as for the ground-state band of the boson core. Furthermore, the states of this band are characterized by the exact quantum numbers $(K_1=j_1, K_2=j_2)K=j_1+j_2$, defined according to the IBFFM relation The other IBFFM bands in the odd-odd system deviate from the $J(J+1)$ energy rule; in general, more so with increasing energy (decrease of K_1, K_2). Simultaneously, the IBFFM wave functions expressed in the KR basis are a mixture of different K values. However, in each state a particular KR basis state dominates. In this way we can attribute approximate quantum numbers $(K_1, K_2)K$ to each state.

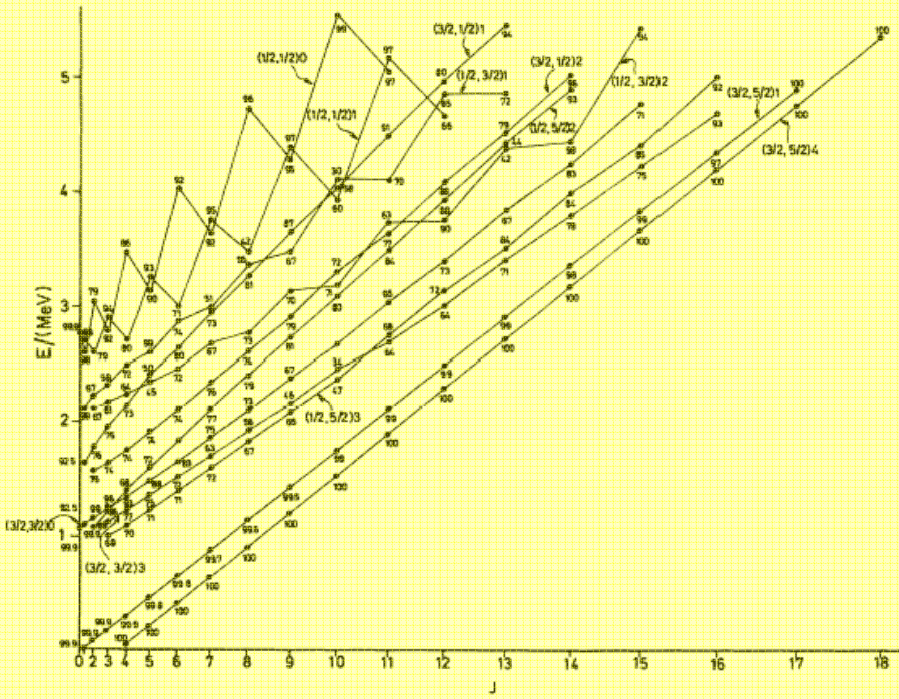

Twelve ground-state bands calculated in the IBFFM for the odd-odd system with $j_1=\frac{3}{2}$ proton hole and $j_2=\frac{5}{2}$ neutron hole coupled to the SU(3) prolate boson core. The $J(J+1)$ scale is employed for the angular momentum axis.

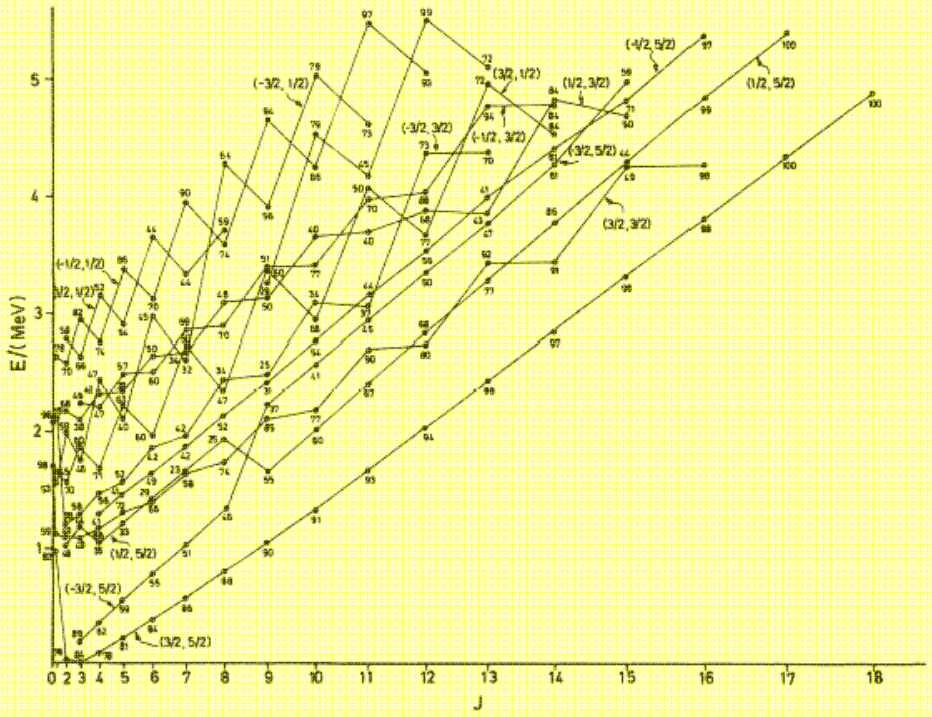

The IBFFM ground-state bands for the odd-odd system with $j_1 = \frac{5}{2}$ proton particle and $j_2 = \frac{5}{2}$ neutron hole coupled to the SU(3) prolate boson core.

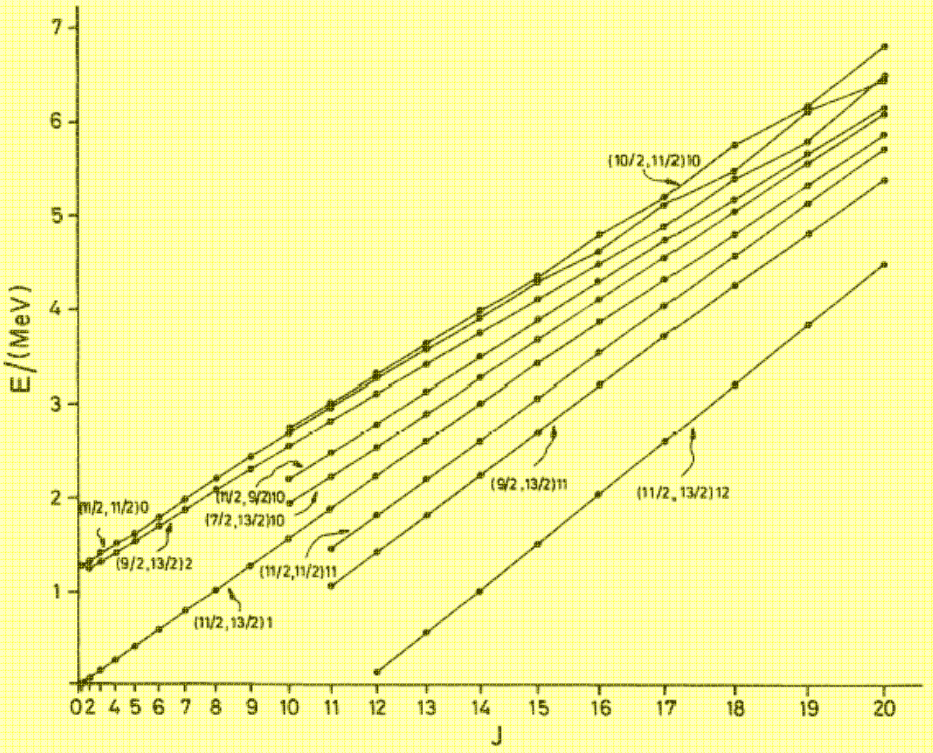

Lowest bands in the odd-odd system with $j_1 = \frac{11}{2}$ proton hole and $j_2 = \frac{13}{2}$ neutron hole coupled to the SU(3) prolate boson core.

Realistic case: Dynamical and exchange interactions different from zero and not limited by supersymmetry constraints

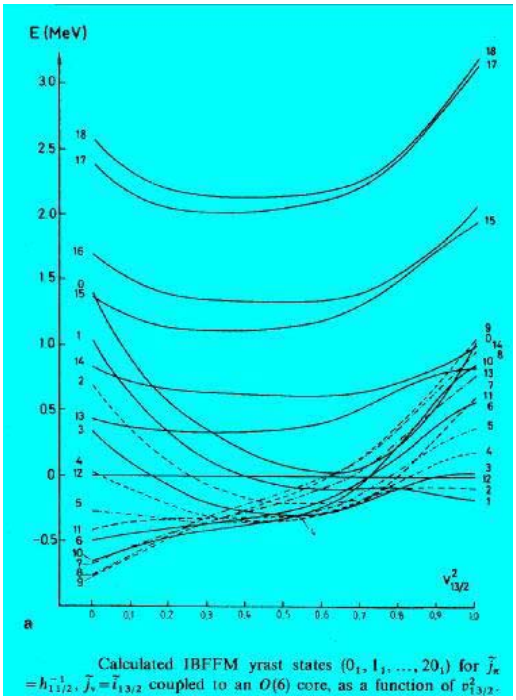

Calculated IBFFM yrast states $(0_1, 1_1, \ldots, 20_1)$ for $\tilde{j}_\pi = h^{-1}_{13/2}$, $\tilde{j}_\nu = \tilde{i}_{13/2}$ coupled to an $O(6)$ core, as a function of $v^2_{13/2}$.

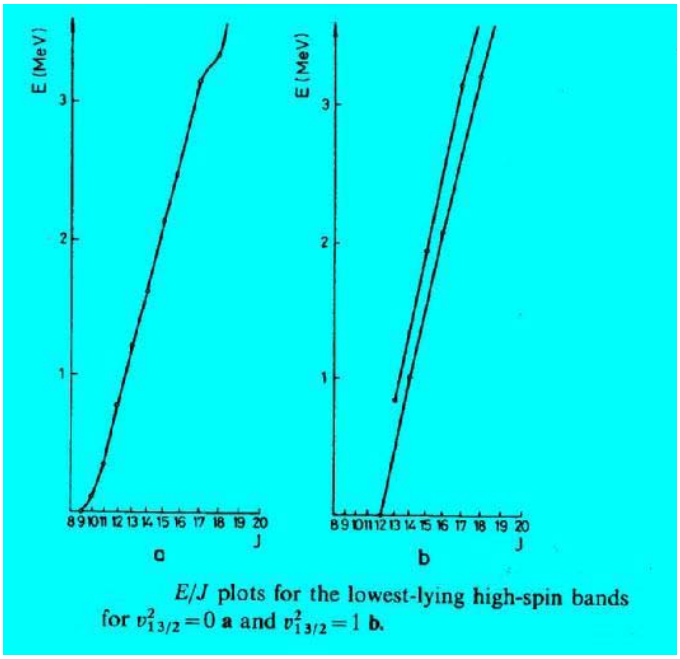

E/J plots for the lowest-lying high-spin bands for $v^2_{13/2}=0$ **a** and $v^2_{13/2}=1$ **b**.

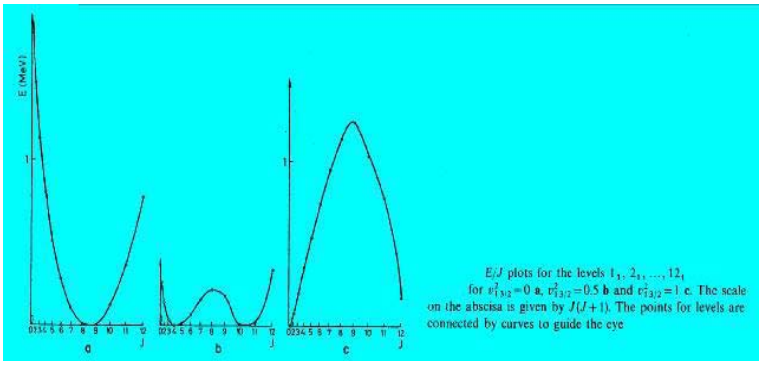

E/J plots for the levels $1_1, 2_1, \ldots, 12_1$ for $v^2_{3/2}=0$ **a**, $v^2_{13/2}=0.5$ **b** and $v^2_{13/2}=1$ **c**. The scale on the abscisa is given by $J(J+1)$. The points for levels are connected by curves to guide the eye

The head of the lowest high-spin band is

$J=j_\pi+j_\nu-3=9$ for $v^2_{13/2}\lesssim 0.2$,
$J=j_\pi+j_\nu-2=10$ for $0.2\lesssim v^2_{13/2}\lesssim 0.5$,
$J=j_\pi+j_\nu-1=11$ for $0.5\lesssim v^2_{13/2}\lesssim 0.8$

and

$J=j_\pi+j_\nu=12$ for $0.8\lesssim v^2_{13/2}$.

A pronounced feature is rather broad region with $J=j_\pi+j_\nu-1=11$ level as the lowest high-spin state. This resembles the $J=j-1$ anomaly for rather broad region around $v^2=0.5$ in odd-even nuclei

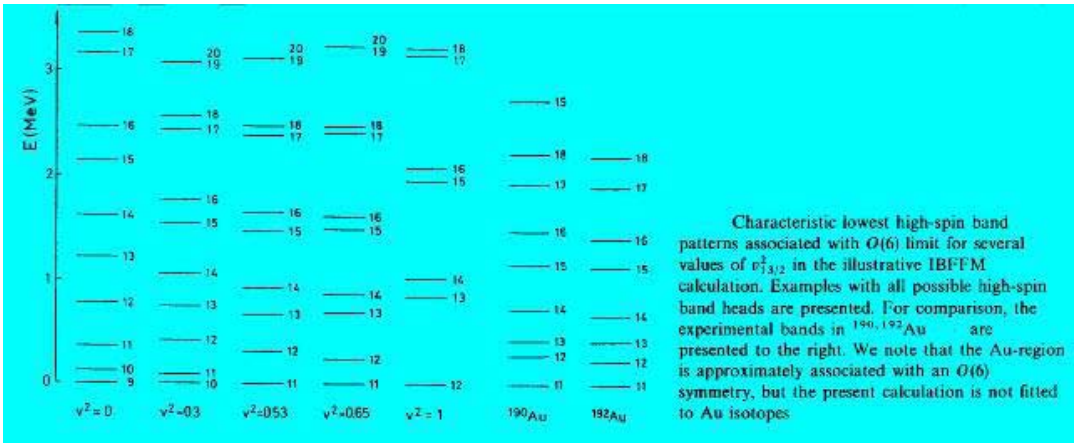

Characteristic lowest high-spin band patterns associated with $O(6)$ limit for several values of $v^2_{13/2}$ in the illustrative IBFFM calculation. Examples with all possible high-spin band heads are presented. For comparison, the experimental bands in ^{190,192}Au are presented to the right. We note that the Au-region is approximately associated with an $O(6)$ symmetry, but the present calculation is not fitted to Au isotopes

Calculated IBFFM yrast states (0_1, 1_1, ..., 20_1) for $\vec{J}_R = \vec{h}_{11/2}^{-1}$, $\vec{J}_V = \vec{i}_{13/2}$ coupled to an $SU(3)$ core, as a function of $v^2_{13/2}$.

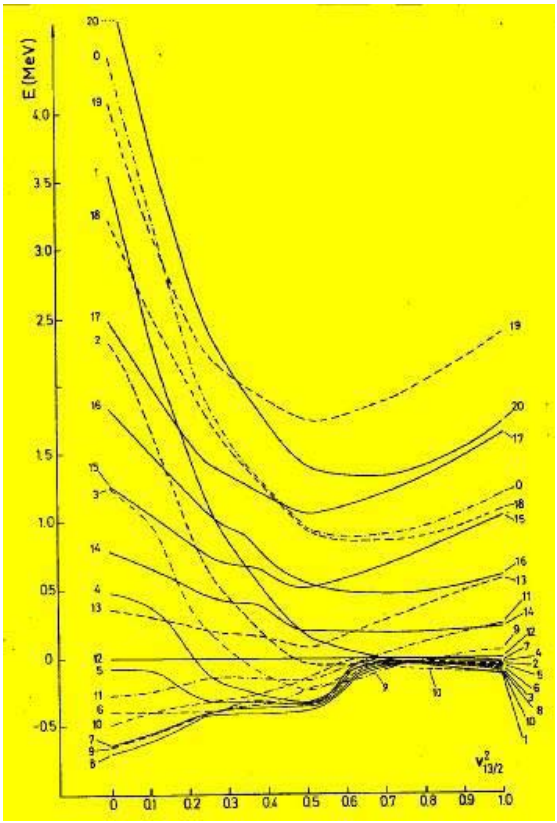

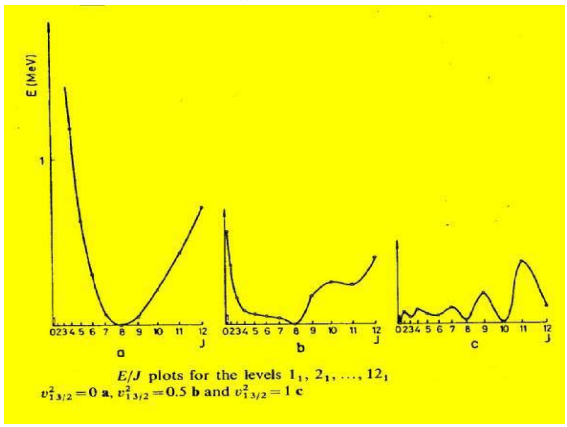

E/J plots for the levels 1_1, 2_1, ..., 12_1 $v^2_{13/2}=0$ **a**, $v^2_{13/2}=0.5$ **b** and $v^2_{13/2}=1$ **c**

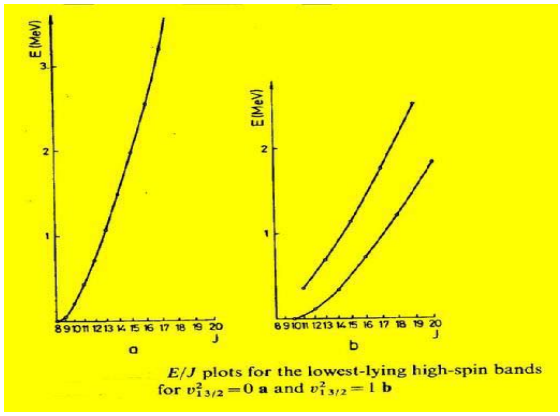

E/J plots for the lowest-lying high-spin bands for $v^2_{13/2}=0$ **a** and $v^2_{13/2}=1$ **b**

Transitional nuclei

^{68}As

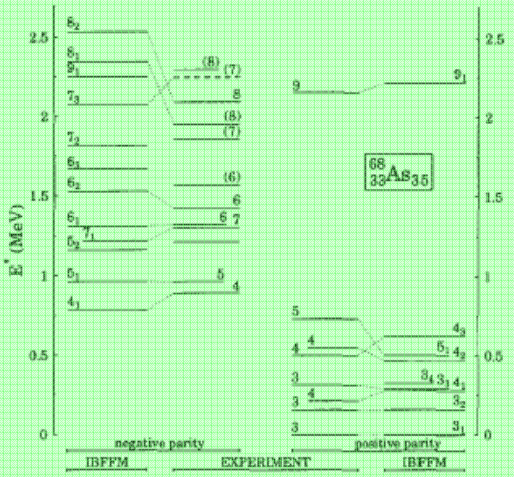

Experimental and theoretical IBFFM energy spectra of the low-lying states in ^{68}As. Up to 0.6 MeV the positive parity levels 3^+, 4^+, 5^+ are shown. In addition, the high spin isomer 9_1^+ is shown. For negative parity the calculated states with $J^\pi = 4_1^-, 5_1^-, 5_2^-, 6_1^-, 6_2^-, 6_3^-, 7_1^-, 7_2^-, 7_3^-, 8_1^-, 8_2^-, 9_1^-$ are shown.

Calculated in IBFFM branching ratios for ^{68}As compared with the experimental data

E_{exp}^* (MeV)	J_{exp}^π ($\hbar$)	$J_i^\pi \rightarrow J_f^\pi$ (theor.)	I_γ Exp.	I_γ Theor.
0.158	3^+	$3_2^+ \rightarrow 3_1^+$	100(6)	100
0.214	4^+	$4_1^+ \rightarrow 3_2^+$	6(2)	5
		$\rightarrow 3_1^+$	100(14)	100
0.313	3^+	$3_3^+ \rightarrow 4_1^+$	<2	4
		$\rightarrow 3_2^+$	16(2)	86
		$\rightarrow 3_1^+$	100(2)	100
0.500	4^+	$4_3^+ \rightarrow 3_3^+$	5(1)	12
		$\rightarrow 4_1^+$	5(1)	5
		$\rightarrow 3_1^+$	100(2)	100
0.550	4^+	$4_2^+ \rightarrow 3_3^+$	9(1)	100
		$\rightarrow 4_1^+$	36(2)	16
		$\rightarrow 3_2^+$	100(4)	9
		$\rightarrow 3_1^+$	48(2)	10
0.733	5^+	$5_1^+ \rightarrow 4_2^+$	17(2)	3
		$\rightarrow 4_3^+$	<6	26
		$\rightarrow 4_1^+$	100(5)	100
3.183	$11^{(+)}$	$11_1^+ \rightarrow 9_1^+$	100(3)	100
0.965	$5^{(-)}$	$5_1^- \rightarrow 4_1^-$	100(3)	100
1.304	$7^{(-)}$	$7_1^- \rightarrow 5_1^-$	100(3)	100
1.323	$6^{(-)}$	$6_1^- \rightarrow 5_1^-$	100(4)	100
		$\rightarrow 4_1^-$	<3	4
1.427	$6^{(-)}$	$6_2^- \rightarrow 5_2^-$	8(2)	2
		$\rightarrow 5_1^-$	100(5)	100
1.956	(8^-)	$8_1^- \rightarrow 6_1^-$	100(8)	100
		$\rightarrow 7_1^-$	23(6)	16
2.094	$8^{(-)}$	$8_2^- \rightarrow 7_1^-$	100(3)	100
2.251	(7^-)	$7_3^- \rightarrow 6_2^-$	<55	75
		$\rightarrow 6_1^-$	100(15)	100
		$\rightarrow 5_2^-$	<40	45

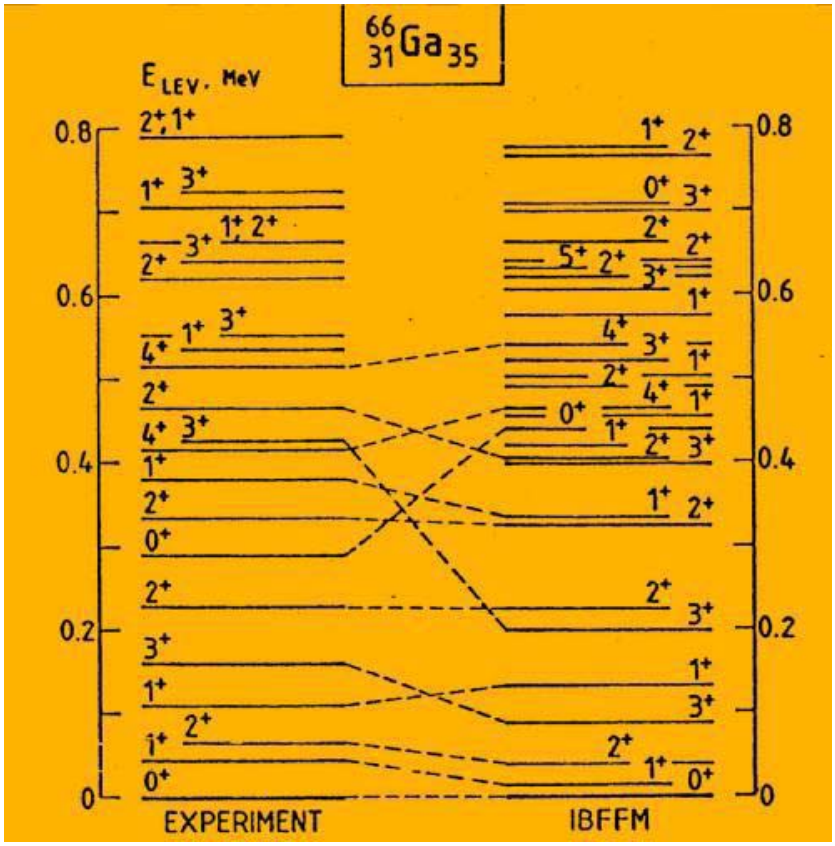
66 31 Ga 35
E LEV. MeV
0.8
0.6
0.4
0.2
0
EXPERIMENT
IBFFM

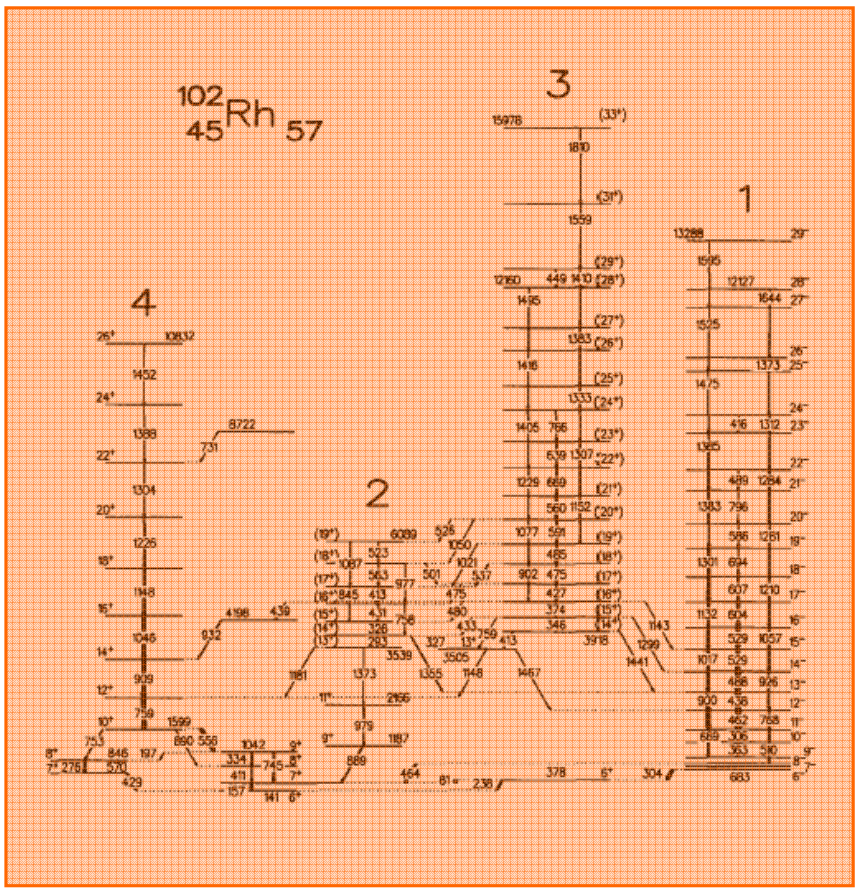
102 45 Rh 57
1
2
3
4

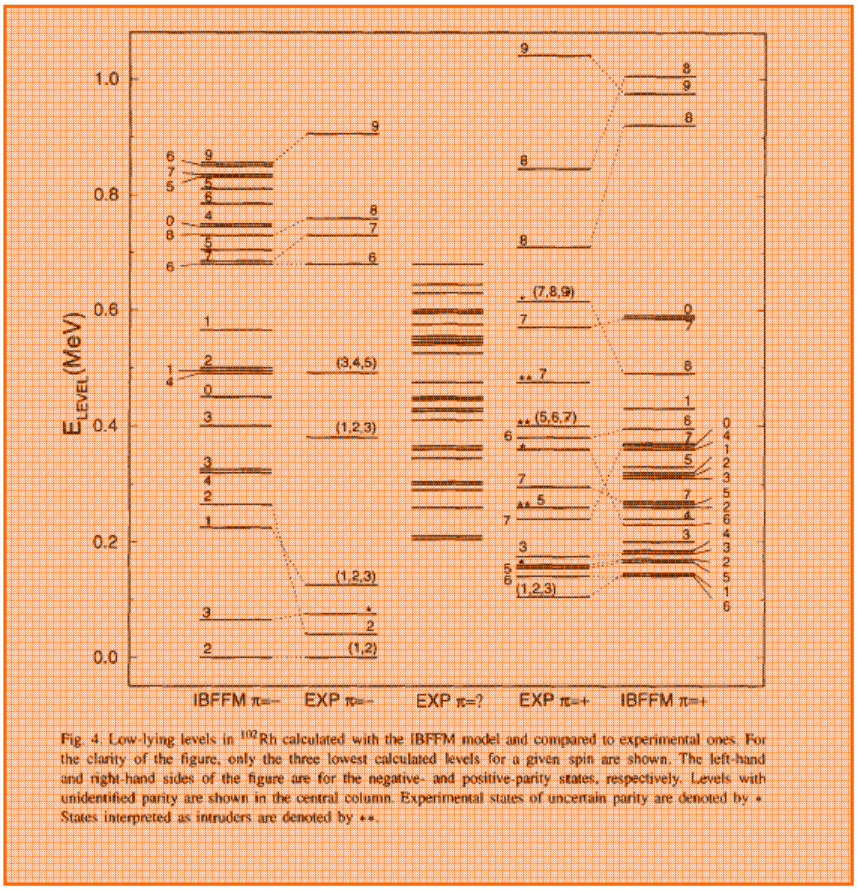

Fig. 4. Low-lying levels in ^{102}Rh calculated with the IBFFM model and compared to experimental ones. For the clarity of the figure, only the three lowest calculated levels for a given spin are shown. The left-hand and right-hand sides of the figure are for the negative- and positive-parity states, respectively. Levels with unidentified parity are shown in the central column. Experimental states of uncertain parity are denoted by $*$. States interpreted as intruders are denoted by $**$.

^{102}Rh

Transition		B(E2) (e^2b^2)		B(M1) (μ_N^2)		I_γ	
$I_i^\pi \to I_f^\pi$	$E_i \to E_f$	Exp.	IBFFM	Exp.	IBFFM	Exp.	IBFFM
$2_3^- \to 2_1^-$	42 → 0		0.0089	0.0054(18)	0.0033	100	100
$3_1^- \to 2_2^-$	76 → 42		0.0206		0.0731		68
$\to 2_1^-$	→ 0		0.0065		0.0097		100
$1_1^- \to 3_1^-$	124 → 76		0.0092				0.0
$\to 2_2^-$	→ 42		0.0068	0.0072(54)	0.0169	12.9	3.4
$\to 2_1^-$	→ 0		0.0307	0.034(18)	0.1436	100	100
$5_1^+ \to 6_1^+$	155 → 141		0.0003		0.0515	100	100
$2_1^+ \to 1_1^+$	157 → 105		0.0246		1.1948	100	100
$3_1^+ \to 2_1^+$	179 → 157		0.0109		1.2919	82[a]	43[a]
$\to 1_1^+$	→ 105		0.0232				0.1[a]
$7_2^+ \to 5_1^+$	242 → 155		0.0033				0.0
$\to 6_1^+$	→ 141		0.0342		0.1286	100	100
$7_1^+ \to 7_2^+$	297 → 242		0.0057		0.0019		8
$\to 5_1^+$	→ 155		0.0178				20
$\to 6_1^+$	→ 141	≥0.039[b]	0.0164	≥ 0.093[b]	0.0007	100	100
$6_2^+ \to 7_1^+$	360 → 297		0.0322		0.2138		100
$\to 7_2^+$	→ 242		0.0181		0.0287		90
$6_3^+ \to 6_2^+$	378 → 360		0.0099		0.0002		0.0
$\to 7_1^+$	→ 297		0.0009	0.045[b]	0.5392	92	69
$\to 7_2^+$	→ 242		0.0023	0.016[b]	0.0046	58	3
$\to 5_1^+$	→ 155	0.0063[b]	0.0006		0.0375	83	100
$\to 6_1^+$	→ 141	0.0044[b]	0.0038	0.0018[b]	0.0309	100	100
$7_3^+ \to 6_3^+$	570 → 378		0.0343		0.1572		19
$\to 6_2^+$	→ 360		0.0000		0.0088		1.4
$\to 7_1^+$	→ 297		0.0018		0.0000	5	0.1
$\to 7_2^+$	→ 242		0.0000		0.0035		2.1
$\to 5_1^+$	→ 155		0.0076		0.0000		1.1
$\to 6_1^+$	→ 141		0.0016		0.0728	100	100
$8_1^+ \to 7_3^+$	616 → 570		0.0080		0.2705		0.3
$\to 6_3^+$	→ 378		0.0009				0.0
$\to 6_2^+$	→ 360		0.0228				0.2
$\to 7_1^+$	→ 297		0.0374		0.2572	100	100
$\to 7_2^+$	→ 242		0.0022		0.0006		0.5
$\to 6_1^+$	→ 141		0.0020				0.4

^{102}Rh

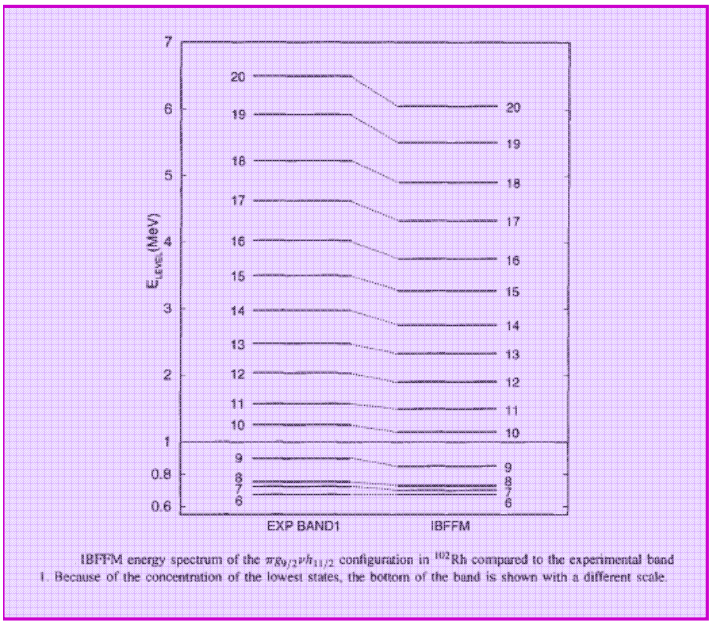

IBFFM energy spectrum of the $\pi g_{9/2}\nu h_{11/2}$ configuration in ^{102}Rh compared to the experimental band 1. Because of the concentration of the lowest states, the bottom of the band is shown with a different scale.

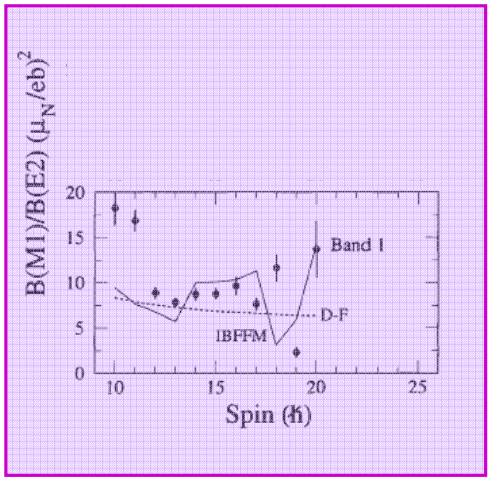

π g9/2 ν h11/2

Full line IBFFM

Dashed line Donau-Frauendorf model

The ΔI=2 positive-parity band 4

In the present IBFFM calculation we obtain two positive-parity high-spin bands, based on $\pi p_{1/2}\nu h_{11/2}$ and $\pi g_{9/2}\nu g_{7/2}$ two-quasiparticle configurations, respectively These bands are clearly formed above the 10^+ state, while for lower spins there is a stronger configuration mixing. The two lowest 10^+ states are based on the $(\pi p_{1/2}\nu h_{11/2})6, 2\ 4; 10$ (50%) and $(\pi g_{9/2}\nu g_{7/2})8, 1\ 2; 10$ (59%) configurations These two calculated bands appear close lying and they cross at angular momentum $I \approx 15\hbar$. Contrary to the experimental band 4 which is of $\Delta I = 2$ type with signature $\alpha = 0$, the calculated bands show doublet-type structures. The $\pi p_{1/2}\nu h_{11/2}$ configuration is associated with a much larger signature splitting than the $\pi g_{9/2}\nu g_{7/2}$ configuration and exhibit a pronounced tendency towards decoupled band (On this basis we attribute the $\pi p_{1/2}\nu h_{11/2}$ configuration to band 4.

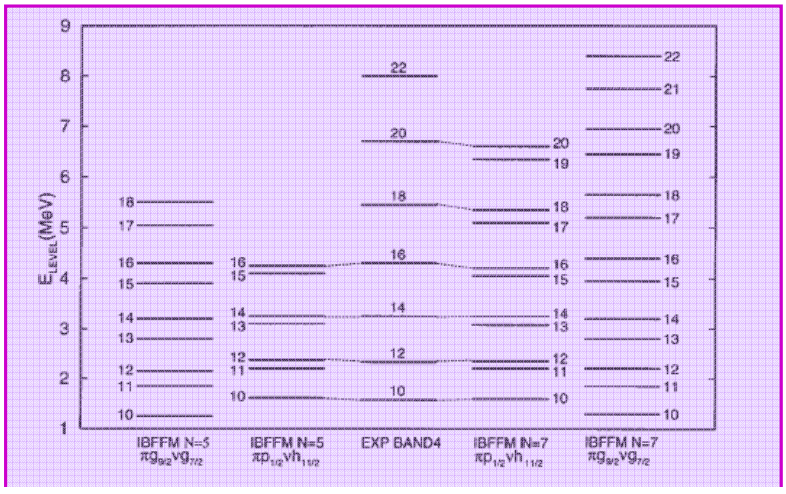

$B(E2)$ and $B(M1)$ reduced transition probabilities calculated between states of the $\pi p_{1/2}\nu h_{11/2}$ configuration with $N = 7$ in ^{102}Rh and comparison of the intensities of γ-rays observed in band 4 with those calculated for the above configuration

Transition	$B(E2)(e^2b^2)$	$B(M1)(\mu_N^2)$	I_γ	
	IBFFM	IBFFM	Exp.	IBFFM
$12^+ \rightarrow 11^+$	0.0016	0.0073		0.0
$12^+ \rightarrow 10^+$	0.4295		100	100
$14^+ \rightarrow 13^+$	0.0021	0.0001		0.0
$14^+ \rightarrow 12^+$	0.1003		100	100
$16^+ \rightarrow 15^+$	0.0005	0.0049		0.1
$16^+ \rightarrow 14^+$	0.0418		100	100
$18^+ \rightarrow 17^+$	0.0010	0.0019		0.0
$18^+ \rightarrow 16^+$	0.1076		100	100
$20^+ \rightarrow 19^+$	0.0011	0.0061		0.1
$20^+ \rightarrow 18^+$	0.0634		100	100

The two remaining experimental bands, bands 2 and 3, are expected to be based on four-quasiparticle states involving broken neutron pairs, in particular the $\nu h_{11/2}^2$ broken pair, so that four-quasiparticle states should be coupled to the boson core. The model including broken pairs of fermions has not been applied yet to odd–odd nuclei and therefore the corresponding theoretical states are missing in the present IBFFM calculations.

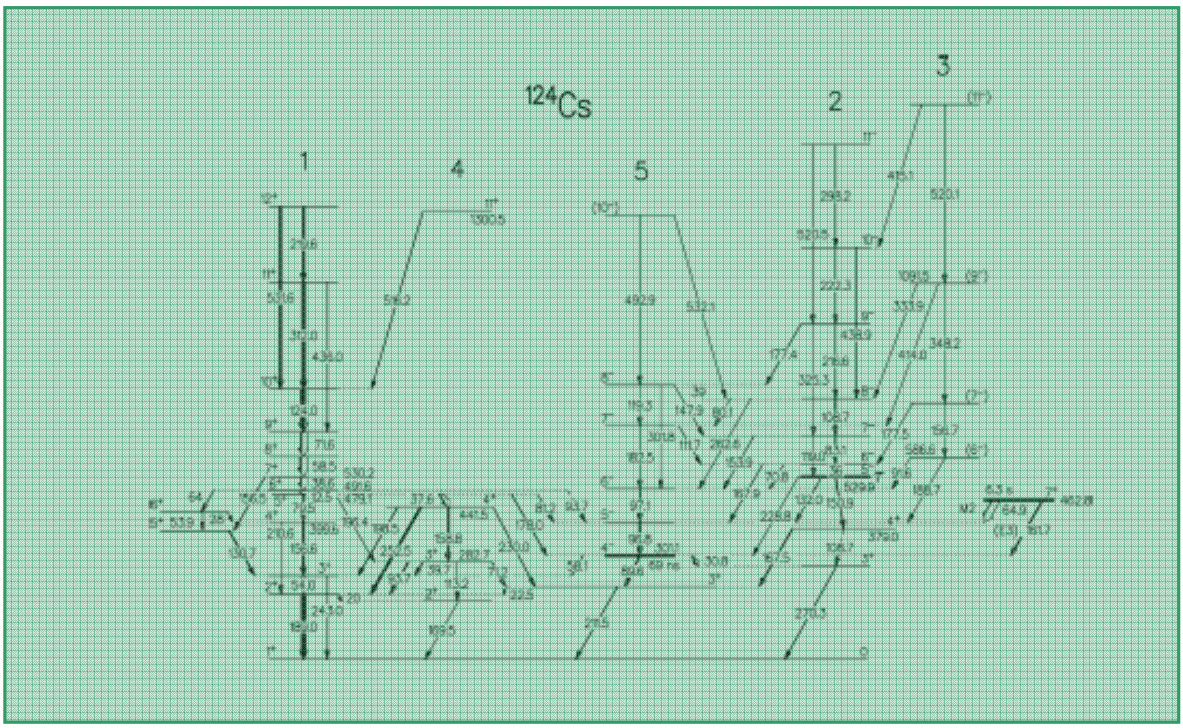

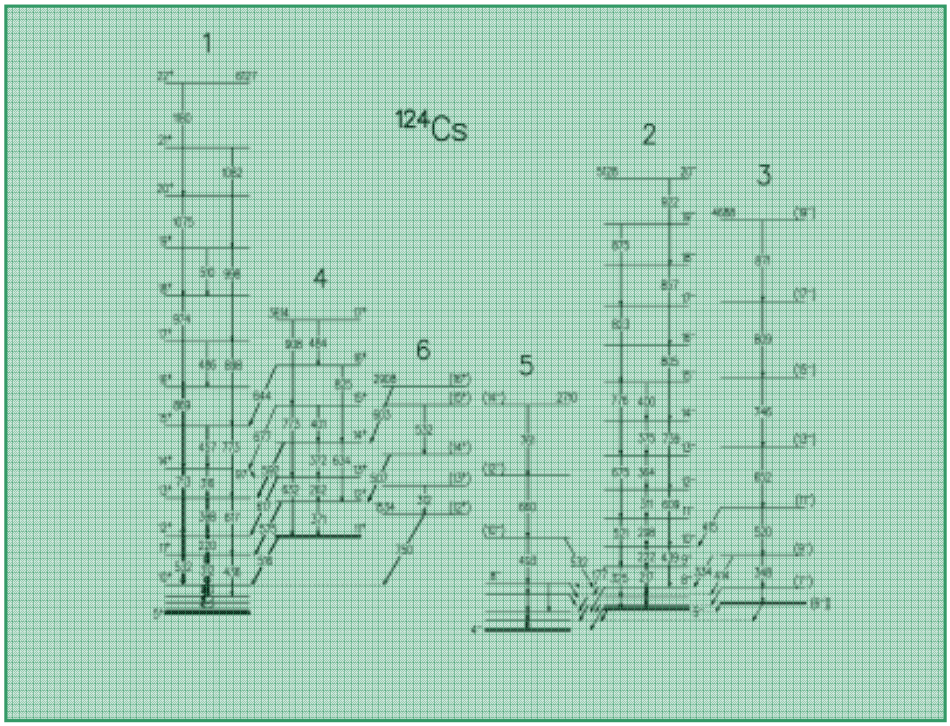

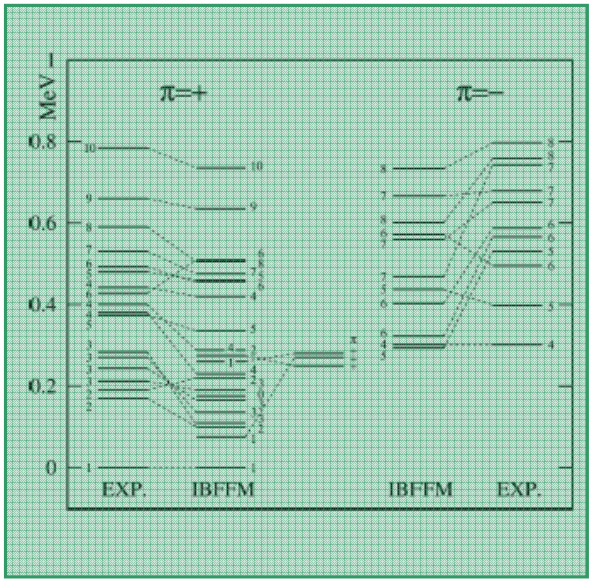

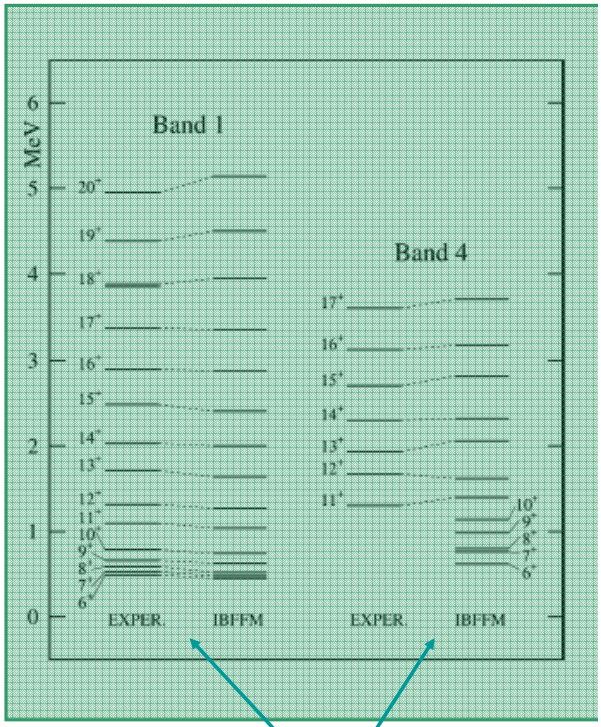

^{124}Cs

π h11/2 ν h11/2

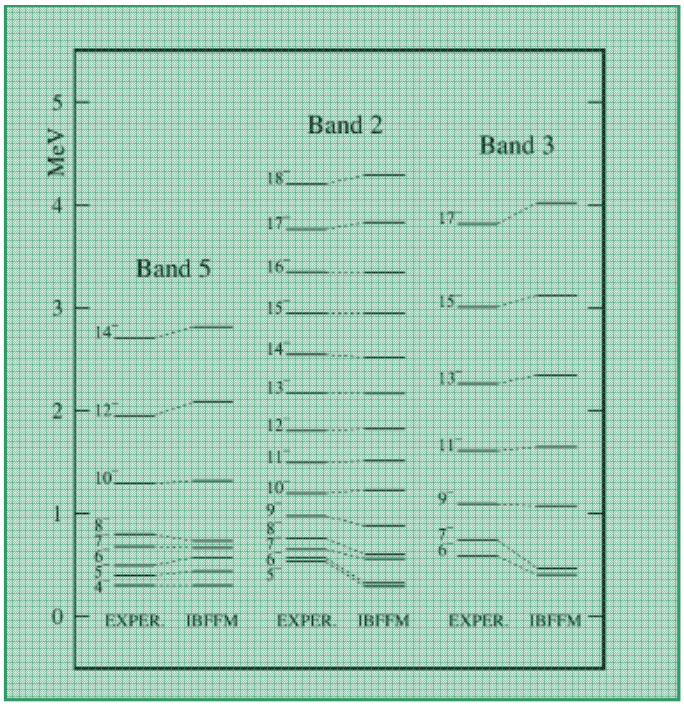

^{124}Cs

Wave functions are very complex !!!!

There is a strong configuration mixing

IBFFM is able to properly predict the structure of high spin states in a multy-j case

on the basis of the IBFFM analysis we propose that the negative-parity bands presented have a $\pi(d_{5/2}g_{7/2})\nu h_{11/2}$ configuration in their low-spin part and, starting from $I \approx 12$, are almost pure $\pi h_{11/2}\nu g_{7/2}$, with band 2 being the yrast structure and bands 3 and 5 the yrare structures. Thus the collective band structures start at spin $I \approx 12$.

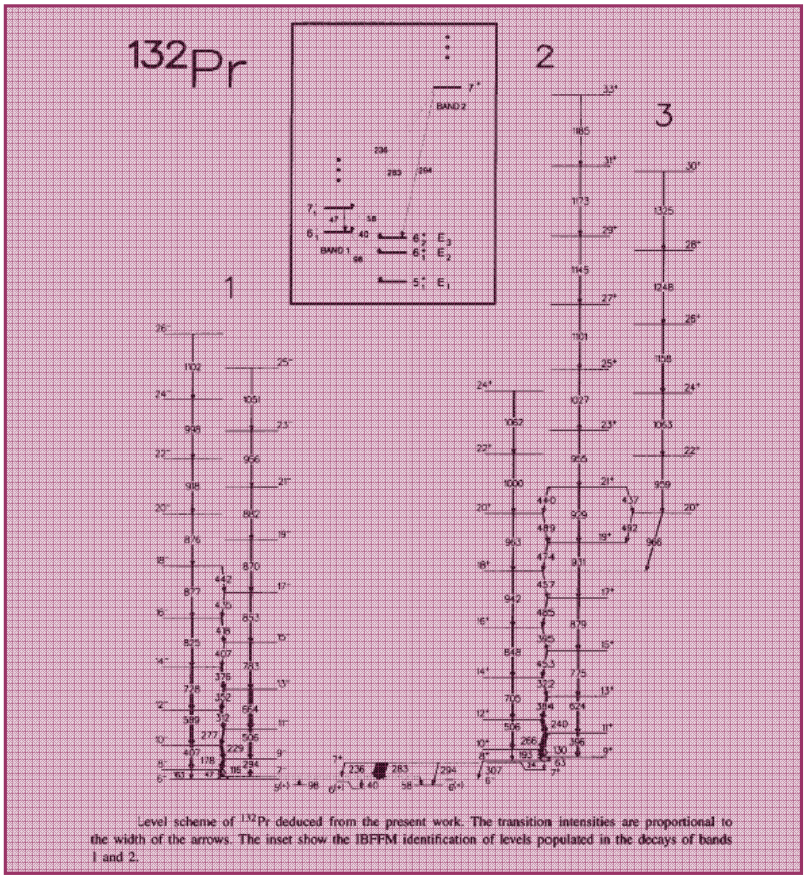

Level scheme of ^{132}Pr deduced from the present work. The transition intensities are proportional to the width of the arrows. The inset show the IBFFM identification of levels populated in the decays of bands 1 and 2.

Mixing of configurations with different parity both for protons and for neutrons (high with low spin states)

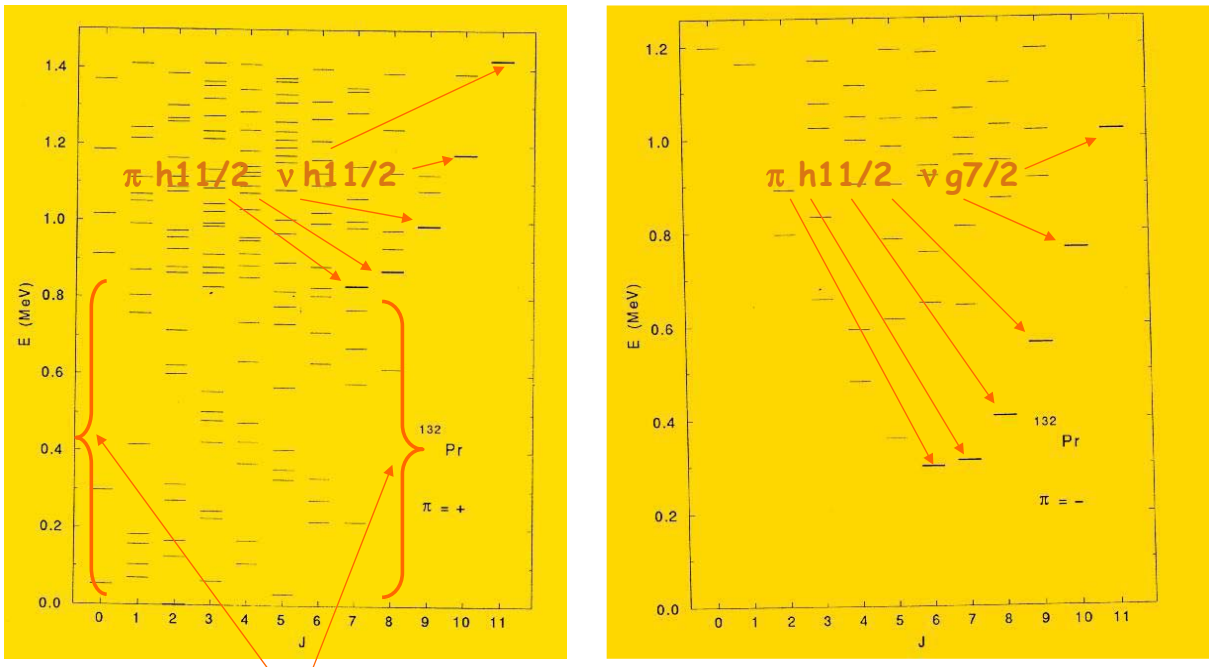

Positive parity proton and positive parity neutron configurations

The formation of regular $\Delta I = 1$ high-spin band pattern in odd-even and odd-odd nuclei with O(6) boson core presents a challenging problem for the IBFM and IBFFM models, respectively. Namely, both models predict normal or decoupled band patterns with close-lying unfavored and favored bands, resulting in characteristic "doublet structures" and $\Delta I = 2$ transitions. This is because the standard IBFM interactions can not induce a sufficiently strong effective interaction which would establish a regular $\Delta I = 1$ band pattern, without sizeably altering the low-energy part of the spectrum.

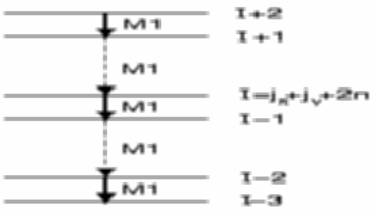

Schematic presentation of the conflicting pattern in odd-odd nuclei associated with unique-parity proton and neutron quasiparticles of opposite occupancy coupled to the O(6) boson core (n is an integer).

In order to account for this problem, in the quadrupole operator of the dynamical boson-fermion interaction we introduce a new term

$$H_{dyn} = \Gamma_0\sqrt{5}\sum_{j_1 j_2}(u_{j_1}u_{j_2} - v_{j_1}v_{j_2})\times < j_1 \parallel Y_2 \parallel j_2 > \{Q_2^B(c_{j_1}^\dagger \tilde{c}_{j_2})_2\}_0$$

$$Q_{2\mu}^B = d_{2\mu}^\dagger s + s^\dagger \tilde{d}_{2\mu} + \chi(d^\dagger \tilde{d})_{2\mu} + \eta\sum_{L_1 L_2}[(d^\dagger \tilde{d})_{L_1}(d^\dagger \tilde{d})_{L_2}]_{2\mu}$$

The effect of the last term is to induce an effective deformation of a soft O(6) core due to polarization caused by odd fermions. In this way a regular $\Delta I = 1$ yrast band is established in odd-odd nuclei with O(6) boson core. Without the η - term a familiar "doublet structure" is obtained in IBFFM, while taking $\eta \neq 0$ leads to a regular $\Delta I = 1$ pattern, both in energies and M1 transitions on the yrast.

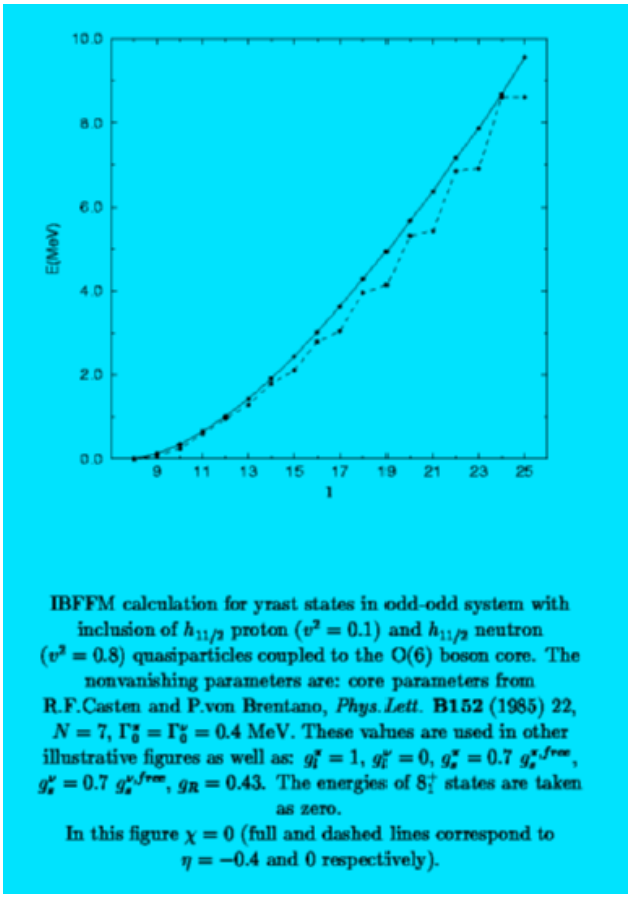

IBFFM calculation for yrast states in odd-odd system with inclusion of $h_{11/2}$ proton ($v^2 = 0.1$) and $h_{11/2}$ neutron ($v^2 = 0.8$) quasiparticles coupled to the O(6) boson core. The nonvanishing parameters are: core parameters from R.F.Casten and P.von Brentano, *Phys.Lett.* **B152** (1985) 22, $N = 7$, $\Gamma_0^\pi = \Gamma_0^\nu = 0.4$ MeV. These values are used in other illustrative figures as well as: $g_l^\pi = 1$, $g_l^\nu = 0$, $g_s^\pi = 0.7\ g_s^{\pi,free}$, $g_s^\nu = 0.7\ g_s^{\nu,free}$, $g_R = 0.43$. The energies of 8_1^+ states are taken as zero.
In this figure $\chi = 0$ (full and dashed lines correspond to $\eta = -0.4$ and 0 respectively).

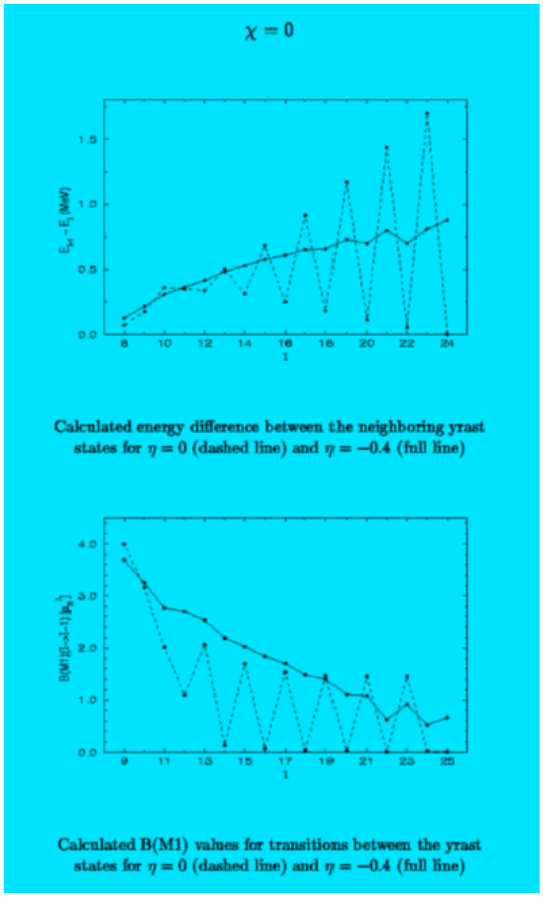

Calculated energy difference between the neighboring yrast states for $\eta = 0$ (dashed line) and $\eta = -0.4$ (full line)

Calculated B(M1) values for transitions between the yrast states for $\eta = 0$ (dashed line) and $\eta = -0.4$ (full line)

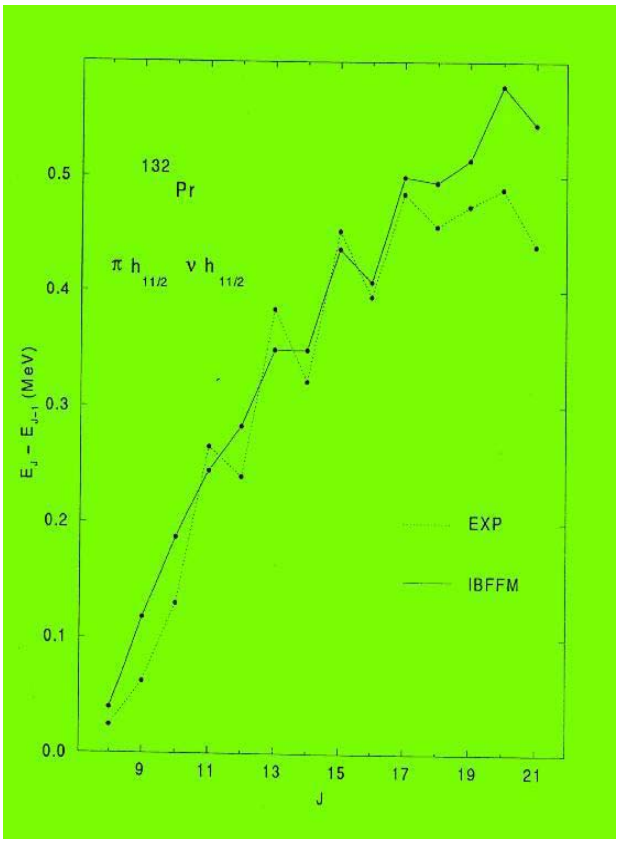

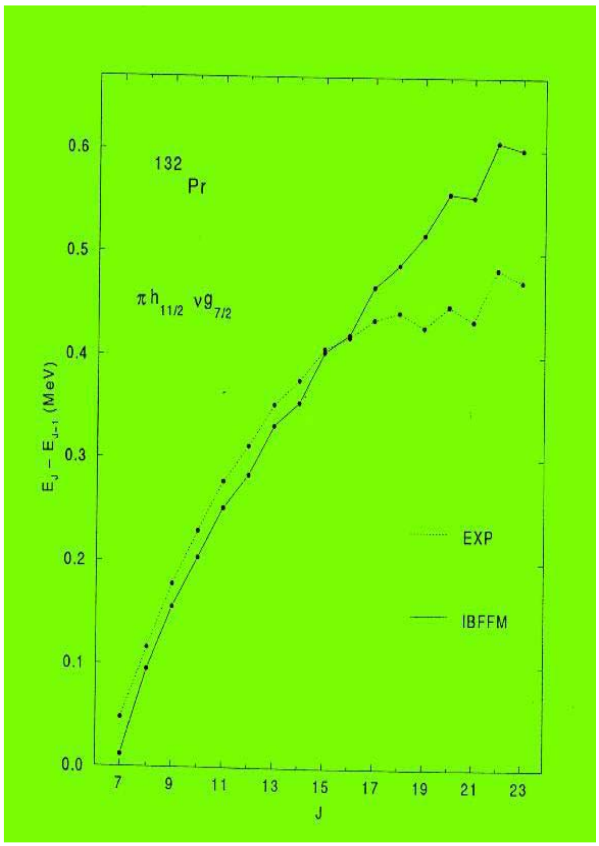

Signature inversion has been investigated in various models. Taking a very strong (!!??) boson-fermion exchange interaction a change of signature pattern from inverted to the normal with increasing spin can be achieved within the unique-parity two-quasiparticle band. However, the strength of the exchange interaction is not a free parameter. A sizeable increase of the strength of exchange interaction would destroy the agreement of the calculation with the low-spin data.

$J_i^\pi \to J_f^\pi$	$B(E2)$ (e^2b^2)	$B(M1)$ (μ_N^2)	I_γ		$B(M1)/B(E2)$	
	IBFFM	IBFFM	EXP.	IBFFM	EXP.	IBFFM
$7_1^- \to 6_1^-$	0.698	0.949	100	100	-	-
$8_1^- \to 7_1^-$	0.668	0.727	100	100	0.97(2)	1.62
$\to 6_1^-$	0.448	-	5	3		
$9_1^- \to 8_1^-$	0.585	0.538	100	100	0.75(10)	0.95
$\to 7_1^-$	0.567	-	36	28		
$10_1^- \to 9_1^-$	0.490	0.459	95	110	0.61(5)	0.71
$\to 8_1^-$	0.648	-	100	100		
$11_1^- \to 10_1^-$	0.406	0.375	61	48	0.66(5)	0.52
$\to 9_1^-$	0.716	-	100	100		
$12_1^- \to 11_1^-$	0.330	0.337	29	27	0.47(6)	0.45
$\to 10_1^-$	0.751	-	100	100		
$13_1^- \to 12_1^-$	0.273	0.294	30	18	0.62(5)	0.38
$\to 11_1^-$	0.763	-	100	100		
$14_1^- \to 13_1^-$	0.219	0.261	20	13	0.52(5)	0.34
$\to 12_1^-$	0.760	-	100	100		
$15_1^- \to 14_1^-$	0.179	0.246	-	11	-	0.34
$\to 13_1^-$	0.727	-	-	100		
$16_1^- \to 15_1^-$	0.142	0.201	14	8	0.5(1)	0.29
$\to 14_1^-$	0.697	-	100	100		
$17_1^- \to 16_1^-$	0.113	0.215	9	9	0.35(5)	0.34
$\to 15_1^-$	0.635	-	100	100		
$18_1^- \to 17_1^-$	0.087	0.146	-	6	-	0.25
$\to 16_1^-$	0.581	-	-	100		
$19_1^- \to 18_1^-$	0.066	0.192	-	9	-	0.38
$\to 17_1^-$	0.508	-	-	100		
$8_2^+ \to 7_1^+$	0.721	2.103	100	100	-	-
$9_1^+ \to 8_2^+$	0.714	1.365	-	100	-	2.69
$\to 7_1^+$	0.507	-	-	0.5		
$10_1^+ \to 9_1^+$	0.727	1.684	100	100	3.3(5)	2.87
$\to 8_2^+$	0.587	-	3	3		
$11_1^+ \to 10_1^+$	0.629	1.408	100	100	2.3(3)	1.86
$\to 9_1^+$	0.758	-	16	19		
$12_1^+ \to 11_1^+$	0.530	1.457	100	100	2.5(3)	1.83
$\to 10_1^+$	0.798	-	66	91		

$J_i^\pi \to J_f^\pi$	$B(E2)$ (e^2b^2)	$B(M1)$ (μ_N^2)	I_γ		$B(M1)/B(E2)$	
	IBFFM	IBFFM	EXP.	IBFFM	EXP.	IBFFM
$13_1^+ \to 12_1^+$	0.430	1.236	100	100	2.6(3)	1.47
$\to 11_1^+$	0.837	-	45	79		
$14_1^+ \to 13_1^+$	0.347	1.194	47	40	1.7(2)	1.44
$\to 12_1^+$	0.828	-	100	100		
$15_1^+ \to 14_1^+$	0.263	1.152	100	100	2.4(1)	1.48
$\to 13_1^+$	0.778	-	87	141		
$16_1^+ \to 15_1^+$	0.203	0.856	32	23	1.6(5)	1.15
$\to 14_1^+$	0.748	-	100	100		
$17_1^+ \to 16_1^+$	0.132	1.128	61	57	1.95(10)	1.83
$\to 15_1^+$	0.615	-	100	100		
$18_1^+ \to 17_1^+$	0.092	0.351	24	11	1.3(3)	0.61
$\to 16_1^+$	0.580	-	100	100		
$19_1^+ \to 18_1^+$	0.051	1.103	35	51	1.6(5)	2.32
$\to 17_1^+$	0.476	-	100	100		
$20_1^+ \to 19_1^+$	0.031	0.233	26	14	1.3(3)	0.71
$\to 18_1^+$	0.328	-	100	100		
$21_1^+ \to 20_1^+$	0.018	0.980	-	63	-	3.52
$\to 19_1^+$	0.279	-	-	100		

^{132}Pr

Transitional SU(3) – O(6) ^{126}Pr nucleus

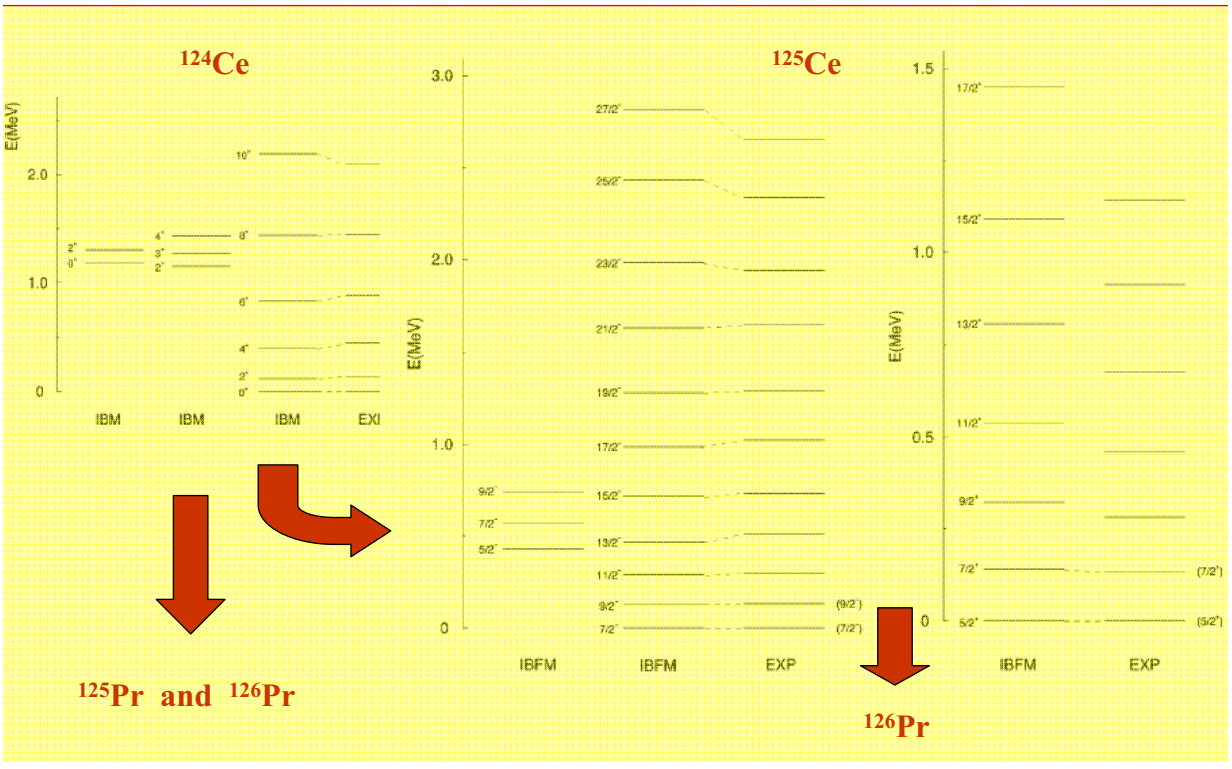

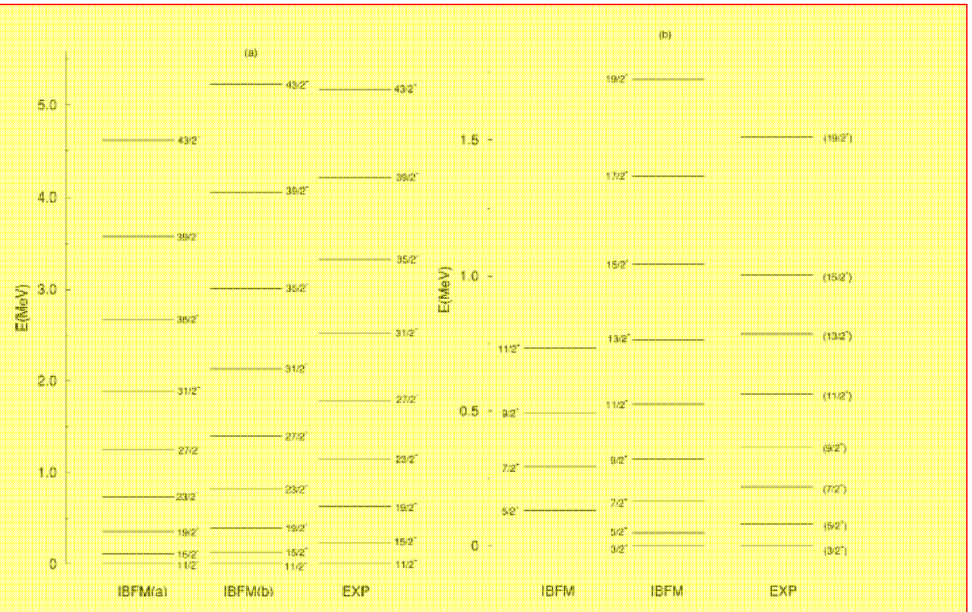

FIG. 12. The negative parity (a) and positive parity (b) yrast states in the odd-Z nucleus ^{125}Pr are compared with the experimental states of ^{127}Pr.

^{126}Pr

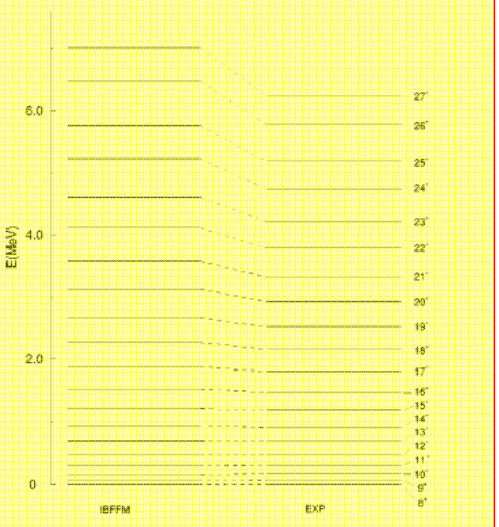

FIG. 13. The yrast sequence of high angular momentum positive parity states based on the $\pi h_{11/2} \otimes \nu h_{11/2}$ configuration is compared with its experimental counterpart in ^{126}Pr. The assignment for the band head, i.e., the lowest observed state is 8^+.

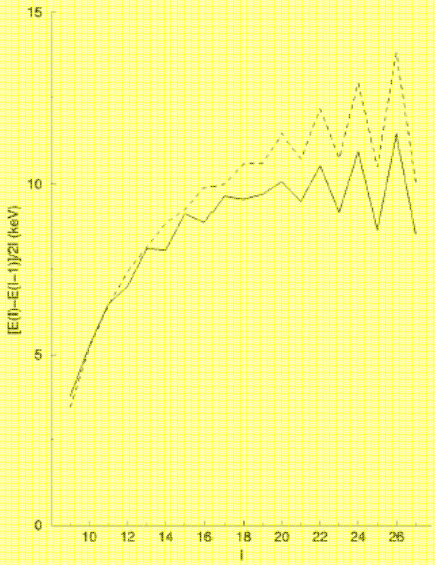

FIG. 14. The IBFFM (dashed line) and the experimental (solid line) $[E(I)-E(I-1)]/2I$ vs I plots for the $\pi h_{11/2} \otimes \nu h_{11/2}$ yrast band in ^{126}Pr. The state 8^+ is assigned to the band head.

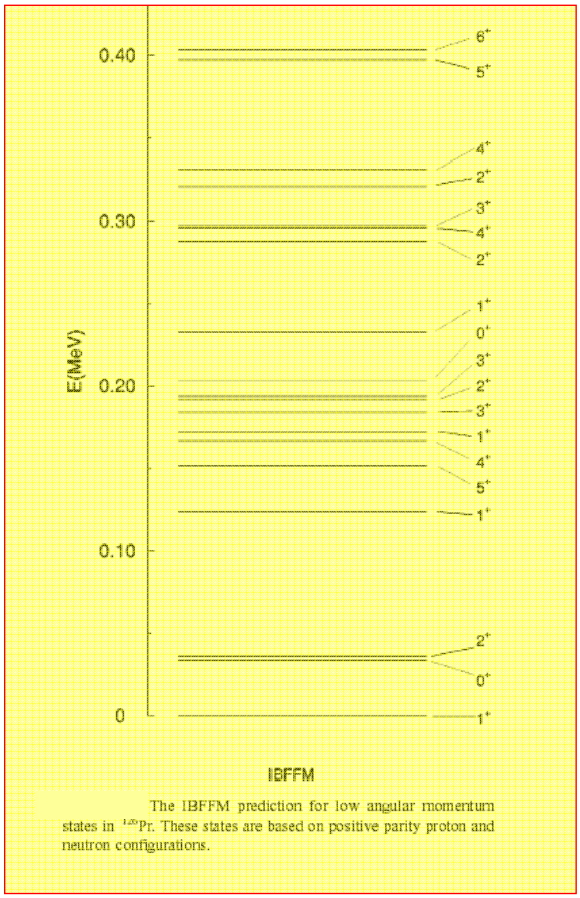

The IBFFM prediction for low angular momentum states in ^{126}Pr. These states are based on positive parity proton and neutron configurations.

The IBFFM analysis predicts the existence of another isomer in ^{126}Pr: 5^+ at $\approx$150 keV excitation energy. Its isomeric character depends strongly on the choice of the proton-neutron interaction. In the present calculation, 5^+_1 is below 4^+_1 and therefore it is an isomer with a possible γ decay to 2^+_1. This transition is slow enough to allow for a β decay that has been reported

^{198}Au

The first odd-odd nucleus calculated in IBFFM

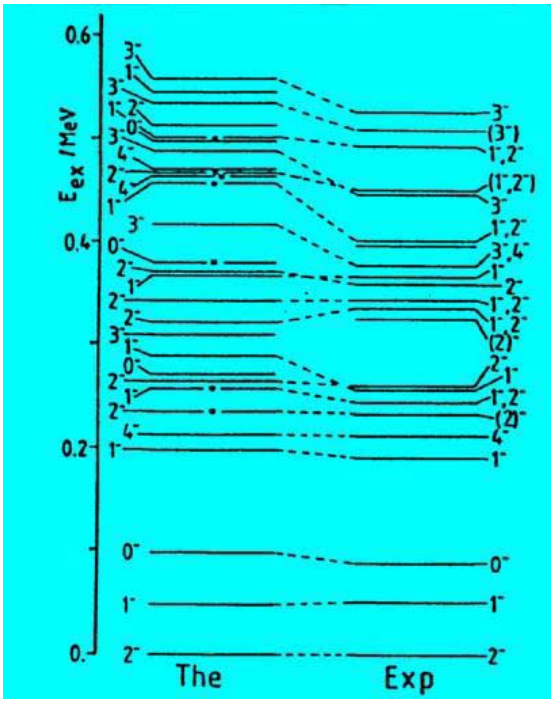

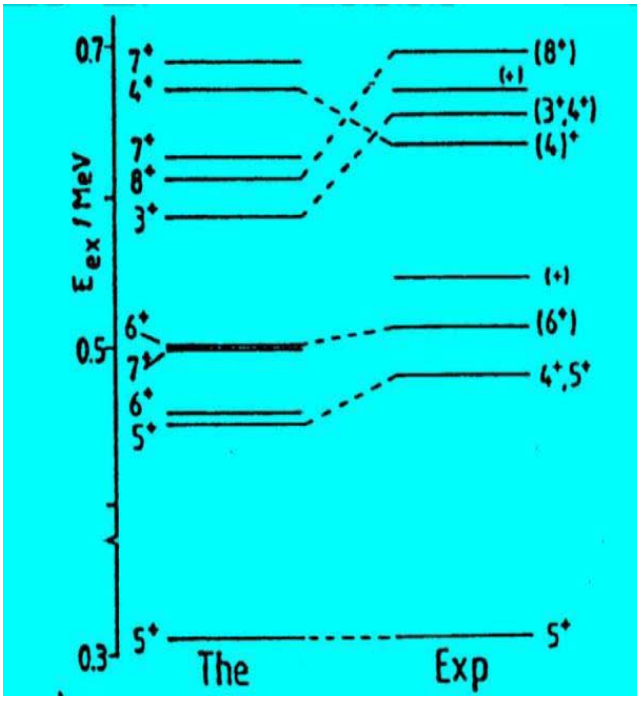

Chiral bands in IBFFM

The rotation of triaxial nuclei may give rise to pairs of identical $\Delta I = 1$ bands with the same parity in odd-odd nuclei – chiral doublet bands. These structures arise from configurations in which the angular momenta of the valence proton, the valence neutron and the core are mutually perpendicular, and can be arranged to form two systems that differ by intrinsic chirality, a left- and a right-handed system. When chiral symmetry is thus broken in the body-fixed frame, the restoration of the symmetry in the laboratory frame results in the occurrence of degenerate doublet $\Delta I = 1$ bands. It has been suggested that such nearly degenerate rotational bands might be observed in the region of transitional nuclei with $A \approx 130$. A number of nuclei in this region are susceptible to triaxial deformation and the yrast bands of odd-odd nuclei are built on the $\pi h_{11/2}$ particle-like – $\nu h_{11/2}$ hole-like configuration. The existence of self-consistent rotating mean field solutions with chiral character has been demonstrated for ^{134}Pr and ^{188}Ir. The theoretical prediction of chiral doublet structures has prompted quite a number of experimental studies of odd-odd $N = 75$ and $N = 73$ isotones in the $A \approx 130$ region, and nearly degenerate $\Delta I = 1$ bands built on the $\pi h_{11/2} \otimes \nu h_{11/2}$ configuration have been identified in many of these nuclei. Sideband partners of the $\pi h_{11/2} \otimes \nu h_{11/2}$ yrast band have been identified in $_{55}$Cs, $_{57}$La and $_{61}$Pm $N = 75$ isotones of ^{134}Pr. For ^{134}Pr the energy spacing between the doublet rotational bands gradually decreases from ≈ 0.19 MeV at low spin to the point where the two bands cross between $I = 14$ and $I = 15$. For the other $N = 75$ isotones the two lowest $\pi h_{11/2} \otimes \nu h_{11/2}$ bands are almost parallel in the E *vs* I plot, and the energy spacing between the corresponding states with the same spin is ≈ 0.3 MeV.

In ^{134}Pr the two lowest, yrast and yrare $\pi h_{11/2} \otimes \nu h_{11/2}$ bands have been interpreted as chiral restored doublet bands. In order to explain similar doublet bands in the other $N = 75$ odd-odd nuclei, it has been suggested that in these cases the triaxial core deformation is not stable, but perhaps more γ-soft, resulting in collective chiral vibration of the core angular momentum between the left- and right-handed chiral systems. It has to be emphasized that in all studies of chiral doublet bands it has been argued that the empirical separation of ≤ 300 keV is too small for the sideband to be interpreted as a band built either on the unfavored signature of the proton orbital, or on the γ-vibrational excitation. A γ-vibration coupled to the yrast band has been ruled out because in this region the γ-vibration energies are ≥ 600 keV.

In the IBM/IBFM framework calculations are performed in the laboratory frame and the results can be directly compared with experimental data. All states within the model space and their electromagnetic properties are compared with experiment, rather than just band-head energies. In the particular case of ^{134}Pr it will be assumed that the nucleus is triaxial but, unlike in a geometric description based on the tilted axis cranking model, the occurrence of nearly degenerate doublet $\Delta I = 1$ bands is not related to a definite alignment of the angular momenta of the odd proton and odd neutron along the body-fixed axes of the core nucleus.

The spectrum of the core nucleus $^{134}_{58}Ce_{76}$ is described by the Hamiltonian

$$H_{IBM} = \epsilon_d \, \hat{n}_d + p \; P \cdot P + k' \; L \cdot L + k \; Q \cdot Q + \Theta_3 \left[(d^\dagger \; d^\dagger)_2 \; d^\dagger \right]_3 \cdot \left[(\tilde{d} \; \tilde{d})_2 \; \tilde{d} \right]_3$$

The first four terms represent the standard Hamiltonian of the Interacting Boson Model (IBM-1). The cubic interaction in the last term, with the strength parameter Θ_3, introduces a degree of triaxiality. The best agreement with the experimental spectrum is obtained for the following choice of parameters:

$\epsilon_d = 0.75$, $p = 0.25$, $k' = 0.014$, $k = -0.003$, $\Theta_3 = 0.025$ (all in MeV), and $\chi = -0.3$ in the quadrupole operator Q_2. This value of χ is also used in the boson quadrupole operator appearing in the boson-fermion dynamical interaction, as well as in the E2 operator.

With the inclusion of the three-body term in the boson Hamiltonian, the boson quadrupole operator appearing in the dynamical boson-fermion interaction and in the E2 operator should also be extended to higher order. The standard boson quadrupole operator is modified by including the additional term

$$\eta \left[(d^\dagger \; \tilde{d})_3 \; (d^\dagger \; \tilde{d})_3 \right]_2$$

This term is included in the dynamical boson-fermion interaction and in the E2 operator, with the strength parameter $\eta = -0.46$ MeV.

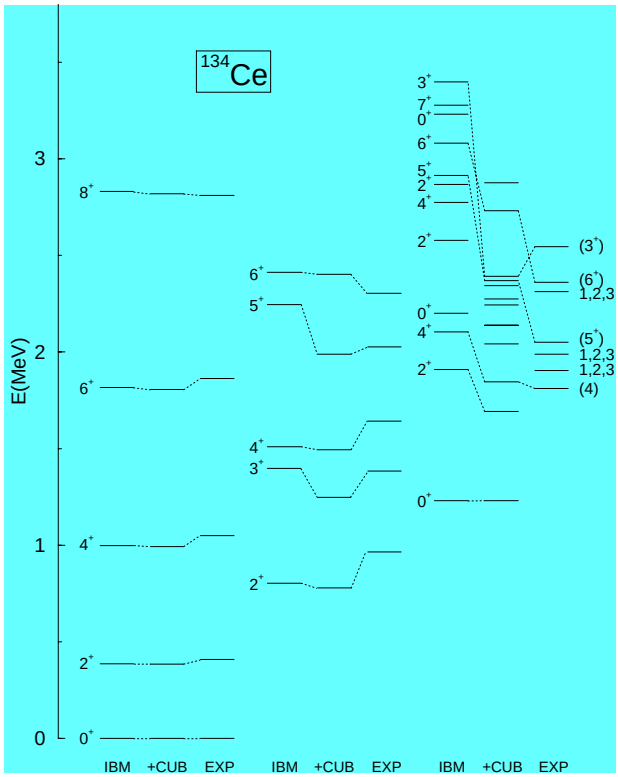

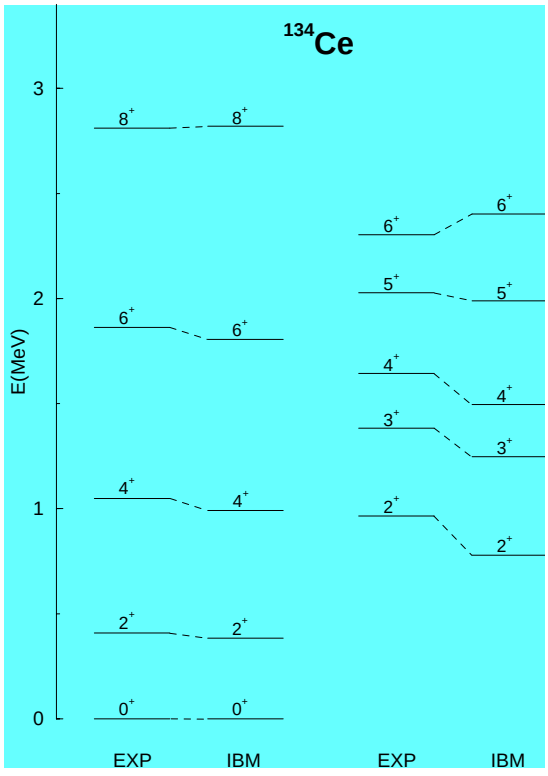

The spectrum of positive-parity states in ^{134}Pr, based on negative-parity orbitals of the odd proton and odd neutron, is calculated by using the quasiparticle energies, occupation probabilities and boson-fermion interaction strengths obtained in the IBFM calculations of negative-parity spectra in $^{135}_{59}Pr_{76}$ and $^{133}_{58}Ce_{75}$. Most of the model parameters, therefore, are determined by the structure of collective and single-nucleon states in the even-even and odd-even neighbors of ^{134}Pr and, in principle, only the residual interaction between the odd proton and odd neutron has to be adjusted to the experimental data in the odd-odd nucleus.

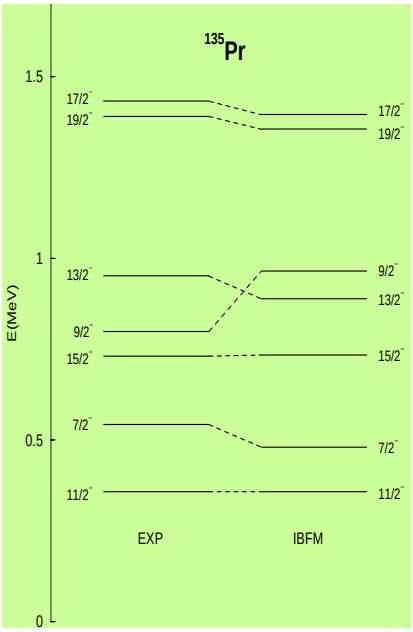

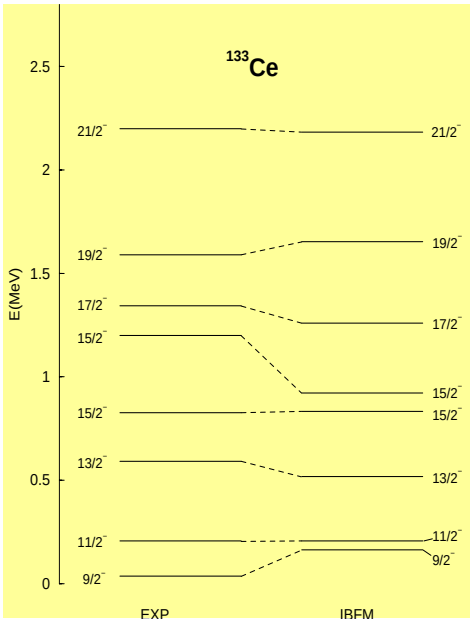

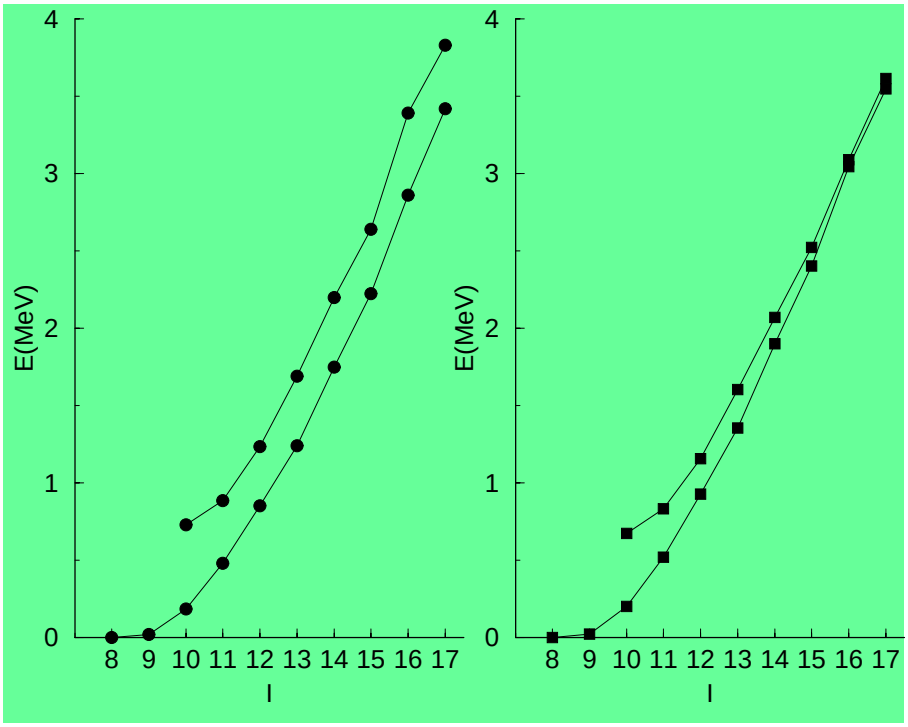

The yrast and yrare $\pi h_{11/2} \otimes \nu h_{11/2}$ bands in ^{134}Pr calculated in the IBFFM for the ^{134}Ce core without triaxiality (left panel, $\Theta_3 = 0$), and with stable triaxial deformation (right panel, $\Theta_3 = 0.03$ MeV).

For $\Theta_3 = 0$ the core is γ-soft and the two bands do not cross or become degenerate. Rather, an almost constant energy spacing ≈ 400 keV between the two bands is predicted. For a stable triaxial deformation ($\Theta_3 = 0.03$ MeV) the energy difference between the yrast and yrare bands gradually decreases, and between angular momenta 16^+ and 17^+ the two bands cross. Except for the exact position of the band crossing (which can be also affected by four-quasiparticle configurations not included in the model space), the "energy *vs* spin" diagram is in excellent agreement with the experimentally observed evolution of the two lowest positive-parity bands in ^{134}Pr. The results are also in agreement with the conclusions of calculations in the body-fixed frame, where it has been suggested that in the odd-odd $N = 75$ nuclei other than ^{134}Pr the triaxial core deformation is not stable, rather it is γ-soft, resulting in the two lowest $\pi h_{11/2} \otimes \nu h_{11/2}$ bands being almost parallel in the E *vs* I plot, with the energy spacing of ≈ 0.3 MeV. In ^{134}Pr, on the other hand, the stable triaxial deformation causes the two lowest positive-parity bands to become almost degenerate.

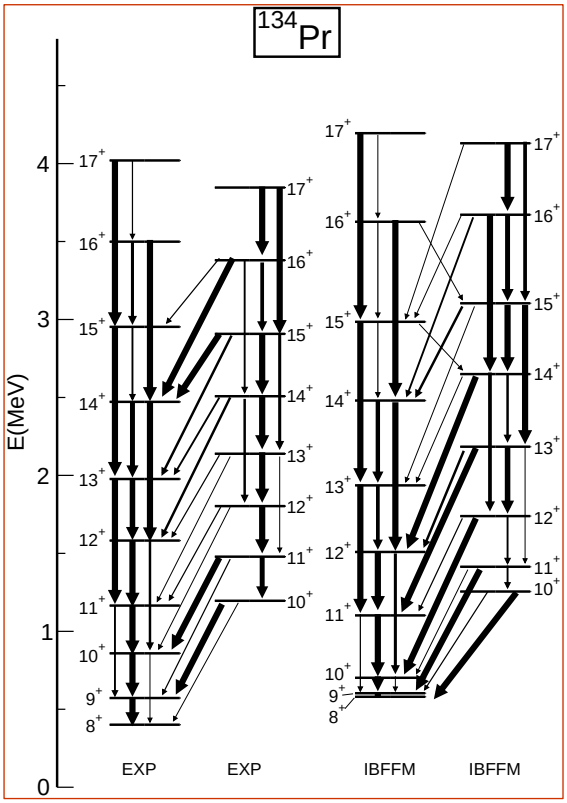

The yrast band is basically built on the ground-state band of the even-even core. With increasing angular momentum the admixture of the γ-band of the core becomes more pronounced. The structure of the second – yrare band, however, is that of the odd proton and odd neutron coupled to the γ-band of the core, especially in the lower part of the band. With increasing angular momentum both ground-state band and γ-band components contribute to the wave functions of the yrare band in ^{134}Pr. In the region of band crossing, in particular, the wave functions of the yrare band contain sizeable components of the higher-lying core structures. The IBFFM prediction, therefore, is that the two lowest $\pi h_{11/2} \otimes \nu h_{11/2}$ bands in ^{134}Pr are built, in leading order, on the ground-state band and the γ-band of the core nucleus, respectively. Their wave functions closely follow the triaxial structure of the core nucleus. This result is at variance with previous analyses of the doublet bands in ^{134}Pr, based on the tilted axis cranking approach, which have basically excluded the possibility that the second band might be built on the γ-band of the core. This was done only on the basis of the relatively high excitation energy of the γ-vibration.

As the IBFFM calculations are performed in the laboratory frame, they cannot determine the alignment of the odd particles along the body fixed axes. The IBFFM analysis indicates that the γ degree of freedom plays an important role in the formation of these bands.

4.

β decay in the interacting boson-fermion model

OBJECTIVES

- To test the nuclear model by analyzing experimental data

  Wave functions (two odd-even and one even-even nucleus are involved)

  Transition operators

- To provide reliable information for astrophysical applications

The process is very sensitive to configuration mixing both in the initial and final states. A detailed knowledge of the wavefunctions is required. Beta decay properties can be calculated by using:

- Shell model (in light nuclei and in medium-mass and heavy nuclei in the neighborhood of doubly magic nuclei)
- Other models for medium-mass and heavy nuclei.

Example: Simple pairing theory

⇩

Overestimates the Gamow-Teller strengths by a large factor (up to a factor 70 !!!!!)

How to account for the large hindrance:

Nuclear deformation
Mixing with 2p-2h states
Mesonic degrees of freedom

In the IBFM there is NO quenching factor (once the wave functions have been calculated, the calculation of beta decay properties is parameter free), or the quenching factor is SMALL.

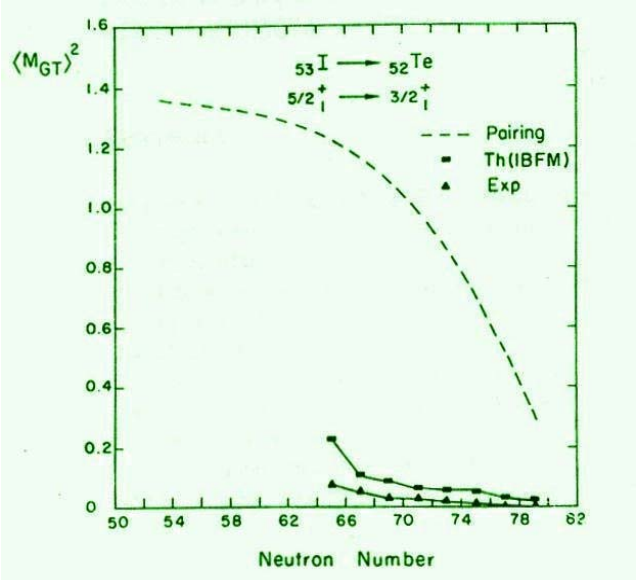

Comparison of experimental Gamow–Teller matrix elements with pairing theory and results of the calculation using the interacting boson–fermion model (IBFM).

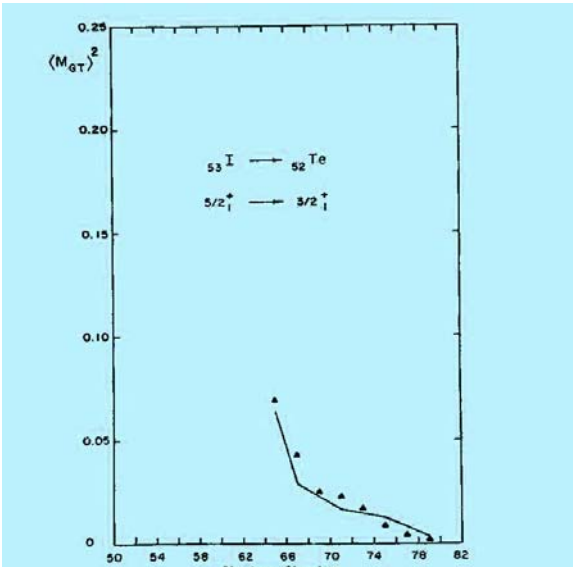

Comparison between experimental Gamow–Teller matrix elements (triangles) and those obtained using IBFM renormalized by a factor 3.5 (continuous line).

PROCEDURE

IBM2 calculations of the structure of even-even core nuclei:

Energy levels and wave functions

↓

Electromagnetic properties (electric quadrupole and magnetic dipole moments, B(E2) and B(M1) values, branching ratios).

↓

Wave functions

IBFM2 calculations of the structure of odd-even parent and daughter nuclei:

Energy levels and wave functions

↓

Electromagnetic properties (electric quadrupole and magnetic dipole moments, B(E2) and B(M1) values, branching ratios).

↓

Wave functions

↻ ↺

Beta decay calculations:

Matrix elements, logft values

Cs → Xe

A = 125, 127, 129

Soft nuclei close to the O(6) limit → complex wave functions

→ **Sensitive test of the model**

IBFM2 Hamiltonian → $H = H^{\mathrm{B}} + H^{\mathrm{F}} + V^{\mathrm{BF}}$

IBM2 Hamiltonian (core nuclei) :

$$
\begin{aligned}
{}^{\mathrm{B}} \;=\; & \epsilon_d \left(n_{d_\nu} + n_{d_\pi}\right) + \kappa \left(Q_\nu^{\mathrm{B}} \cdot Q_\pi^{\mathrm{B}}\right) \\
& + \frac{1}{2}\xi_2 \left((d_\nu^\dagger s_\pi^\dagger - d_\pi^\dagger s_\nu^\dagger) \cdot (\tilde{d}_\nu s_\pi - \tilde{d}_\pi s_\nu) \right) + \sum_{K=1,3} \xi_K \left([d_\nu^\dagger d_\pi^\dagger]^{(K)} \cdot [\tilde{d}_\pi \tilde{d}_\nu]^{(K)} \right. \\
& + \frac{1}{2} \sum_{L=0,2,4} c_L^\nu \left([d_\nu^\dagger d_\nu^\dagger]^{(k)} \cdot [\tilde{d}_\nu \tilde{d}_\nu]^{(k)} \right) + \frac{1}{2} \sum_{L=0,2,4} c_L^\pi \left([d_\pi^\dagger d_\pi^\dagger]^{(k)} \cdot [\tilde{d}_\pi \tilde{d}_\pi]^{(k)} \right.
\end{aligned}
$$

$$Q^{\rm B}_\nu = d^\dagger_\nu s_\nu + s^\dagger_\nu \tilde{d}_\nu + \chi_\nu [d^\dagger_\nu \tilde{d}_\nu]^{(2)}$$
$$Q^{\rm B}_\pi = d^\dagger_\pi s_\pi + s^\dagger_\pi \tilde{d}_\pi + \chi_\pi [d^\dagger_\pi \tilde{d}_\pi]^{(2)}$$

Boson quadrupole operators

IBM2 parameters. The unit is MeV except for the dimensionless χ_ν. The parameters $\chi_\pi = -0.80$ and $\xi_1 = \xi_2 = 0.24$ MeV, $\xi_3 = -0.18$ MeV are fixed.

odd nuclei	core nucleus	ϵ_d	κ	χ_ν	c^ν_0	c^ν_2
^{125}Cs	^{124}Xe	0.70	−0.145	0.00	0.05	−0.10
^{125}Xe, ^{127}Cs	^{126}Xe	0.70	−0.155	0.20	0.10	−0.10
^{127}Xe, ^{129}Cs	^{128}Xe	0.70	−0.170	0.33	0.30	0.00
^{129}Xe	^{130}Xe	0.76	−0.190	0.50	0.30	0.10

$$H^{\rm F} = \sum_i \epsilon_i n_i$$

Hamiltonian of the odd fermion

BCS ➡ ϵ_i is the quasi-particle energy of the ith orbital
n_i is its number operator

Interaction between bosons and the odd fermion :

$$\begin{aligned} V^{\rm BF} = & \sum_{i,j} \Gamma_{ij} \left([a^\dagger_i \tilde{a}_j]^{(2)} \cdot Q^{\rm B}_\rho \right) \\ & + \sum_{i,j} \Gamma'_{ij} \left([a^\dagger_i \tilde{a}_j]^{(2)} \cdot Q^{\rm B}_{\rho'} \right) \\ & + \sum A_i \, n_i n_{d_\rho} + \sum A'_i \, n_i n_{d_{\rho'}} \\ & + \sum_{i,j} \Lambda^j_{ki} \Big\{ : \left[\left[d^\dagger_\rho \tilde{a}_j \right]^{(k)} a^\dagger_i s_\rho \right]^{(2)} : \cdot \left[s^\dagger_{\rho'} \tilde{d}_{\rho'} \right]^{(2)} \\ & + H.c. \Big\} \\ & + B \, J \cdot L_\rho + B' \, J \cdot L_{\rho'}. \end{aligned}$$

ρ and ρ' denote π (ν) and ν (π) if the odd fermion is a proton (a neutron).

Orbital dependence of the interaction strengths

$$\Gamma_{i,j} = (u_i u_j - v_i v_j)\, Q_{i,j}\, \Gamma$$

$$\Lambda^j_{k,i} = -\beta_{k,i}\beta_{j,k} \left(\frac{10}{N_\rho (2j_k + 1)} \right)^{1/2} \Lambda$$

$$\beta_{i,j} = (u_i v_j + v_i u_j)\, Q_{i,j}$$

$$Q_{i,j} = < l_i, \frac{1}{2}, j_i || Y^{(2)} || l_j, \frac{1}{2}, j_j >$$

uj and vj from BCS

Electromagnetic transition operators

$$T^{(E2)} = e^B_\pi Q^B_\pi + e^B_\nu Q^B_\nu + \sum_{i,j} e'_{i,j} [a^\dagger_i \tilde{a}_j]^{(2)}$$

$$e'_{i,j} = -\frac{e^F_\rho}{\sqrt{5}} (u_i u_j - v_i v_j) < i || r^2 Y^{(2)} || j >$$

$$T^{(M1)} = \sqrt{\frac{3}{4\pi}} \left(g^B_\pi L^B_\pi + g^B_\nu L^B_\nu + \sum_{i,j} e^{(1)}_{i,j} [a^\dagger_i \tilde{a}_j]^{(1)} \right)$$

$$e^{(1)}_{i,j} = -\frac{1}{\sqrt{3}} (u_i u_j + v_i v_j) < i || g_l \mathbf{l} + g_s \mathbf{s} || j >$$

u_j and v_j from BCS

Cs isotopes (odd proton)

Single particle energies (MeV)

$d_{5/2}$	$g_{7/2}$	$s_{1/2}$	$d_{3/2}$	$h_{11/2}$	$h_{9/2}$	$f_{7/2}$
0.05	0.00	3.35	3.00	1.50	7.00	8.00

Boson-fermion interaction strengths

isotope	Γ	A	Λ
^{125}Cs	0.90	−0.60	1.65
^{127}Cs	0.76	−0.66	2.30
^{129}Cs	0.74	−0.80	2.90

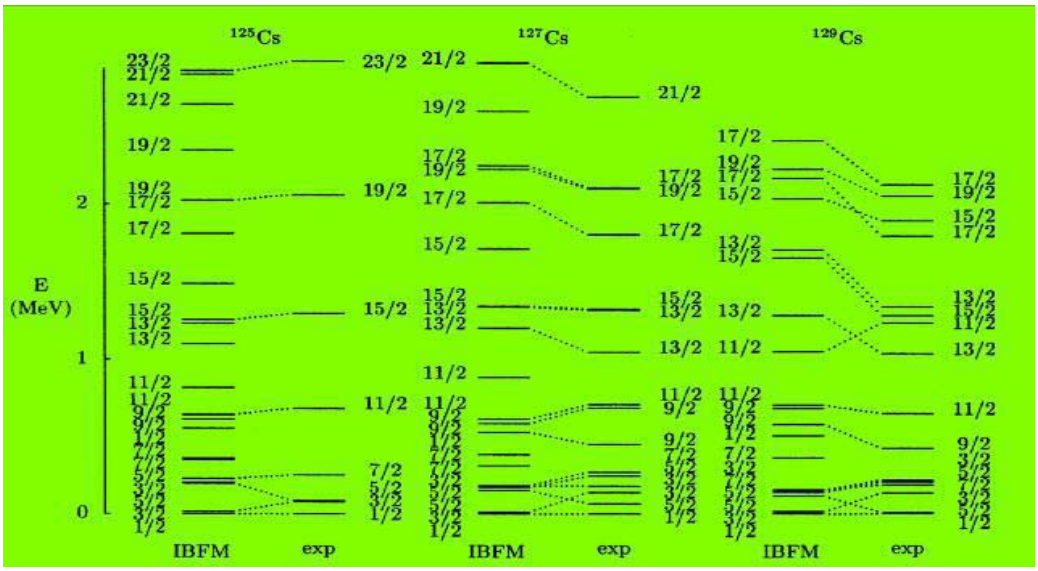

Positive parity levels

Xe isotopes (odd neutron)

Single particle energies (MeV)

Boson-fermion interaction strengths

	$d_{5/2}$	$g_{7/2}$	$s_{1/2}$	$d_{3/2}$	$h_{11/2}$
^{125}Xe	0.00	0.30	1.55	2.00	1.30
^{127}Xe	0.00	0.35	1.55	2.00	1.30
^{129}Xe	0.00	0.40	1.60	2.00	1.30

isotope	Γ	A	Λ
^{125}Xe	0.39	−0.42	0.40
^{127}Xe	0.44	−0.42	0.40
^{129}Xe	0.50	−0.42	0.40

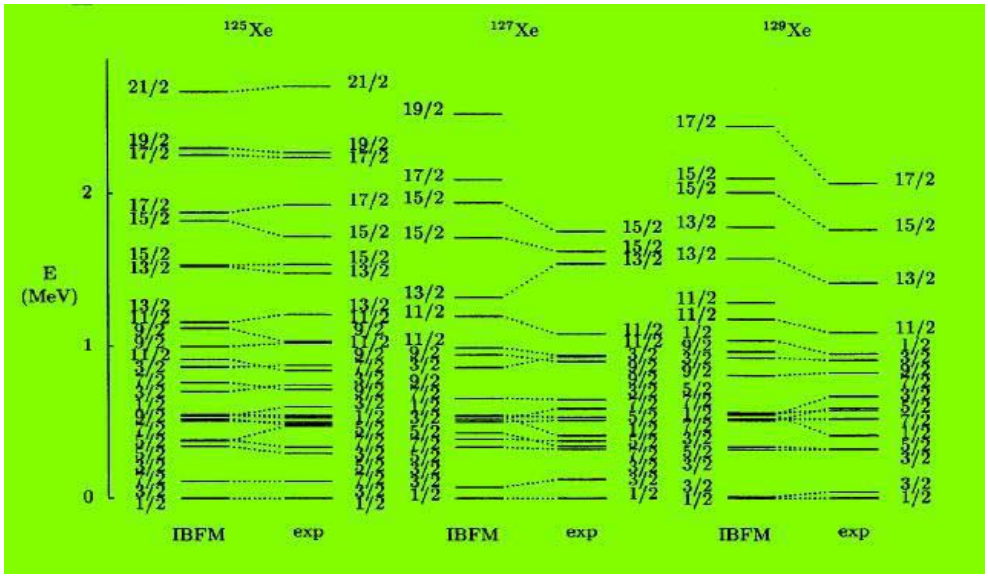

Positive parity levels

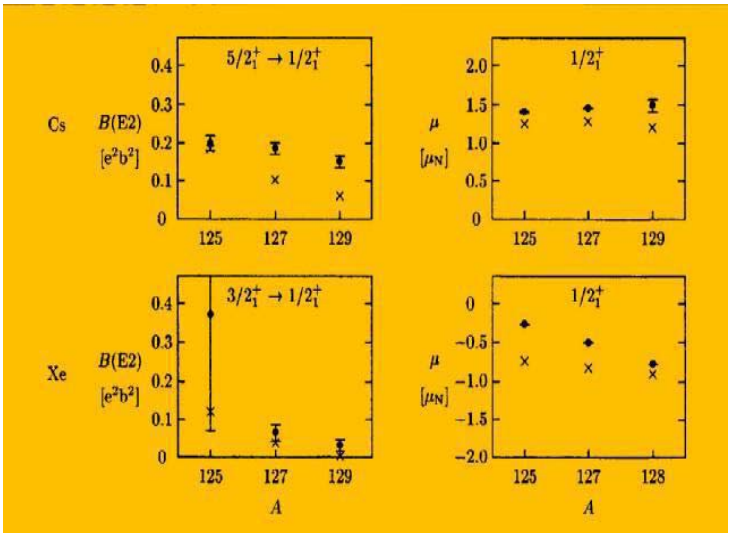

B(E2) and B(M1) values, static moments, branching ratios are calculated for the sequence of Cs and Xe nuclei

B(E2) values and magnetic moments. The symbol • with the error bar denotes the experimental data, while x shows the calculated values

Wave functions are realistic

The Fermi $\sum_k t^{\pm}(k)$ and the Gamow-Teller $\sum_k t^{\pm}(k)\sigma(k)$ transition operators can be expressed in the framework of IBFM2. They can be constructed from the transfer operators.

$$A^{\dagger(j)}_m = \zeta_j a^{\dagger}_{jm} + \sum_{j'} \zeta_{jj'} s^{\dagger} [\tilde{d} a^{\dagger}_{j'}]^{(j)}_m \qquad (\Delta n_j = 1,\ \Delta N = 0)$$

$$B^{\dagger(j)}_m = \theta_j s^{\dagger} \tilde{a}_{jm} + \sum_{j'} \theta_{jj'} [d^{\dagger} \tilde{a}_{j'}]^{(j)}_m \qquad (\Delta n_j = -1,\ \Delta N = 1)$$

The former creates a fermion, while the latter annihilates a fermion simultaneously creating a boson. Either operator increases the quantity $n_j + 2N$ by one unit. The conjugate operators are:

$$\tilde{A}^{(j)}_m = (-1)^{j-m} \left\{ A^{\dagger(j)}_{-m} \right\}^{\dagger} = \zeta^*_j \tilde{a}_{jm} + \sum_{j'} \zeta^*_{jj'} s [d^{\dagger} \tilde{a}_{j'}]^{(j)}_m \qquad (\Delta n_j = -1,\ \Delta N = 0)$$

$$\tilde{B}^{(j)}_m = (-1)^{j-m} \left\{ B^{\dagger(j)}_{-m} \right\}^{\dagger} = -\theta^*_j s a^{\dagger}_{jm} - \sum_{j'} \theta^*_{jj'} [\tilde{d} a^{\dagger}_{j'}]^{(j)}_m \qquad (\Delta n_j = 1,\ \Delta N = -1)$$

The asterisks mean complex conjugate. These operators decrease the quantity $n_j + 2N$ by one unit.

The IBFM image of the Fermi $\sum_k \mathrm{t}^{\pm}(k)$ and the Gamow-Teller transition operator $\sum_k t^{\pm}(k)\sigma(k)$

$$O^{\mathrm{F}} = \sum_j -\sqrt{2j+1} \left[P^{(j)}_{\nu} P^{(j)}_{\pi} \right]^{(0)}$$

$$O^{\mathrm{GT}} = \sum_{j'j} \eta_{j'j} \left[P^{(j')}_{\nu} P^{(j)}_{\pi} \right]^{(1)}$$

$$\eta_{j'j} = -\frac{1}{\sqrt{3}} < l' \tfrac{1}{2}; j' || \sigma || l \tfrac{1}{2}; j >$$

The transfer operators $P_\rho^{(j)}$ depend on nuclei. In the present case

$$P_\pi^{(j)} = \tilde{A}_\pi^{(j)}$$
$$P_\nu^{(j)} = \tilde{B}_\nu^{(j)}$$

$$< M_{\mathrm{F}} >^2 = \frac{1}{2I_i+1} | < I_f || O^{\mathrm{F}} || I_i > |^2$$
$$< M_{\mathrm{GT}} >^2 = \frac{1}{2I_i+1} | < I_f || O^{\mathrm{GT}} || I_i > |^2$$

$$ft = \frac{6163}{< M_{\mathrm{F}} >^2 + (G_{\mathrm{A}}/G_{\mathrm{V}})^2 < M_{\mathrm{GT}} >^2}$$

in units of second where $(G_{\mathrm{A}}/G_{\mathrm{V}})^2 = 1.59$

The coefficients η_j, $\eta_{jj'}$, θ_j, $\theta_{jj'}$ appearing in transfer operators

$$\zeta_j = u_j \frac{1}{K'_j}$$
$$\zeta_{jj'} = -v_j \beta_{j'j} \left(\frac{10}{N(2j+1)} \right)^{1/2} \frac{1}{K K'_j}$$
$$\theta_j = \frac{v_j}{\sqrt{N}} \frac{1}{K''_j}$$
$$\theta_{jj'} = u_j \beta_{j'j} \left(\frac{10}{2j+1} \right)^{1/2} \frac{1}{K K''_j}$$

N is N_π or N_ν, depending on the transfer operator, and K, K'_j, K''_j are determined by

$$K = \left(\sum_{jj'} \beta_{jj'}^2 \right)^{1/2}$$
$$\sum_{\alpha J} < \mathrm{odd};\alpha J || A^{\dagger j} || \mathrm{even};0_1^+ >^2 = (2j+1) u_j^2$$
$$\sum_{\alpha J} < \mathrm{even};0_1^+ || B^{\dagger j} || \mathrm{odd};\alpha J >^2 = (2j+1) v_j^2$$

When the odd fermion is a hole in respect to the boson core, u_j and v_j have to be interchanged

Beta-decay rates from ^{A}Cs to ^{A}Xe shown in terms of $\log_{10} ft$ values. The symbol • with the error bar denotes experimental data, while × presents the calculated value.

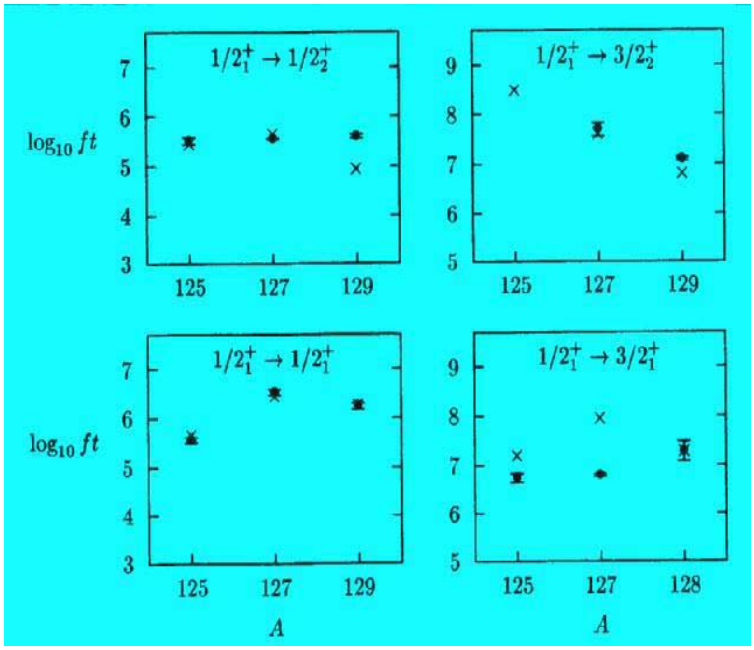

Rh → Pd

A = 105, 107, 109

U(5) ⟷ O(6) nuclei

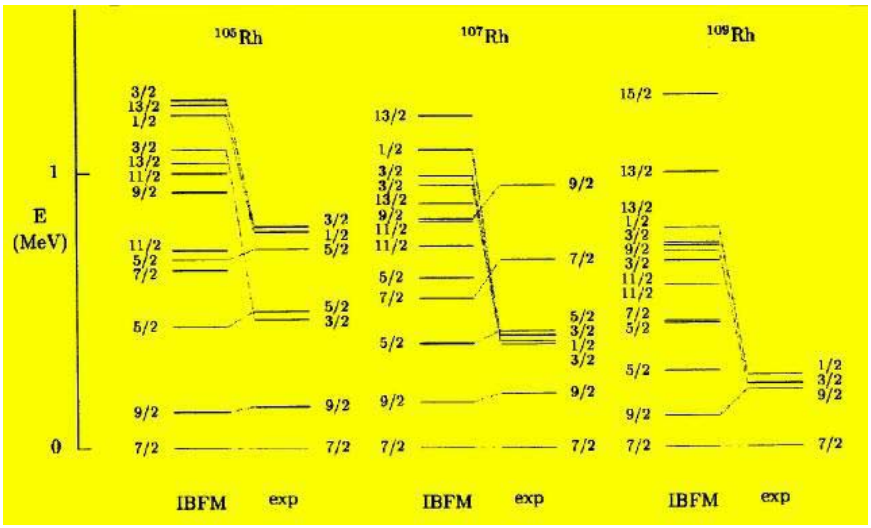

Positive parity levels

j – 1 anomaly !!!!

on $g_{9/2}$

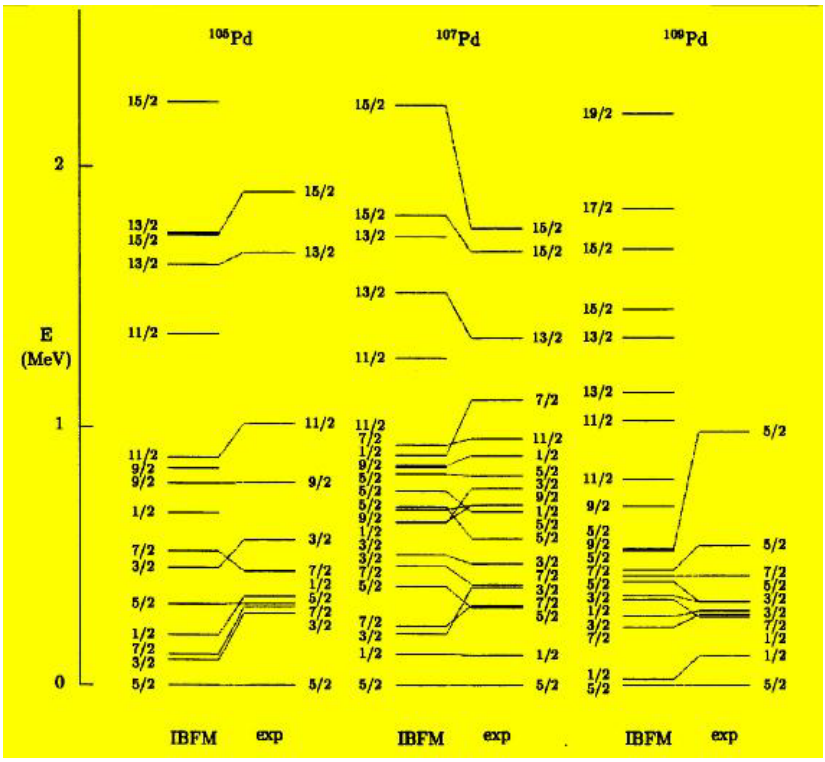

Positive parity levels

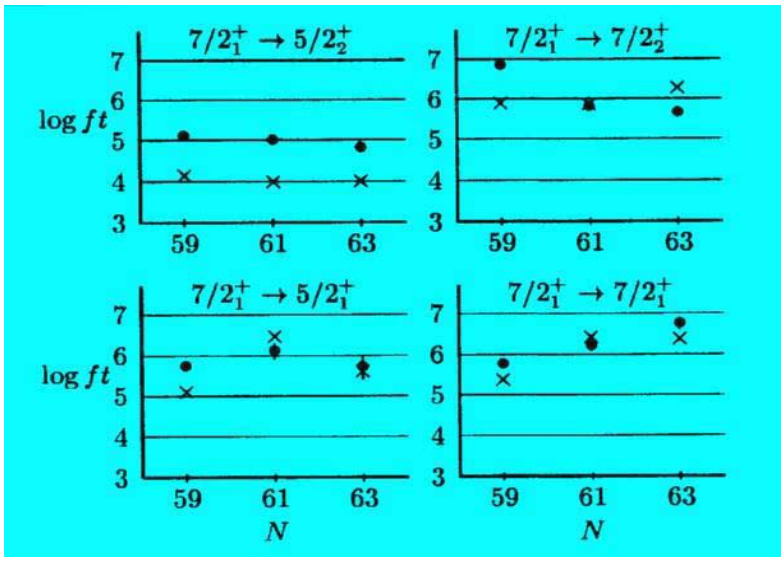

$\log_{10} ft$ values in the decays $_{45}\mathrm{Rh}_{N+1} \to {}_{46}\mathrm{Pd}_N$. The experimental data are presented by • while the calculated values are shown by $\times$.

As → Ge

A = 69, 71, 73

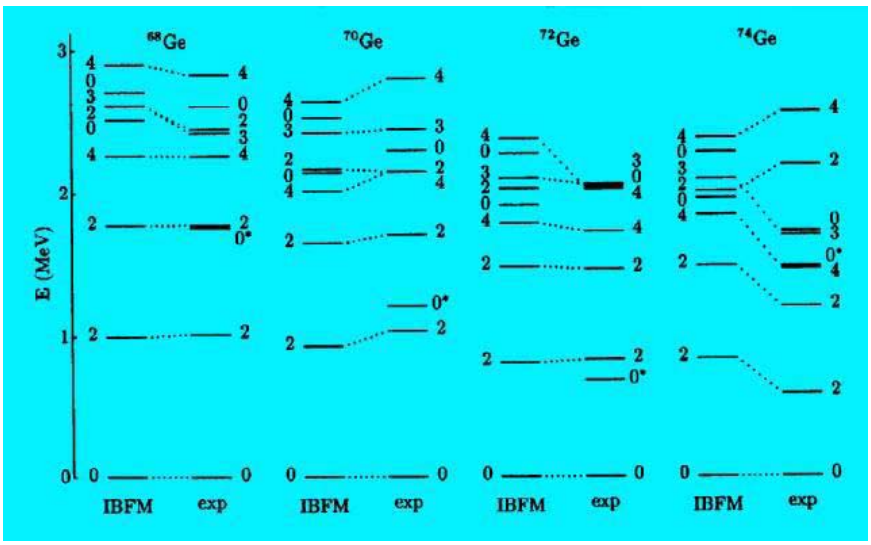

0_2^+ states are intruders !!!!

→ outside the boson space

Consequences ?????

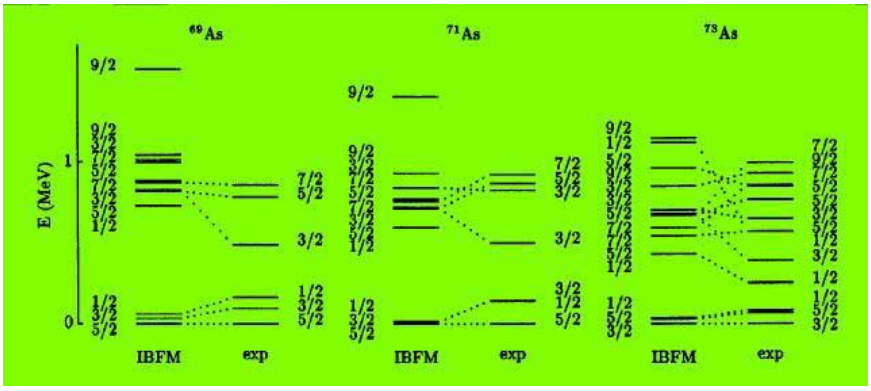

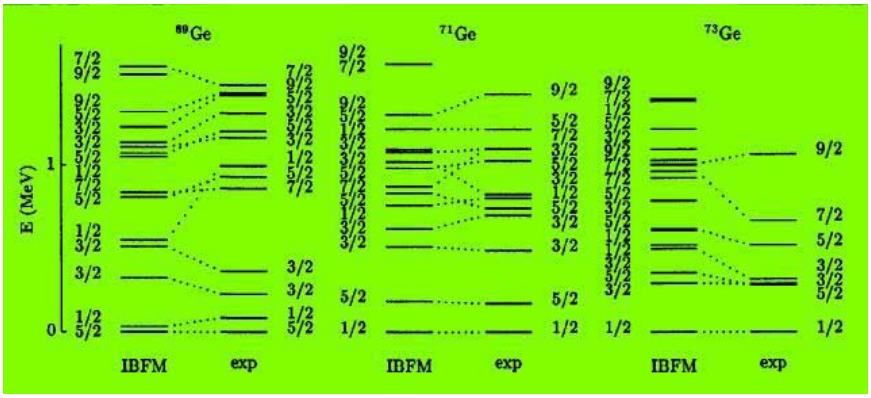

Negative parity levels

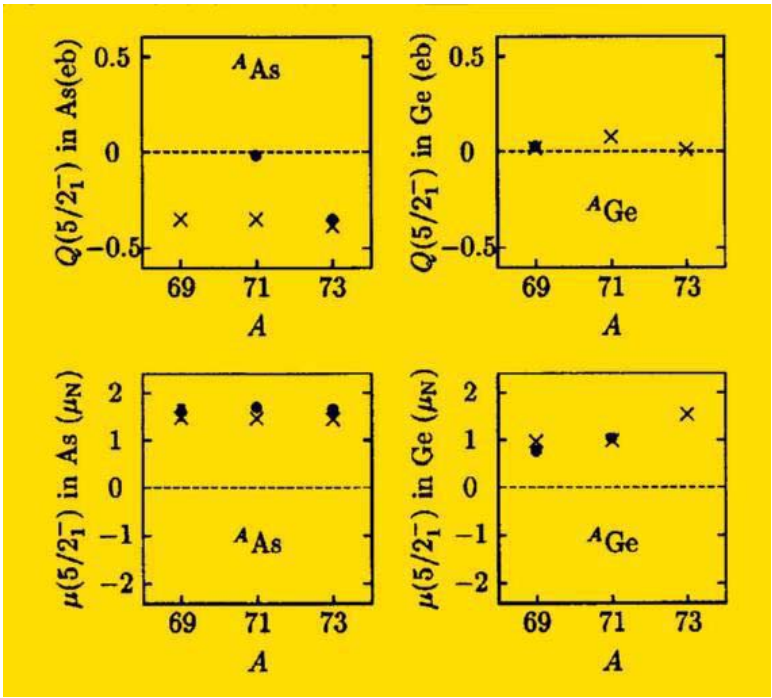

The exclusion of intruder components does not influence strongly the theoretical values of static moments

and branching ratios

Branching ratios in ^{71}As

level (MeV)	transition	$I_\gamma(IBFM2)$	$I_\gamma(EXP)$
0.143	$1/2_1^- \to 5/2_1^-$	100	100
0.147	$3/2_1^- \to 1/2_1^-$	0.0	
	$3/2_1^- \to 5/2_1^-$	100	100
0.506	$3/2_2^- \to 3/2_1^-$	100	100 (5)
	$3/2_2^- \to 1/2_1^-$	7.1	27 (14)
	$3/2_2^- \to 5/2_1^-$	8.2	
0.829	$3/2_3^- \to 3/2_2^-$	9.3	
	$3/2_3^- \to 3/2_1^-$	100	100 (14)
	$3/2_3^- \to 1/2_1^-$	30.3	9.3 (7)
	$3/2_3^- \to 5/2_1^-$	29.4	
0.870	$5/2_2^- \to 3/2_3^-$	0.0	
	$5/2_2^- \to 3/2_2^-$	28.8	
	$5/2_2^- \to 3/2_1^-$	36.4	40 (1)
	$5/2_2^- \to 1/2_1^-$	27.0	1.8 (7)
	$5/2_2^- \to 5/2_1^-$	100	100.0(7)
0.925	$7/2_1^- \to 5/2_2^-$	0.0	
	$7/2_1^- \to 3/2_3^-$	0.0	
	$7/2_1^- \to 3/2_2^-$	0.0	
	$7/2_1^- \to 3/2_1^-$	1.1	5.8 (16)
	$7/2_1^- \to 5/2_1^-$	100	100 (3)

Branching ratios in ^{69}Ge

level (MeV)	transition	$I_\gamma(IBFM2)$	$I_\gamma(EXP)$
0.087	$1/2_1^- \to 5/2_1^-$	100	100
0.233	$3/2_1^- \to 1/2_1^-$	43.2	48.3 (13)
	$3/2_1^- \to 5/2_1^-$	100	100 (3)
0.374	$3/2_2^- \to 3/2_1^-$	0.7	4.6 (8)
	$3/2_2^- \to 1/2_1^-$	100	100.0 (15)
	$3/2_2^- \to 5/2_1^-$	0.1	31.5 (8)
0.862	$7/2_1^- \to 3/2_2^-$	0.4	0.76 (13)
	$7/2_1^- \to 3/2_1^-$	0.1	8.4 (21)
	$7/2_1^- \to 5/2_1^-$	100	100 (3)
0.933	$5/2_2^- \to 7/2_1^-$	0.0	
	$5/2_2^- \to 3/2_2^-$	0.5	32 (7)
	$5/2_2^- \to 3/2_1^-$	16.7	8
	$5/2_2^- \to 1/2_1^-$	35.5	24 (7)
	$5/2_2^- \to 5/2_1^-$	100	100 (5)
0.995	$1/2_2^- \to 5/2_2^-$	0.0	
	$1/2_2^- \to 3/2_2^-$	7.9	9 (6)
	$1/2_2^- \to 3/2_1^-$	26.8	41 (9)
	$1/2_2^- \to 1/2_1^-$	0.7	
	$1/2_2^- \to 5/2_1^-$	100	100 (21)

$\log_{10} ft$ values for levels in ^{69}Ge.

level	$\log_{10} ft$ $(IBFM2)$	$\log_{10} ft$ (EXP)
$3/2_1^-$	5.88	6.05 (2)
$3/2_2^-$	7.90	7.21 (5)
$3/2_3^-$	5.07	6.79 (4)
$3/2_4^-$	6.46	6.71 (6)
$3/2_5^-$	6.73	7.02 (6)
$5/2_1^-$	4.26	5.49 (2)
$5/2_2^-$	6.65	6.94 (7)
$5/2_3^-$	5.33	6.65 (5)
$5/2_4^-$	5.49	6.80 (6)
$7/2_1^-$	7.54	6.98 (5)
$7/2_2^-$	6.54	6.81 (5)
$7/2_3^-$	5.96	6.20 (5)

$\log_{10} ft$ values for levels in ^{71}Ge.

level	$\log_{10} ft$ $(IBFM2)$	$\log_{10} ft$ (EXP)
$3/2_1^-$	6.52	7.19 (1)
$3/2_2^-$	7.79	
$3/2_3^-$	5.73	
$3/2_4^-$	5.21	6.33 (1)
$3/2_5^-$	7.34	6.94 (1)
$5/2_1^-$	4.60	5.85 (1)
$5/2_2^-$	6.08	
$5/2_3^-$	5.63	6.87 (2)
$5/2_4^-$	5.55	6.84 (2)
$7/2_1^-$	7.60	8.79 (25)

The ground states of parent ^{69}As and ^{71}As nuclei are $5/2_1^-$ levels. The erarchy of values for transitions into different states of each angular momen- m is reproduced for ^{69}Ge (except for the transition to the $3/2_3^-$ level that predicted to have a rather small $\log_{10} ft$ value). The same is true for ^{71}Ge. he theory predicts that the smallest $\log_{10} ft$ value among all $3/2^-$ levels in Ge has the $3/2_4^-$ level. This result is in agreement with the experimental ata. The only available experimental $\log_{10} ft$ value in ^{73}Ge is for the $1/2_1^-$ vel ($\log_{10} ft = 5.4$). The corresponding theoretical value (4.27) is the smallest lculated.

Systematic effect : For most decays the calculated values are smaller than the experimental values

a) Wave functions ?

If one takes the transition operators without normalization parameters, then the difference between the calculated and experimental values are caused by the transition matrix elements, that in this case have to be overestimated. This may indicate that other components are admixed in the wave functions (for example those involving intruder states), which would decrease the amplitudes of the present IBFM2 components, leading to an increase of the theoretical $\log_{10} ft$ values.

Accurate test of wave functions

b) Transfer operators ?

- **Normalization factors ?**
- **Additional terms ?**
- **Normalization factors + Additional terms ?**

$$A_m^{\dagger(j)} = [\ \zeta_j a^\dagger_{jm} + \sum_{j'} \zeta_{jj'}\ (\ s^\dagger [\tilde{d} a^\dagger_{j'}]^{(j)}_m + \quad)\ ]$$

Overall normalization factor N ?

Normalization factor γ

a) Parameter
b) Microscopic

Additional term(s)

$\tilde{s}[d^\dagger a^\dagger_{j'}]^{(j)}_m$

or

$\sum_{j',J} \phi^J_{jj'} [(a^\dagger_{j'} \times d^\dagger)^{(J)} \times \tilde{d}]^{(j)}_m$

or

.....

^{58}Ni (d, ^{3}He) ^{57}Co reaction

Normalization factor γ and the term $\tilde{s}[d^\dagger a^\dagger_{j'}]^{(j)}_m$

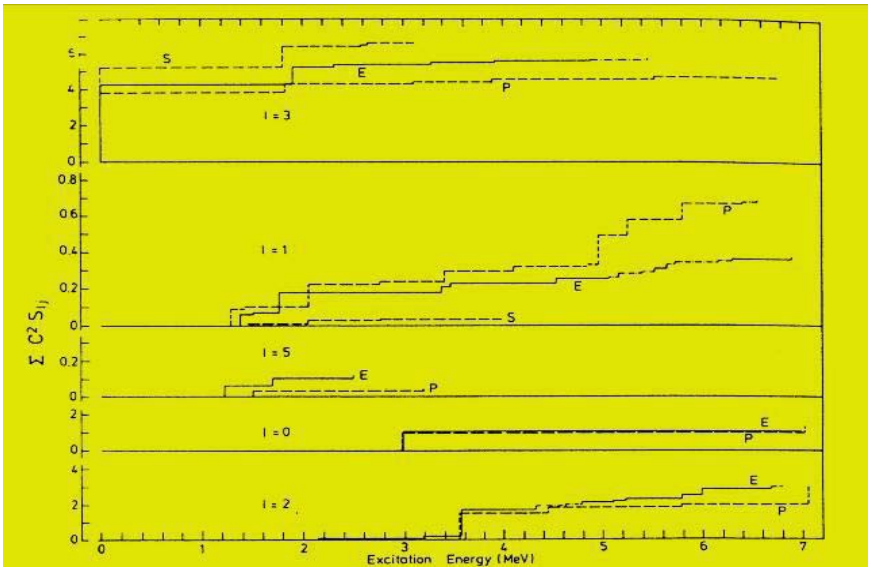

Sums of spectroscopic strengths

E experiment S shell model P IBFM1

^{62}Ni (d, ^{3}He) ^{61}Co reaction

Normalization factor γ and the term $\tilde{s}[d^\dagger a^\dagger_{j'}]^{(j)}_m$

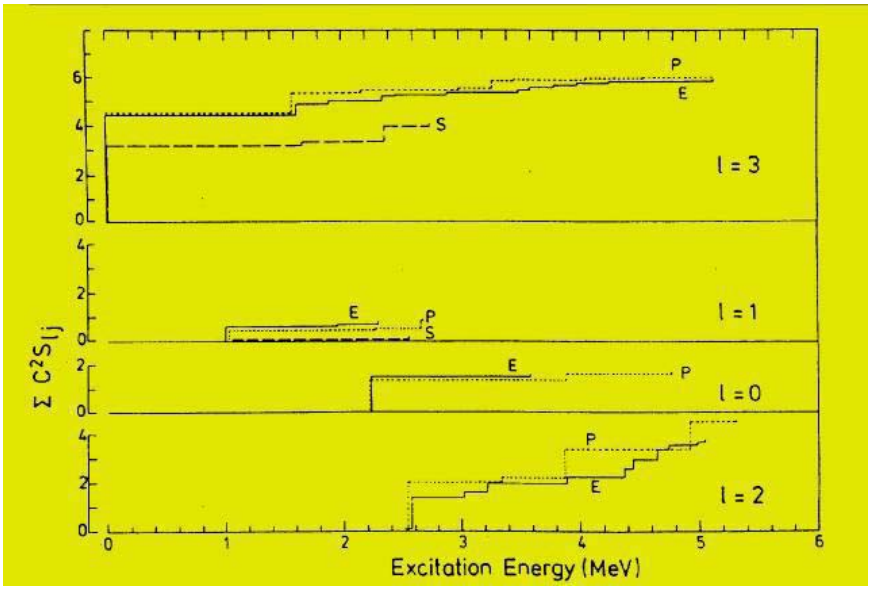

Sums of spectroscopic strengths

E experiment S shell model P IBFM1

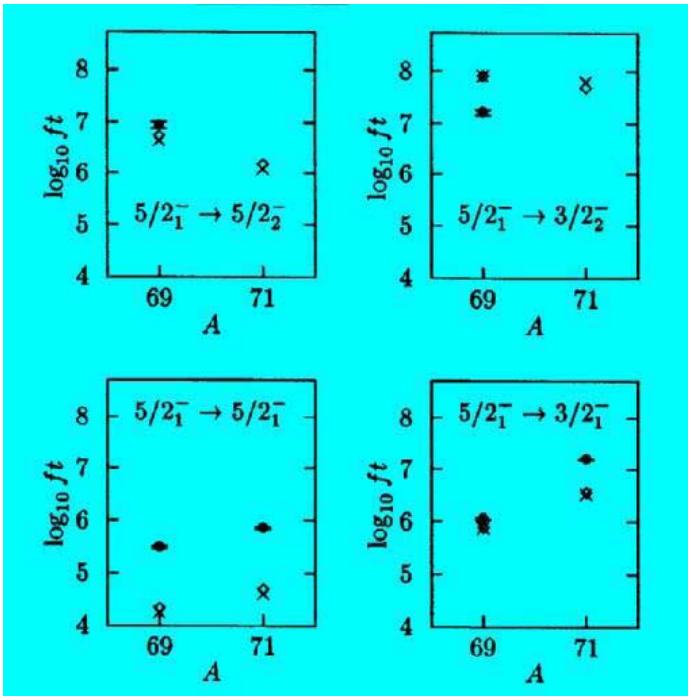

$\log_{10} ft$ values of the β-decay from the As to the Ge isotopes. The symbol • shows the experimental values with their errors, while the symbol × shows the results of calculations with the conventional operators. The symbol ○ shows the results of calculations with the additional d-boson number conserving terms.

The effect of the additional term

$$\sum_{j',J} \phi^J_{jj'}[(a^\dagger_{j'} \times d^\dagger)^{(J)} \times \tilde{d}]^{(j)}_m$$

is small

CONCLUSIONS

The extensions of IBM with fermion degrees of freedom provide a consistent description of nuclear structure phenomena in:

- spherical nuclei
- deformed nuclei
- transitional nuclei

- The structure results from a consistent calculation that includes interaction strengths obtained in the analysis of neighboring nuclei
- All calculations are performed in the laboratory frame, and therefore the results can be directly compared with experimental data
- The models can be related to the shell model
- The symmetry approach can be applyed in special cases
- There is a strong evidence that collective and single-particle degrees of freedom are closely related